AC-AC CONVERTER WITH SOFT COMMUTATION FOR INDUCTION HEATING APPLICATION

A THESIS SUBMITTED TO THE GRADUATE SCHOOL OF APPLIED SCIENCES OF NEAR EAST UNIVERSITY

By

ABDURAHIM ALHASHMI H. IDWAIB

In Partial Fulfillment of the Requirements for the Degree of Master of Science in Electrical and Electronic Engineering

NICOSIA

2019

AC-AC CONVERTER WITH SOFT COMMUTATION FOR INDUCTION HEATING APPLICATION

A THESIS SUBMITTED TO THE GRADUATE SCHOOL OF APPLIED SCIENCES
OF
NEAR EAST UNIVERSITY

By

ABDURAHIM ALHASHMI H. IDWAIB

In Partial Fulfillment of the Requirements for the Degree of Master of Science
in
Electrical and Electronic Engineering

NICOSIA

2019

ABDURAHIM ALHASHMI H. IDWAIB: AC-AC CONVERTER WITH SOFT COMMUTATION FOR INDUCTION HEATING APPLICATION

Approval of Director of Graduate School of Applied Sciences

Prof. Dr. Nadire CAVUS

Wecertify this thesis is satisfactory for theaward of the degree of Master of Science in Electrical and Electronic Engineering

Examining Committee in Charge:

Prof. Dr. Senol Bektas	Committee Chairman, Department of Electrical and Electronic Engineering, NEU
Prof. Dr. Seyedhossein Hosseini	Supervisor, Department of Electricaland Computer Engineering, University of Tabriz-Iran
Assist. Prof. Dr. Sertan Serte	Department of Electrical and Electronic Engineering, NEU

I hereby declare that all information in this document has been obtained and presented in accordance with academic rules and ethical conduct. I also declare that, as required by these rules and conduct, I have fully cited and referenced all material and results that are not original to this work.

Name, Last name: ABDURAHIM ALHASHMI H. IDWAIB

Signature:

Date:

ACKNOWLEDGEMENTS

Firstly, I would like to thank my thesis supervisor Prof. Dr. Seyedhossein Hosseini a professor at Near East University . My completion of this thesis could not have been possible without his continuous academic guidance and support. Dr. Hosseini enabled me to reach my greatest and full potential and showed me that I can accomplish my dreams.

I would also like to extend my warm thanks to the head of the Electrical And Electronic Engineering Department Prof. Dr. Bulen Bilgehan.

I would also like to acknowledge the jury members (Prof. Dr. Senol Bektas and Assist. Prof. Dr. Sertan Serte) their valuable input and comments .
Finally , and most importantly , I must express my profound gratitude to my beloved father and mother for their unconditional love and support . To my loving and caring wife for her patience and continuous encouragement .

My endless appreciation to my siblings who despite their distance have always been a source of empowerment and strength for me .Also , To my closest and dearest friends.

ABSTRACT

In this research a single unidirectional power switch based parallel resonant converter is presented. This converter is utilized in providing power for inducting heating applications. The structure of the proposed converter is composed three main parts; an LC source filter, H-Bridge diode rectifier circuit and the single power switch. The resonant tank provides the needed soft commutation of the power switch and as in the case of all cycloconverters; the proposed topology is a generator of high frequency. The converter load power is regulated by using an appropriate switching frequency. Investigation of the proposed converter is done in two modes; mathematical analysis and simulation analysis using MATLAB 2015Ra edition.

***Keywords*:** Ac-Ac Converter, Soft Commutation, Induction Heating, Zero Voltage Switching, Zero Current Switching .

ÖZET

Bu araştırmada paralel rezonans dönüştürücü bazlı tek yönlü bir güç anahtarı sunulmuştur. Bu dönüştürücü, ısıtma uygulamalarını indüklemek için güç sağlamada kullanılır. Önerilen dönüştürücünün yapısı üç ana bölümden oluşur; bir LC kaynak filtresi, H-Bridge diyot doğrultucu devresi ve tek güç anahtarı. Rezonans tankı, güç şalterinin ihtiyaç duyulan yumuşak komutasyonunu ve tüm döngü çevricilerinde olduğu gibi sağlar; Önerilen topoloji, yüksek frekanslı bir jeneratördür. Dönüştürücü yük gücü, uygun bir anahtarlama frekansı kullanılarak düzenlenir. Önerilen dönüştürücünün araştırılması iki modda yapılır; MATLAB 2015Ra baskısını kullanarak matematiksel analiz ve simülasyon analizi.

Anahtar Kelimeler: Ac-Ac Çevirici, Yumuşak İletişim, İndüksiyonla Isıtma, Sıfır Gerilim Anahtarlama, Sıfır Akım Anahtarlama.

TABLE OF CONTENTS

LIST OF FIGURES

LIST OF TABLES

LIST OF ABBREVIATIONS

AC:	Alternating Current
DC:	Direct Current
BJT:	Bipolar Junctions Transistor
EMI:	Electromagnetic Interference
PWM:	Pulse Width Modulation
IBC:	Isolated Boost Converter
MC:	Matrix Converter
ZV:	Zero Voltage
ZC:	Zero Current

CHAPTER ONE
INTRODUCTION

1.1 Overview

Power electronic (PE) converters have revolutionized electric power generation, transmission, distribution and most importantly the efficient application of this vital commodity which is the backbone of every developed society.

Power electronic converter is a broad terminology used in both academia and industry to describe power electronic device/circuit which are used to condition power/voltage to the desired characteristics such as phase, magnitude of amplitude, harmonic content, frequency amplitude etc. In power conditioning, the following devices are utilized to achieve a certain desired results;*rectifiers* are used to change ac power into dc power whiles *inverters* perform the opposite function of rectifiers i.e. changing of dc power into ac power. *Cycloconverters* and *choppers*do not change the "nature" of the power but rather control the amplitude from one level to another, it could be an increase from the original value or a decrease from the original value, they (cycloconverters and choppers) can be used to provide "clean" power hence not much difference between the input value and output values but rather performs the function of cleaning the input power of impurities or noise such as harmonics, frequency etc. In the case of choppers, they are used to regulate the input and output values of dc power systems only, basically both the input power and the output power are dc in nature. In the case of cycloconverters, they are utilized in controlling the magnitude of the input ac power to a desired value at the output. The output of the cycloconverters are also ac in nature, and are also used in frequency regulation.

Power electronic converters have several applications; they can be found in almost every sector of human life, from communication to education, power generation, transmission systems and distribution systems, transportation, military etc. Some specific application of PE converter are:

- Motor drive control
- RES
- UPS
- FACTS

Renewable energy has seen much intense growth in the last decade, this can mostly be attributed to the negative effects of using fossil fuels. Increased development of renewable energy means an increase in the application of converters. The new goal of applying converters is not only to condition power to the requisite characteristics but also an efficient application.

Several topologies of converters exist but our focus in this research will analyse ac-ac converters for application in induction heating. Even under ac-ac converters, several types or different topologies exist, some examples are matrix converters which also known as cycloconverter, direct and indirect converters, converters based on impedance or ZS (gamma) structure.

In the case of cycloconverters, they are used as buck converters for voltage because of the limitation of boosting capabilities but also used as boost converter for frequency control systems. Basically, the input voltage of cycloconverters are always lower than the output voltage whiles the input frequency is always less than the output frequency. Switches utilized in this type of converter are always bidirectional type for both voltage and current due this, the total losses is much high because more switches conduct during a specific period. However the cycloconverter is a robust device which has several applications. It can be utilized in power conditioning i.e. changing of the phase of the source to a specific phase, used as any of the four state of converters.

The direct and indirect types of ac-ac converters are the usual voltage source inverters which have a storage element embedded in the structure. The indirect topology has the energy storage element whiles the direct topology does not have any form of energy storing component, the input voltage is conditioned to the desired characteristics and directly supplied to the load. The cost benefit analysis of the two topologies can be done from many point of merits such as, loses due to the converter, application areas, cost of converter, number of components utilized etc. The direct ac-ac topology is better when analysed from the cost point of view because large capacitors are required in the indirect topologies as energy storage devices. The indirect ac-ac converters are most suitable for applications where variable or changing frequency and voltages are required, but if only changeable voltage is required, the direct ac-ac converter is most suitable because of the following advantages; small size, maximum output efficiency and reduced cost. In applications where ac-ac converters are employed with high power, Thyristor switches are used for power regulation because of the following: durability and low cost and also suitable for high power applications, however they require filters to reduce or eliminate current harmonics and also very slow response time.

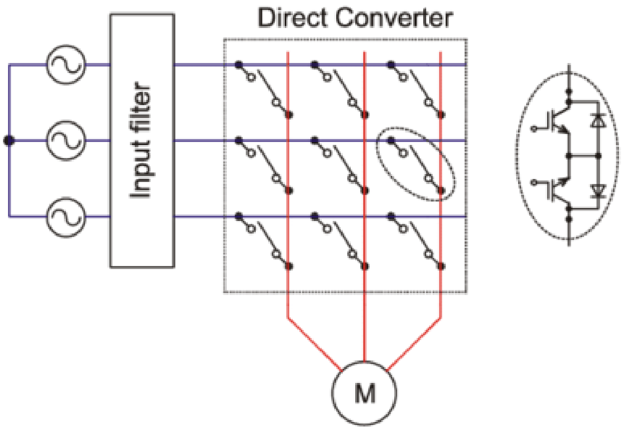

Figure 1.1: Direct MC

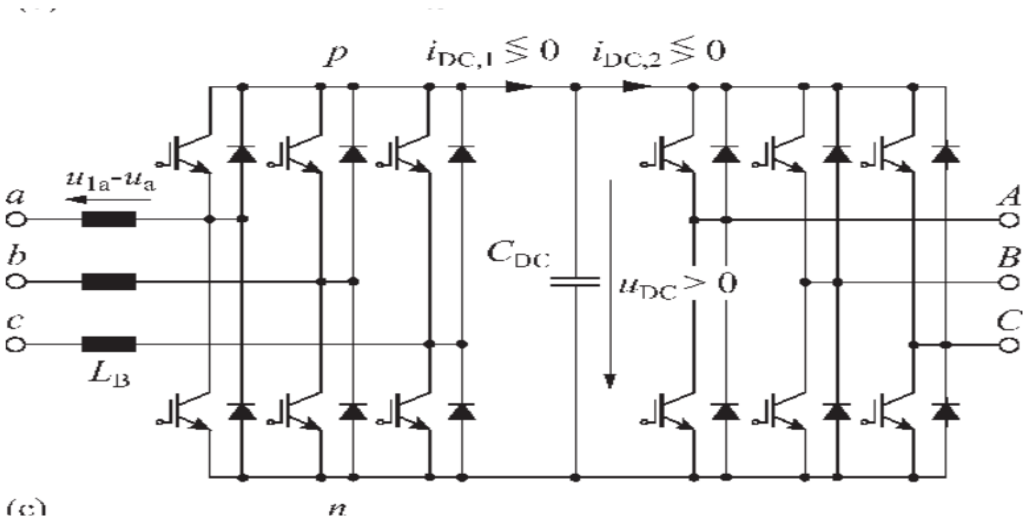

Figure 1.2: Indirect converter

The introduction of the ZS structure can be considered a novel structure because ZS has resolved all the demerits of the conventional VS and CS converters. The impedance based ac-ac converters are new generational converters which are able to give enormous advantages when compared to the conventional ac-ac topologies. They are able to provide buck-boost capabilities, very high boosting characteristics and large number of different topologies to choose for specific applications. The only difference between these impedance based converter and the conventional converter in terms of structure is the introduction of the Z-S or impedance structure which is inserted between the source and the main inverter structure. The impedance based topologies which are most suitable for ac-ac converters can be found but not limited in the following:

- Trans ZS
- Quasi
- Conventional Z-S
- Switched Coupled
- T-ZS
- Gamma ZS
- Magnetically coupled

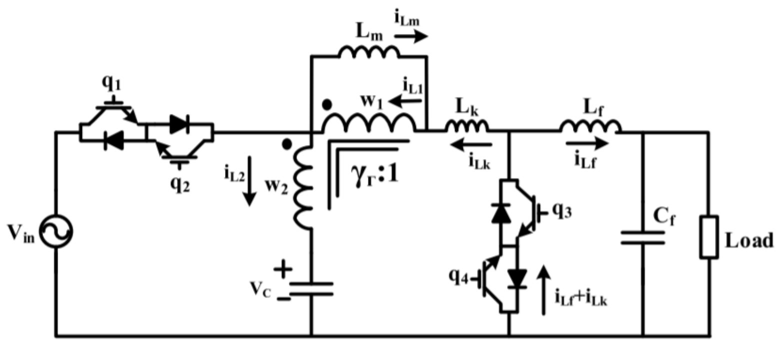

Figure 1.3: Gamma ZS converter

The proposed structure under review is a single phase topology, however two, three or more phase's topologies exist for ac-ac converters. One major advantage of ac-ac converters which makes them suitable for induction heating application is its ability to provide very high frequencies however ac-ac converters cannot provide electrical isolation from the main system unless transformers are utilized.

Induction cooking derived from a copper wound spiral coil which is usually located beneath a pan made or iron.

Induction cooking is the application of heat directly unto a cooking pan to efficiently cook the provided food substance. A power source having very high frequency is connected to the coil which produces very magnetic field which makes eddy current path in the coil hence heating the pan for cooking. The provide heat is as a result of eddy current dissipation. An exciting coil is used to produce magnetic field which varies. A circular path of eddy current is produced by this system. The conventional induction systems have the disadvantages of being able power only electric irons or steel (stainless) substances. A good or reliable induction heating system should provide the following merits:

a. High output power and minimum cost.
b. High efficiency
c. Wide variable power control system
d. Wide range load functionality
e. Reduced harmonic content.

The heart of every reliable induction heating or cooking system is the converter based device which is able to efficiently provide the desired power, hence the introduction of low cost inverters has helped in the mass production of induction cookers. Current induction cookers have the following advantages over the conventional technologies:

a. Fast response time
b. Efficient
c. Low cost
d. High Safety
e. Flexibility
f. Pan detection

The following factors which are associated with induction cooking system; which when improved will greatly increase the efficiency of the system has seen major focus in terms of research over the past few years;

a. Resonant converters
b. Control techniques
c. Magnetic circuits

Current trends in induction cooking systems is linked to other systems such a self-cooking robot. Also the size and weight of the cooking utensil, and power and temperature regulation are all interlinked. One major which affects induction cookers are the types of cooking utensil available on the market, these products due to their different characteristic have different levels of temperature functionality hence a wide range of control exists; this causes huge limitations for the efficient control of the induction cooker.

1.2 Thesis Problem

Several single phase topologies of ac-ac circuit exist; from matrix converter to impedance based topologies. The structure of these topologies rely heavily on bidirectional switches; these type of switches are mostly composed of two IGBT and two diodes connected in an ant-parallel form, mostly for common emitter or common collector topologies. In the case of diode bridge topology, four diodes and one switch are used to obtain bidirectional current and voltage flow switch. Because of the large number of components required to obtain bidirectional switch, the total component count for most converters using these types of switches are on the high side. Having high component count directly increases the switching and conduction loses of the converter hence reduced efficiency, increased cost, increased weight and size. These factors seriously hinders the commercialization of these converters.

1.3 The Aim of the Thesis

The aim of this research is design a single phase converter applied in a single phase system which resolves all the problems mentioned above. A single phase converter (ac-ac) which uses only one unidirectional switch is proposed. The proposed converter will be switched with safe commutation and also applied for induction cooking.

1.4 The Importance of the Thesis

The following advantages will be realised when the proposed topology is successfully derived. A single unidirectional switch based converter will possess the following advantages:

a. Reduced cost
b. Reduced losses
c. Increased efficiency
d. Reduced size, volume and weight

1.5 Limitation of Study

This research was successfully carried with minimum limitation. These limitations can be traced to the absence of a well-equipped research facility where experimental results can be investigated and compared to the simulation results, however the software used (MATLAB) has minimum error difference between experimental and simulation results.

1.6 Overview of the Thesis

The body of the thesis is segmented into the following categories:

Chapter 1: Introduction, Thesis Problem, Aim of the Thesis, The importance of the Thesis, Overview of the Thesis

Chapter 2: Literature Review of ac-ac converters

Chapter 3: Resonant And Commutation Circuit Analysis

Chapter 4: Simulation Results

Chapter 5: Conclusion and Future Results

CHAPTER TWO
LITERATURE REVIEW

2.1 Introduction

This chapters seeks to review the various ac-ac converter technologies published over the years or others being used in industry, several ac-ac converter topologies can be found in industry and in academia.AC-AC converters are generally classified into two categories based on the nature of power conversion; these two categories are direct and indirect topologies. The difference between the two topologies is that in the case of the direct topology, both the input and output voltage are ac-type hence the nature of voltage (ac) does not change therefore there's no ESS required whiles in the case of the indirect topology, the nature of the voltage changes to dc between the source and output and ESS is required sometimes to store the dc energy.A few of these topologies will selected and reviewed. The selected topologies will the following headings but not limited to:

- Matrix Converter
- Impedance Based Topologies
- Modular MI Topologies
- Buck-Boost Topologies
- Other Topologies

2.2 Matrix Converter (MC)

The matrix converter is a special type of converter which is also known cycloconverter. This type of converter is able efficiently change the type of phase at the output irrespective of the input phase. MC use bidirectional switches which are derived from any of the known switch arrangements to obtain bidirectional switch. Generally MC are classified based on either the type conversion or the type of phase (although there are cross phase topologies). Based on the conversion type, MC are categorized into direct or indirect MC topologies, whiles based on the type of phase, MC are categorized into the following groups:

- Single Phase
- Two phase
- Three Phase

Without adding any extra structure to the conventional MC, they are commonly referred to buck voltage converters and boost frequency converters. This is to mean that when used for voltage conversion the voltage gain is less than one but when utilized for frequency conversion, the frequency gain is greater than one.

The general structure of the matrix converter is composed of 9-switches which have current and voltage bidirectional flow. Hence the topology of the matrix converter can switch from a specific phase at the input to a different phase at the output or can maintain both phases at the input and output side. Matrix converters can be single stage converters or double stage converters where energy storage components are impeded in the conversion stage; these types of topologies are referred to Direct MC and Indirect MC. The first topology of MC was introduced by Gyugyi in 1970 whilesVenturini carried out further investigation in 1981 . The general structure of the matrix converter is shown by Figure 2.1 and the equations of the input current and the output voltage are given by:

$$I_I=T^T x I_0=\begin{bmatrix} I_a \\ I_b \\ I_c \end{bmatrix}=\begin{bmatrix} S_{Aa} & S_{Ab} & S_{Ac} \\ S_{Ba} & S_{Bb} & S_{Bc} \\ S_{Ca} & S_{Cb} & S_{Cc} \end{bmatrix}\begin{bmatrix} I_A \\ I_B \\ I_C \end{bmatrix} \qquad (2.1)$$

$$V_0=T x V_I\begin{bmatrix} V_A \\ V_B \\ V_C \end{bmatrix}=\begin{bmatrix} S_{Aa} & S_{Ab} & S_{Ac} \\ S_{Ba} & S_{Bb} & S_{Bc} \\ S_{Ca} & S_{Cb} & S_{Cc} \end{bmatrix}\begin{bmatrix} V_a \\ V_b \\ V_c \end{bmatrix} \qquad (2.2)$$

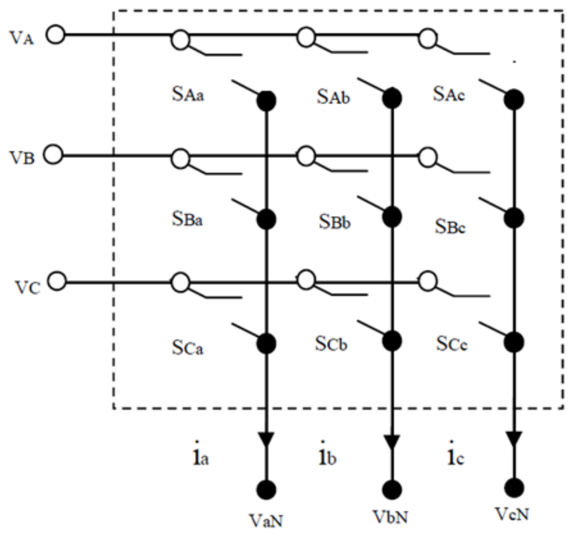

Figure 2.1: General structure of MC

The switches used in MC are bidirectional in nature for current flow in both directions; these types of switches are composed and not bought due to the variations in power ratings.

There are several topologies which are used in designing the bidirectional switches. These are shown by Figure 2.2 and are commonly called:

- common emitter
- common collector
- Antiparallel
- Diode bridge
- Hybrid

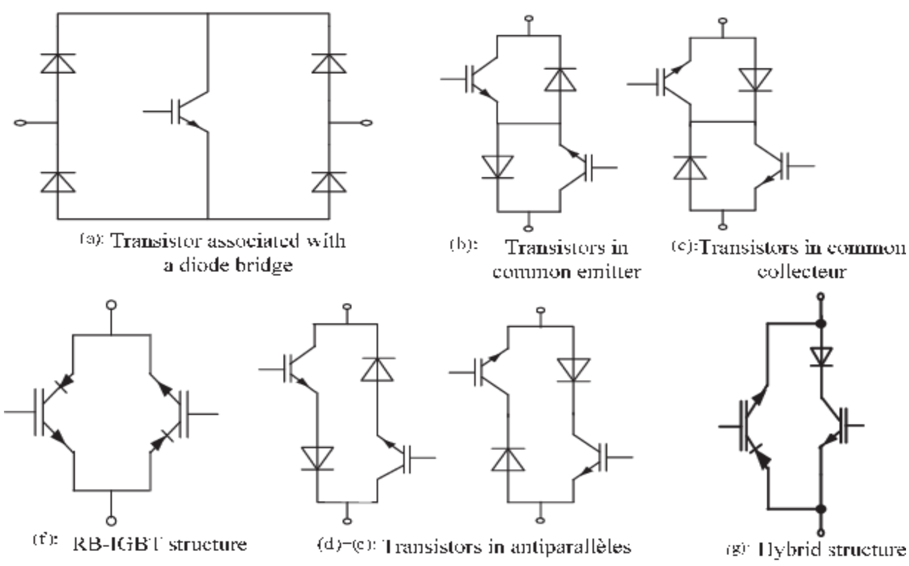

Figure 2.2: Types of bidirectional switches

Investigation of a matrix converter as a general multipurpose converter having all the possible power conditioning capabilities is investigated ; the matrix converter is utilized as an inverter, a rectifier, chopper and cycloconverter. The appropriate control method applied in this analysis the predictive control method. Figure 2.3 shows the general topology of a three phase matrix converter and Figure2.4 shows the cycloconverter mode of the matrix conductor.

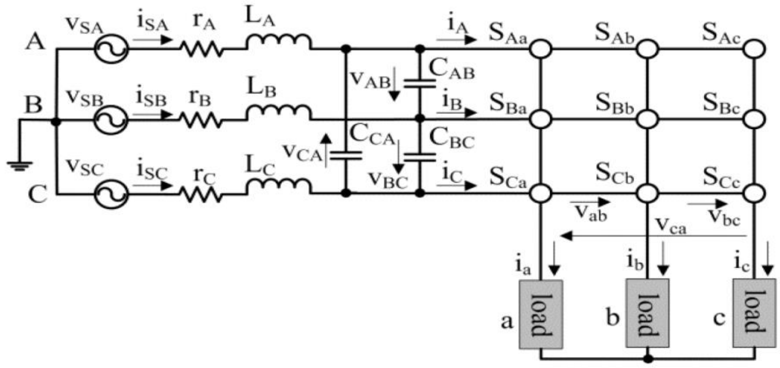

Figure 2.3: Three phase matrix converter

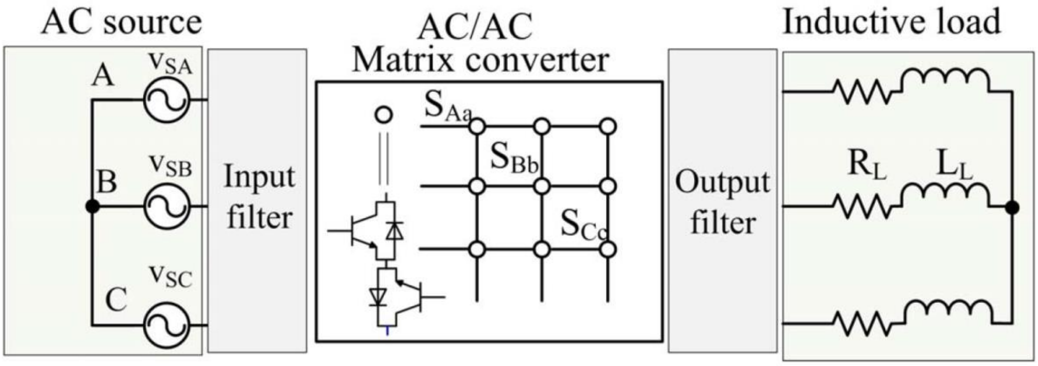

Figure 2.4: Cycloconverter mode of matrix converter

High boosting converters are in high demand because of their imperative advantages over buck converters hence a high boosting ac-ac matrix converter is proposed . This proposed topology achieves high boosting capabilities without increasing the semiconductors switches in a previously proposed topology. Previous methods of gaining high boosting abilities was derived by introducing dc-dc converters to the proposed topology, however with the introduction of impedance based networks popular referred to as Z source networks , high boosting capabilities are achieved by utilizing any of the ZS structures which give both buck and boost functionalities. The proposed high boosting matrix converter is composed of six bidirectional switches, switched inductor cells and 6 diodes. There are four modes of operation of the proposed topology; two modes in the positive cycle which are the charging and discharging modes and two modes of the negative cycle which are also charging and discharging modes. Figure 2.5 shows the circuit of the proposed topology and the rest of the figures shows the modes of operation and the switched inductor cell arrangements.

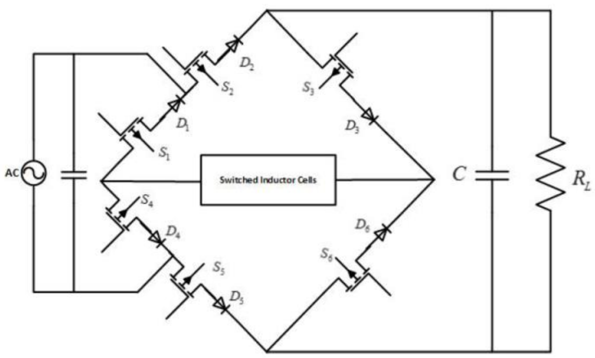

Figure 2.5: High gain matrix converter

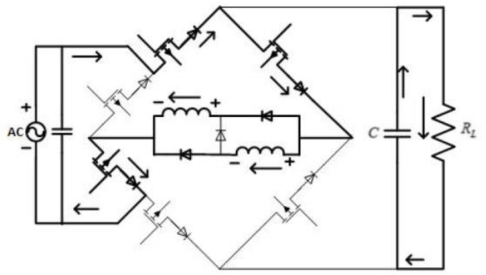

Figure 2.6: Positive mode charging

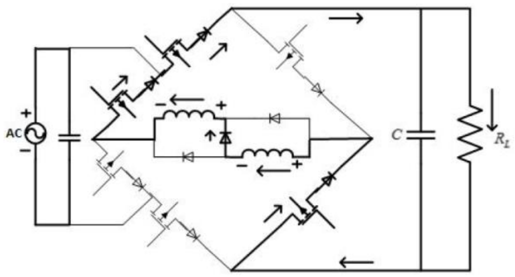

Figure 2.7: Positive mode discharging

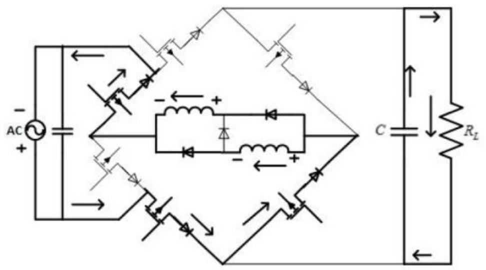

Figure 2.8: Negative mode charging

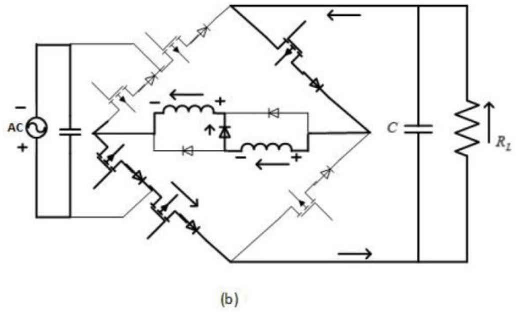

Figure 2.9: Negative mode discharging

The switched inductor cell arrangement is shown in Figure 2.10 where (a) shows the arrangement, (b) and (c) represents the charging and discharging mode respectively.

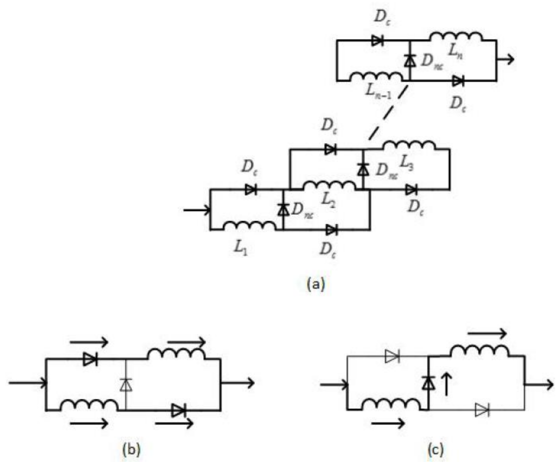

Figure. 2.10: Switched inductor cell disposition

Similarly a high boosting ac-ac single phase matrix converter is presented in (S. Z. Mohammad Noor et al., 2011) . This topology has the ability to synthesize greater voltage at the out than the source voltage. Two modes of operation are permissible in the proposed topology; positive and negative half cycles. Figure 2.11 shows the circuit of the proposed matrix converter and the modes of operation are represented by Figure 2.12 and Figure 2.13. The positive mode of operation is represented by Figure 2.12 whiles the negative mode of operation is shown by Figure 2.13.

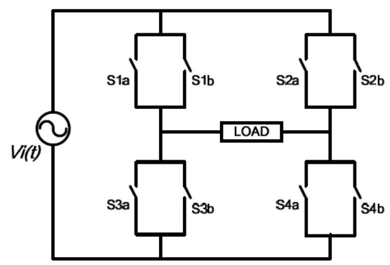

Figure 2.11: Single phase MC (S. Z. Mohammad Noor et al., 2011)

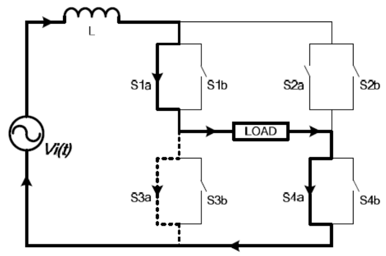

Figure 2.12: Single phase MC in positive mode

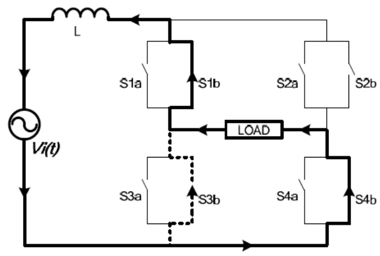

Figure 2.13: Single phase MC in negative mode

A buck-boost single phase MC topology based on the conventional ZS structure is proposed . This topology has the capability to minimum and maximum output voltage provided by the impedance structure using the shoot through phenomenon. A bidirectional switch placed between the source and the ZS network provides bidirectional current flow from the load to the source hence in braking modes of some applications, energy is transferred from the load to the source. The impedance network is composed of symmetric passive components; two capacitors and two inductors. A total of five bidirectional switches are utilized. The bidirectional switches are derived from the common emitter configurations. Figure 2.14 shows the proposed topology in (Minh-Khai Nguyen et al., 2009).

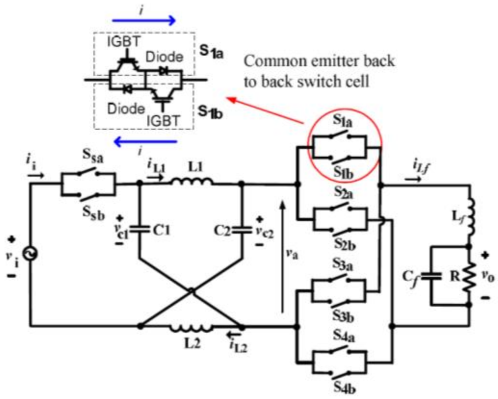

Figure 2.14: ZS based matrix converter (Minh-Khai Nguyen et al., 2009)

A new type of matrix converter is proposed. This novel topology uses minimum component count to achieve the same function as the conventional structure where the component count in much higher. The proposed topology utilizes three bidirectional switches to converter a three-phase system to a single phase system; whiles the conventional topology uses 6 bidirectional switches for the same function. The circuit of both systems are shown below.

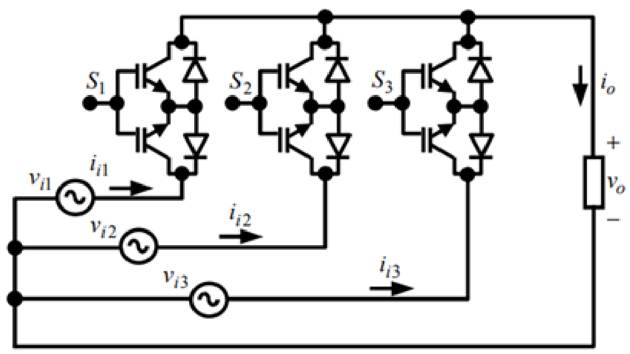

Figure 2.15: The 3 switches MC

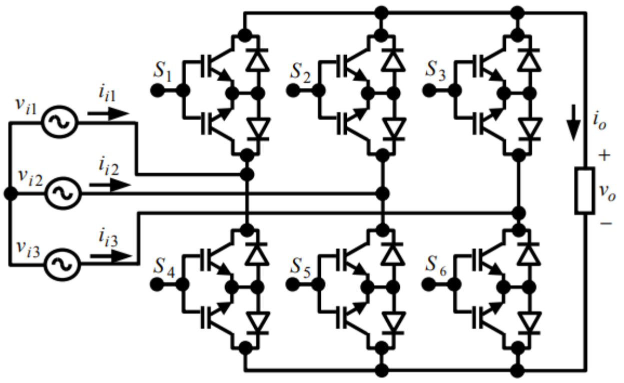

Figure 2.16: 6 switches MC

Table 2.1: Switching Pattern

Mode	Switch	Output Voltage v_0	Output current i_0
3 switches based *1x3* matrix converter			
1	S1	v_{i1}	i_{i1}
2	S2	v_{i2}	i_{i2}
3	S3	v_{i3}	i_{i3}

Table 2.2: Switching Pattern

Mode	Switch	Output Voltage v_0	Output Current i_0
6 switches based *1x3* matrix converter			
1	S_1 and S_5	$v_{i1} - v_{i2}$	$i_{i1} = -i_{i2}$
2	S_1 and S_6	$v_{i1} - v_{i3}$	$i_{i1} = -i_{i3}$
3	S_2 and S_6	$v_{i2} - v_{i3}$	$i_{i2} = -i_{i3}$
4	S_2 and S_4	$v_{i2} - v_{i1}$	$i_{i2} = -i_{i1}$
5	S_3 and S_4	$v_{i3} - v_{i1}$	$i_{i3} = -i_{i1}$
6	S_3 and S_5	$v_{i3} - v_{i2}$	$i_{i3} = -i_{i2}$
7	(S_1 , S_4) or (S_2 , S_5) or (S_3 , S_6)	0	i_0

A new topology of indirect MC is proposed in (Z. Shao et al., 2009). This topology combines the impedance structure with MC to achieve higher boosting capabilities. The impedance network is embedded in the second stage of power conversion hence the proposed topology is a double stage converter or popularly called indirect MC. The applied impedance structure is the first or conventional network composed of passive elements having equal magnitudes. Figure 2.17 shows the diagram of the proposed topology. The main drawback of matrix converters which is limited output power ratio is overcome with the introduction of the impedance network. Also buck-boost capabilities, better spectral performance against EMIs and high voltage gains are achieved.

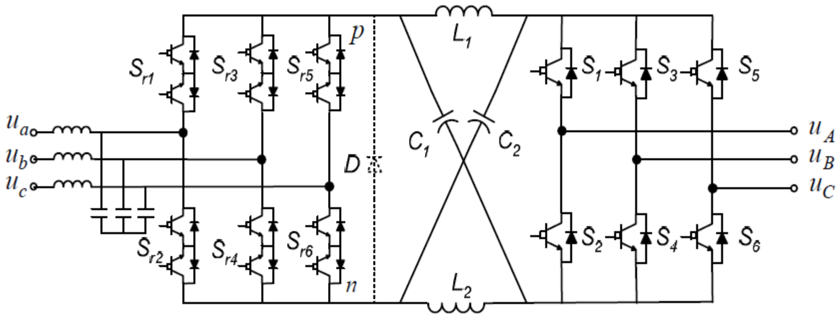

Figure 2.17: Indirect ZS MC (Z. Shao et al., 2009)

Three modes of operation exist for the proposed topology; these modes of operation are shown by Figure 2.18a to Figure 2.18c. In the first mode, the topology functions as a current converter which is also known as the inversion mode. In the second mode of operation, the second part of the topology after the impedance network is in a short circuit hence the output voltage of the network in that mode is zero.

Finally in the third mode of operation, the topology functions in any of the possible 7 shoot through modes and the source or input becomes a short circuited source.

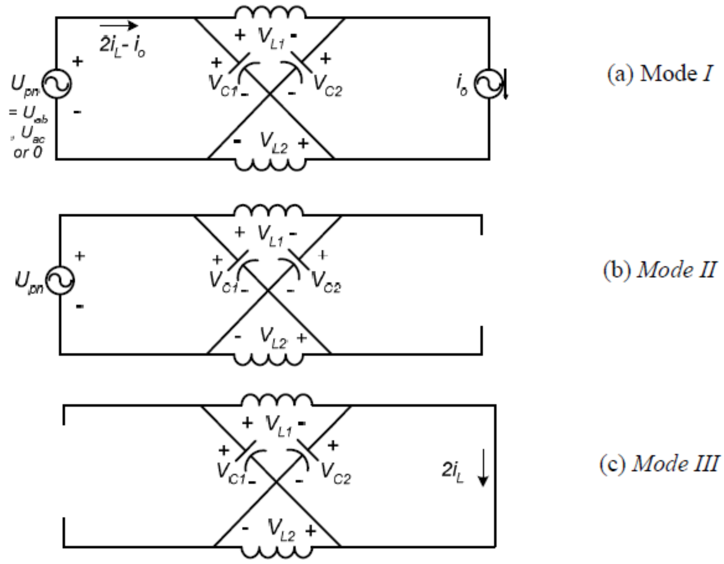

Figure 2.18: Modes of operation (Z. Shao et al., 2009)

2.3 Impedance Based AC-AC Converters

This section of my research will review various impedance based ac-ac converter topologies but will not consider topologies having MC structures. The impedance network proposed has received a lot attention over past decades because it has resolved the main drawbacks associated with voltage source and current source converters. The first proposed impedance based network is the conventional two capacitors and two inductors connected in an X form and placed between the voltage or current input and the main converter structure. The next topology was the quasi network which was introduced to resolve the limitation of the ZS network, several topologies have been introduced after the first two topologies basically to increase the boosting factor and also reduce the component count and voltage stresses on the switches.

A single phase ac-ac ZS topology is proposed in (X. Peng Fang et al., 2005). However this topology uses only two switches having bidirectional functionality. The switches are derived from the diode bridge topology. Both voltage and current sources can be used to feed the converter. By controlling the duty ratio of the proposed topology, solid state transformers are derived. The proposed topology has several advantages when compared to the conventional PWM topologies. Some these advantages are buck-boost capabilities, phase angle variations, reduced in-rush current, better reliability and minimum harmonic content.

Figure 2.19a and Figure 2.19b shows the two structures of the proposed topology; which are voltage source structure and current source structure.

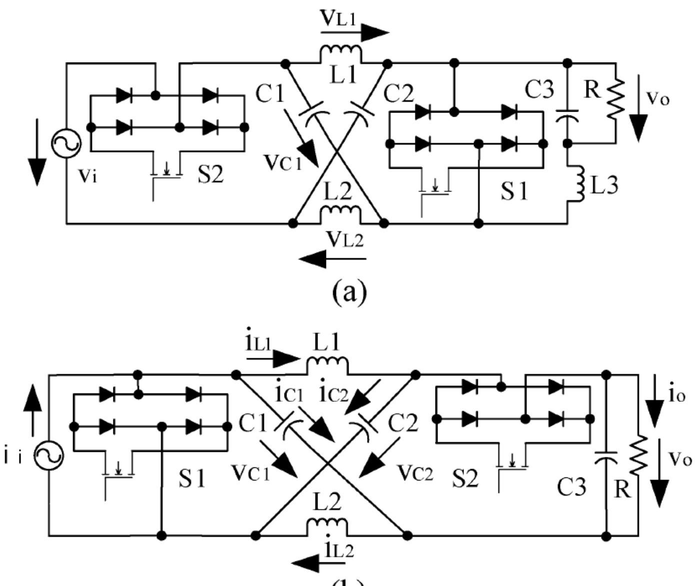

Figure 2.19: Single ac-ac ZS MC (X. Peng Fang et al., 2005)

There are two modes of operation of the proposed inverter, these modes of operation are common with all impedance based topologies. These are the shoot through and non-shoot through modes. Due to the symmetric nature of the passive components in the impedance network, the following equations are valid:

$$i_L = i_{L1} = i_{L2} \tag{2.3}$$

$$i_C = i_{C1} = i_{C2} \tag{2.4}$$

$$V_C = V_{C1} = V_{C2} \tag{2.5}$$

$$\begin{cases} V_o = V_o \sin(\omega t + \emptyset) \\ \quad V_i = V_i sin\ \omega t \end{cases} \tag{2.6}$$

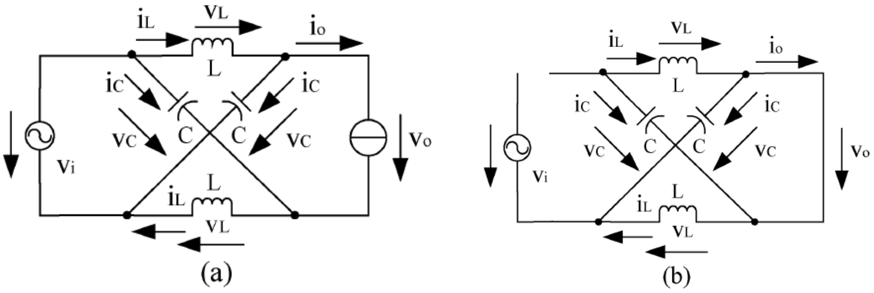

Figure 2.19: Modes of operation

A single phase quasi based ZS topology is presented by (M. K. Nguyen et al., 2010). This topology uses the quasi ZS network because it's an improvement of the conventional ZS structure. This topology combines the advantages of the proposed structure in plus the following advantages common ground between the input and output, higher efficiency and operates in the continuous conduction mode and also sinusoidal phase alignment of the voltage and current waveforms is possible with the proposed topology. All the above advantages are achieved for the proposed topology using the same number of components as the previous topology. Figure 2.20 shows the structure of the proposed network.

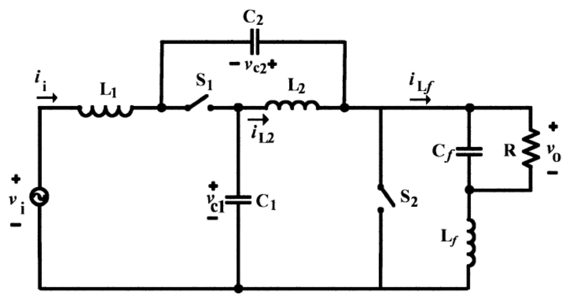

Figure 2.20: Quasi ZS converter

Two modes of operation are possible in the proposed topology; non shoot-through mode which is also known as the active mode because in this mode the converter functions a conventional converter without any special features, the second mode is known as the shoot through mode which allows for the charging of the passive components and the output voltage of the network is zero .Figure 2.21 represents the two modes of operation whiles the equations governing these modes of operations are given below. Equations (2.6) to (2.8) represents the first mode of operation whiles the second mode of operation is represented by (2.9) to (2.11).

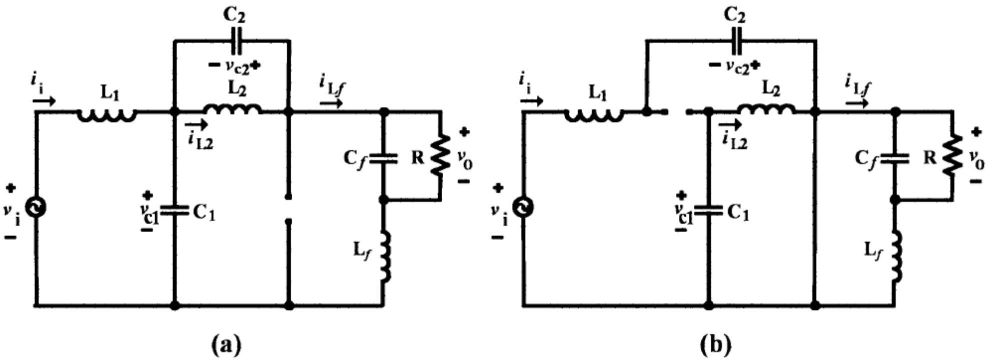

Figure 2.21: Modes of operation

$$v_i - v_{C1} = L_1 \frac{di_{L1}}{dt} \tag{2.6}$$

$$-v_{C2} = L_2 \frac{di_{L2}}{dt} \tag{2.7}$$

$$v_{C1} + v_{c2} - v_o = L_f \frac{di_{Lf}}{dt} \tag{2.8}$$

$$v_{C2} + v_i = L_1 \frac{di_{L1}}{dt} \tag{2.9}$$

$$v_{c1} = L_2 \frac{di_{L2}}{dt} \tag{2.10}$$

$$-v_o = L_f \frac{di_{Lf}}{dt} \tag{2.11}$$

A similar single phase quasi topology is given; this topology however has a safe commutation circuit. The two topologies are similar in structure that is they possess the same number of components, the difference lies in the safe commutation circuit proposed .The various modes of operation of the safe commutation circuit is given by Figure 2.22.

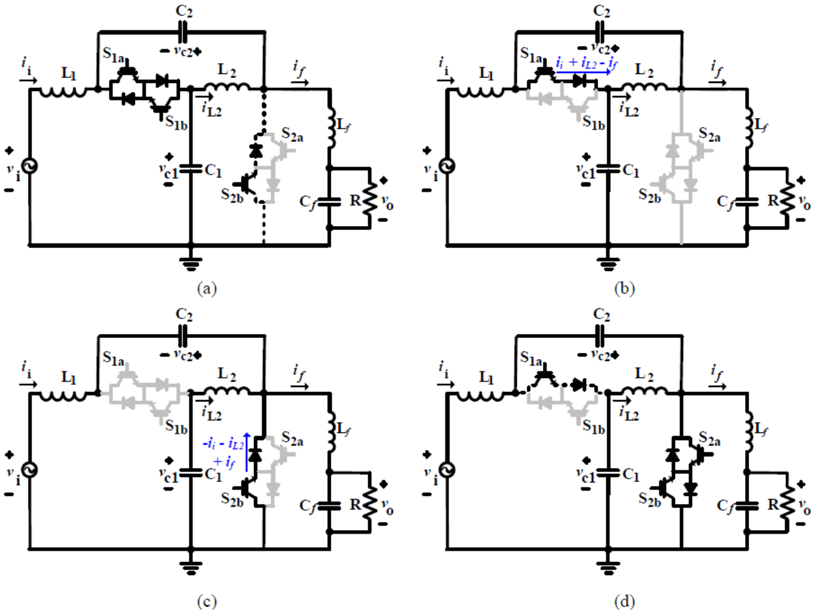

Figure 2.22: Boost state operation

A high frequency transformer (HFT) based quasi ac-ac converter is presented in (H. F. Ahmed et al., 2016). This topology retains all the advantages of the quasi network plus the network isolation using the HFT system. The HFT overcomes the demerits of the conventional line transformers such huge cost, maximum losses, large size and volume, inrush current high saturation and reduced efficiency.

The circuit of the proposed topology is given by Figure 2.23. The component count in this topology is however high when compared to conventional quasi topologies. The switch count increases by one, hence there are 3 switches, one HTF, 5 passive components and a filter. The similarity of the proposed topology and other conventional quasi is the primary side of this topology; they have the same structure. The modes of operation of this network is also two; sate 1 which occurs when switches S_3 and S_2 are closed during the time period DT and state 2 occurs when switch S_1 is closed during the time period T(1-D). The equivalent circuit for the two states are represented by Figure 2.24 and Figure 2.25 respectively.

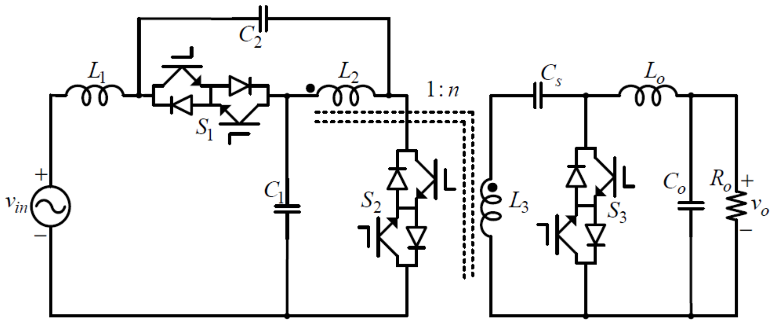

Figure 2.23: HFT quasi converter.

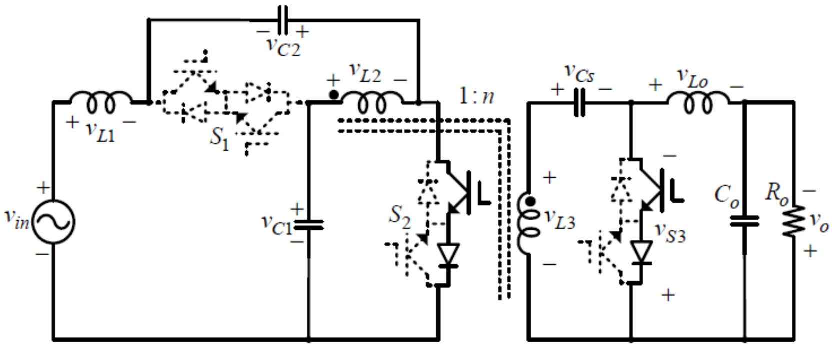

Figure 2.24: DT operation

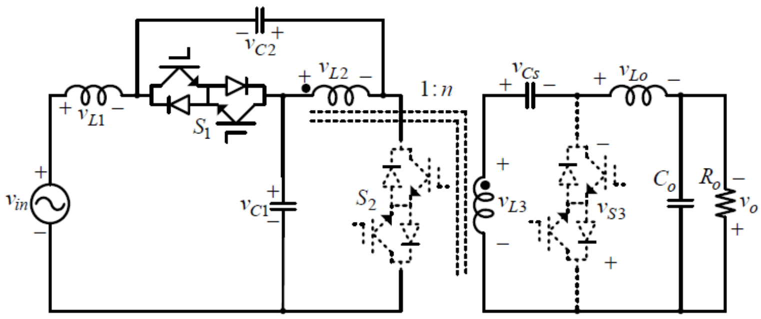

Figure 2.25: (1-D)T operation

The following equations are developed during state 1{(DT)} operation:

$$\begin{cases} v_{in} + v_{C2} = v_{L1} \\ v_{C1} = v_{L2} = v_{L3} \\ v_o = v_{Lo} \\ v_{CS} = v_{L3} \end{cases} \tag{2.12}$$

The following equations are developed during state 2 {T (1-D)} operation:

$$\begin{cases} v_o - v_{S3} = v_{L0} \\ v_{in} - v_{C1} = v_{L1} \\ -v_{C2} = v_{L2} = v_{L3} \\ v_{CS} - v_{S3} = v_{L3} \end{cases} \tag{2.13}$$

The relationship between the input and output voltages is given by:

$$v_o = \frac{1-D}{1-2D} v_{in} \tag{2.14}$$

A transformer based ZS ac-ac converter is proposed in (Z. Aleem et al., 2016). This topology has embedded a transformer in the impedance structure hence the turn’s ratio of the proposed converter is achieved by varying the turn’s ratio of the transformer. Two topologies of the proposed inverter are presented. The following are the unique characteristics of the proposed converter:

a. This topology retains all the merits of the conventional ac-ac ZS converter
b. Has wide buck-boost capabilities
c. Voltage gains is achieved by varying the turns ratio of the transformer
d. Mode of conduction is continuous (CCM)
e. Has a common ground between the input and output

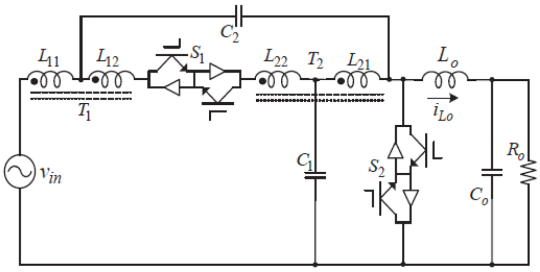

Figure 2.26: 1st Topology

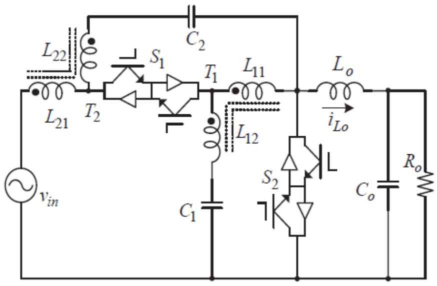

Figure 2.27: 2nd Topology

The relationship between the input and output voltages is given by:

$$v_o = \frac{(1-D)v_{in}}{1-(2+n_1+n_2)D} \tag{2.15}$$

a) Non-shoot through

b) Shoot through

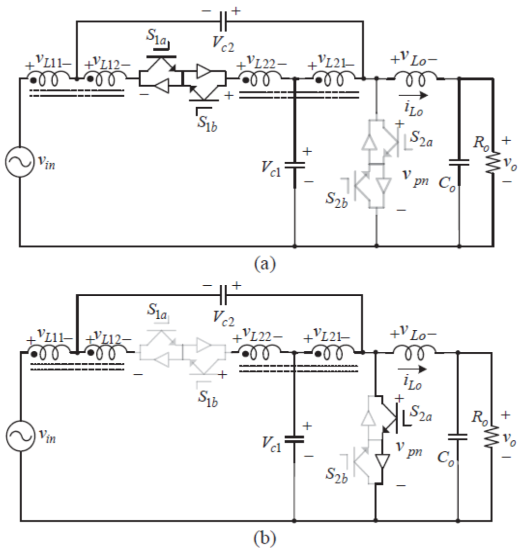

Figure 2.28: Mode of operation 1st topology

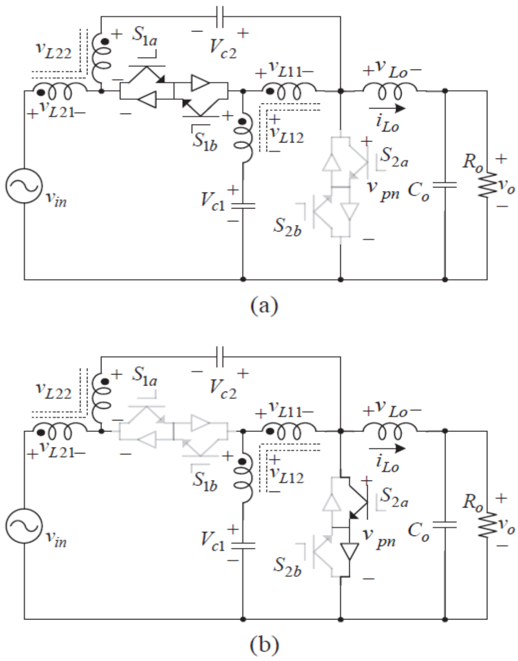

Figure 2.29: Mode of operation 1st topology

Several topologies of impedance based HFT converters have been presented over the years, the following diagrams are some example of the presented topologies (X. Fang et al.,2010).

a) Z-Source b) Quasi ZS c) Trans Z source d)Trans Quasi ZS e) I-Trans ZS f) Gamma ZS

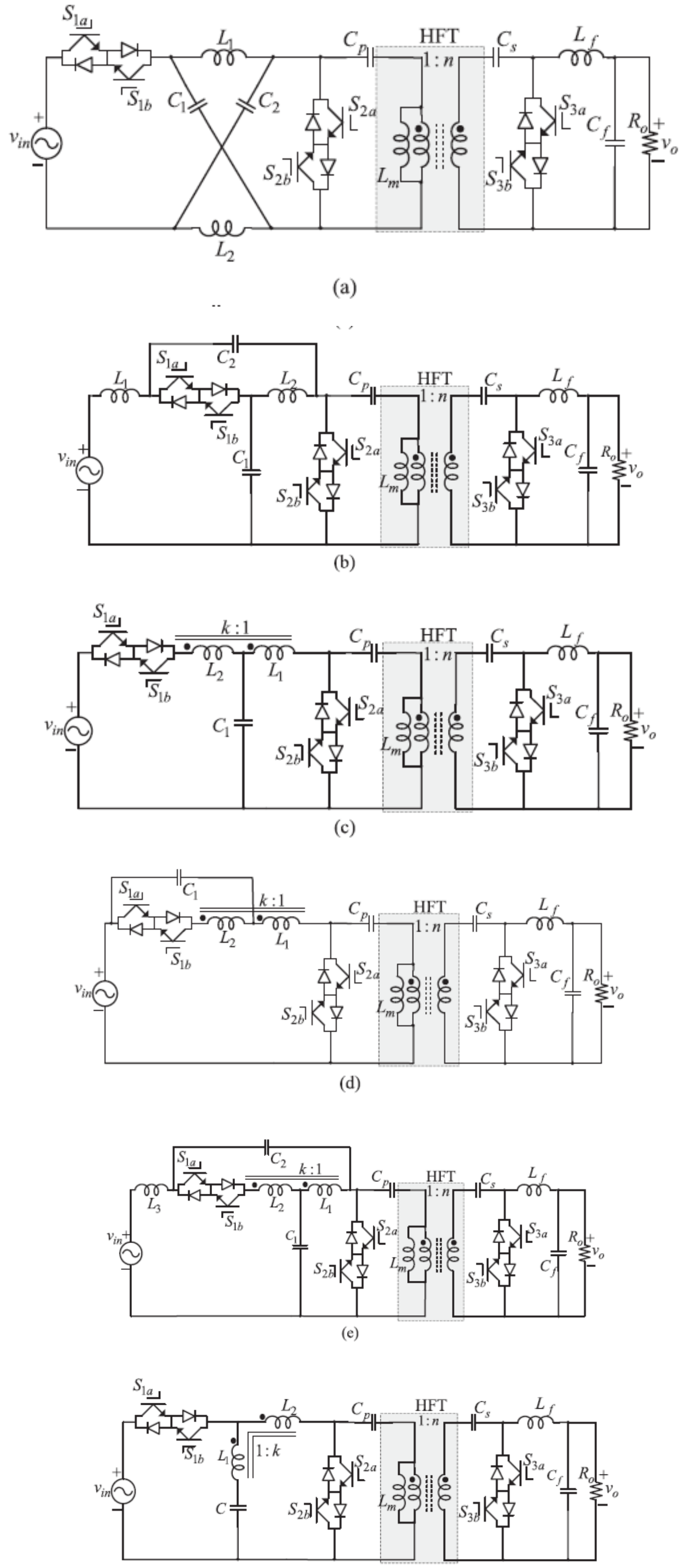

Figure 2.30: HFT topologies

A modified Z source ac-ac converter is presented by (M. R. Banaei et al., 2016). The proposed topology functions as a voltage booster and also a variable frequency provider. Also this topology provides higher efficiency and better circuit attributes when compared to the conventional ZS topology. Figure 26 shows the circuit of the presented topology. The impedance network has the same components as the conventional topology with unidirectional switch with respect to voltage.

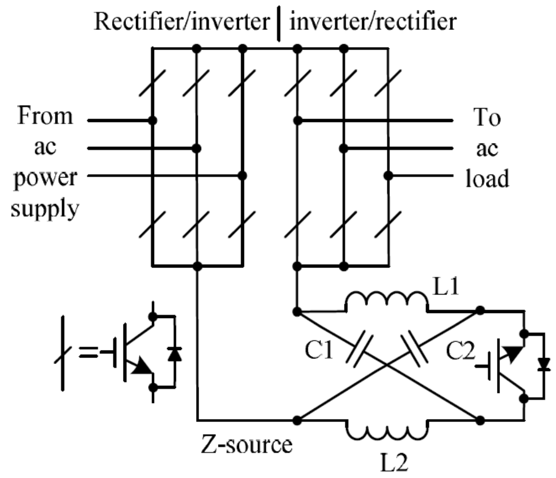

Figure 2.31: Modified ZS converter

The equivalent switch mode circuit is provided by Figure 2.32. There are two modes of operation of the converter. These are shoot through which is represented by Figure 2.33 and the non-shoot through is presented by Figure 2.34.

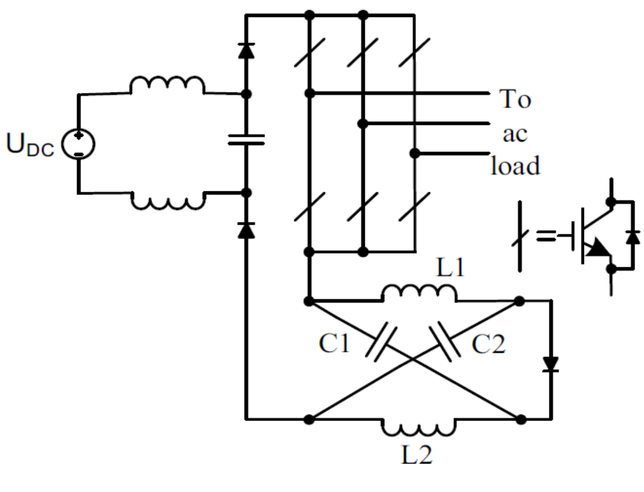

Figure 2.32: Equivalent circuit

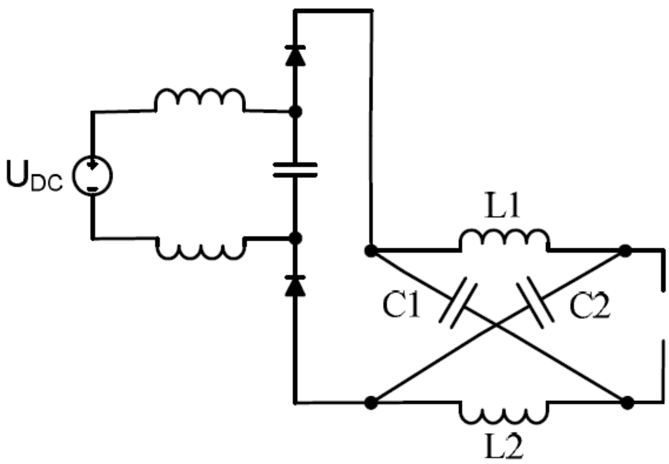

Figure 2.33: Shoot through

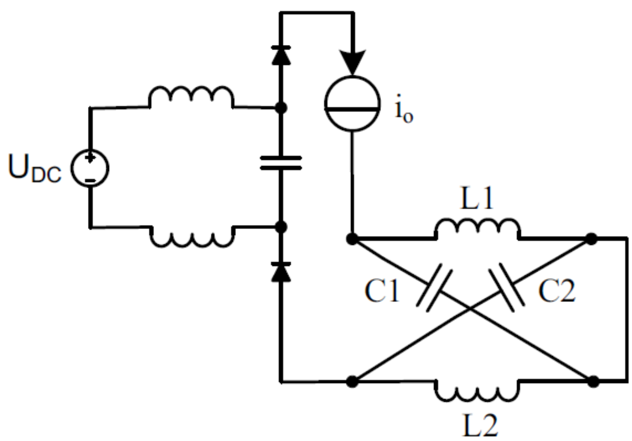

Figure 2.34: Non-shoot through

The capacitor voltage is given by:

$$V_c = V_o \frac{B-1}{2} \tag{2.16}$$

The impedance network output voltage or the inverter input voltage is given by:

$$V_i = V_o \frac{B+1}{2} \tag{2.17}$$

The inverter output voltage is given by:

$$V_{ac} = \frac{V_o}{2} MB \tag{2.18}$$

A single phase gamma ZS converter is presented by (Emerson et al., 2018). This topology is also an ac-ac converter having two bidirectional switches and gamma based impedance components. The proposed topology has high boosting capabilities than many other impedance based converters.

Figure 2.35 shows the circuit of the proposed gamma based ZS converter. The coupled inductor or transformer turns ratio is the major component which provides higher boosting capabilities varying the turns ratio; small turns ratio provides the much higher boosting feature required.

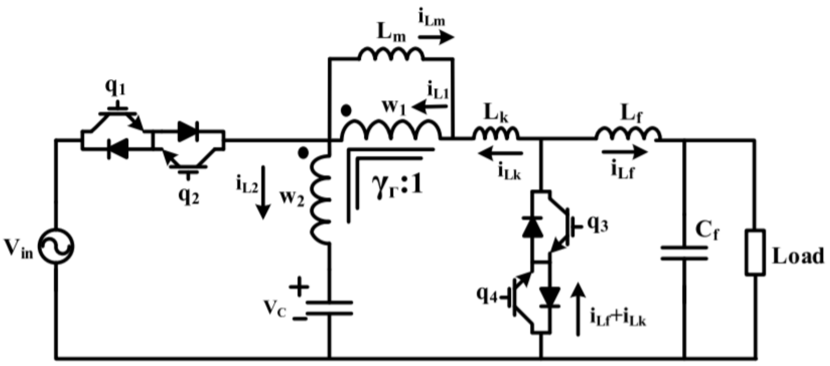

Figure 2.35: Gamma ZS converter.

Figure 2.36 and Figure 2.37 shows the two modes of converter operations.

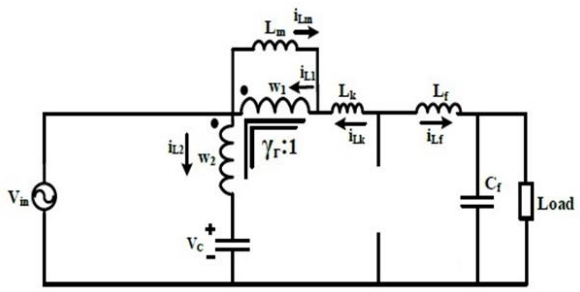

Figure 2.36: Non-shoot through

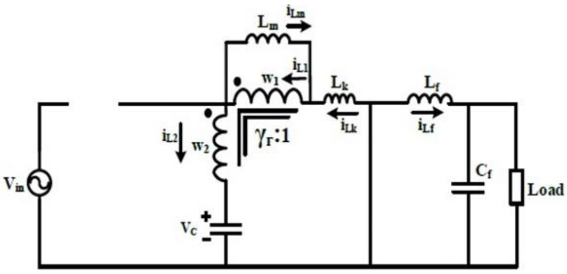

Figure 2.37: Shoot through

Analysis of the modes of operation will yield the boost factor B is given by:

$$B = \frac{1-D}{1-D\left(1+\frac{1}{\gamma_\Gamma-1}\right)} \tag{2.19}$$

2.4 Indirect MC AC-AC Topologies

Matrix converters are generally grouped into direct and indirect topologies. This section of our research will focus on indirect MC topologies. Indirect MC are also referred to as double stage converters because the power conversion process goes through more than one stage of power conversion, mostly the ac source is converted into dc source and then back to ac output. A few of these topologies have been reviewed below.

In (A. Hakemi et al., 2017) an indirect MC having the features of power factor corrections and also high frequency isolation is presented. This topology provides the high isolation via a high frequency transformer. The converter circuit of the presented topology is based on dual DAB (double active bridge) having 3 cell state switching. Some advantages of the proposed topology are high power factor, minimum harmonic content, bidirectional current flow and quick dynamic response. Also conduction and switching losses are reduced because of the utilization of the 3 cell state switching, the filter component size is also minimized hence cost saving. Figure 2.38 show the circuit of the proposed topology.

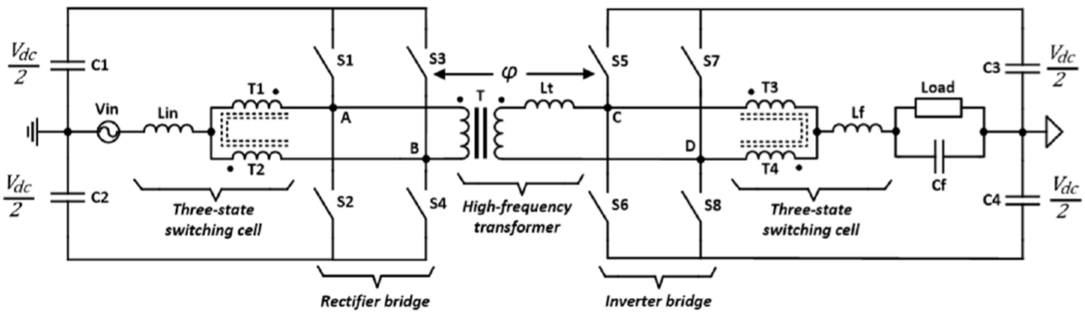

Figure 2.38: Indirect MC

The input impedance which is composed of inductor and capacitor is given by:

$$L_R = V_{DC,R}\frac{1}{16(\Delta I_{L,r}.2f_{sw,\_r})} \qquad (2.20)$$

$$C_{CD,r} = P_{o,r}\,\Delta_{t,r}\frac{1}{\left[V_{DC,r}\left(\frac{1}{2}\right)\right]^2+(-\Delta V_{DC,r}+V_{DCmax})^2} \qquad (2.21)$$

Various impedance based indirect MC topologies have been reviewed in (Zhang et al., 2009) and novel topology also presented. The reviewed topology in (Tang et al., 2013) uses the conventional ZS structure placed between the rectifier and inversion stages of the converter. Whiles the topology presented in (L Wang et al., 2017) place the quasi impedance structure between the dc source the rectifier stage of the converter; this topology is known as continuous quasi ZS indirect MC. The presented topology in (Zhang et al., 2009) combines the two topologies to achieve a continuous and series impedance based indirect MC. Figure 2.39 shows the circuit of the presented topology. The main merits of the presented topology is high voltage gain which is a major disadvantage of the conventional MC. Figure 2.40a and Figure2.40b shows the two states of operation; non shoot through and shoot through modes respectively.

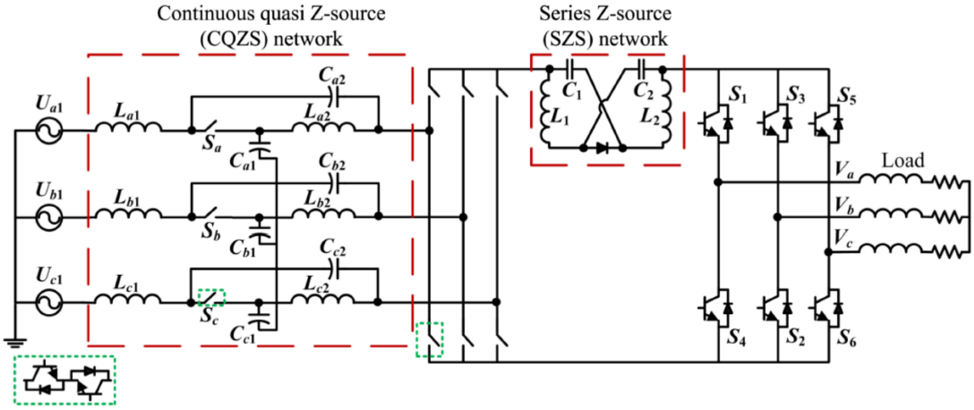

Figure 2.39: High gain MC

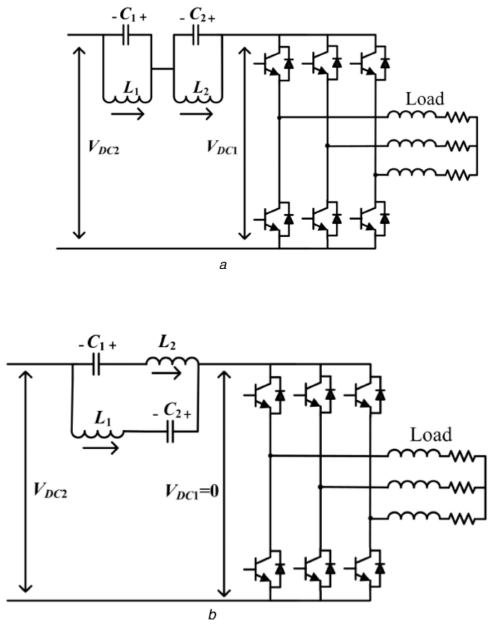

Figure 2.40: Mode of operation

Indirect MC have two major problems which affects them during specific applications, for example in the case of wind power applications, reactive power generation is mostly limited and also balancing of the neutral point voltage is a major problem. To resolve the above problems, third harmonic injection based indirect MC is proposed in (Tiago et al., 2015). This converter is a 3 level converter which combines the advantages of the third harmonic injection topology with the T-type converter. Figure 2.41 shows the circuit of the proposed topology. The circuit can be divided into three main parts, the rectifier part which is a current source rectifier, the VSI stage which composed of the T-type converter and in between them is the injection converter topology.

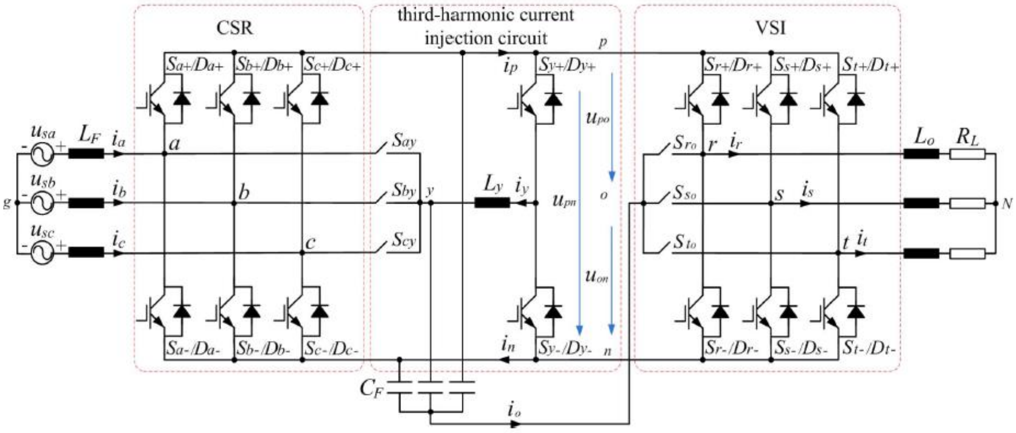

Figure 2.41: T-Type indirect MC (Tiago et al., 2015)

A silicon carbide switch based indirect MC topology is presented by (S Raju et al.,2013). This topology increases the overall efficiency of the converter by 97.7%. A delta switch system is utilized between the two stages of the converter. The converter structure is based on the conventional topology. Figure 2.42 shows the circuit of the presented converter; a) converter structure, b) SiC bidirectional switch c) unidirectional SiC switch.

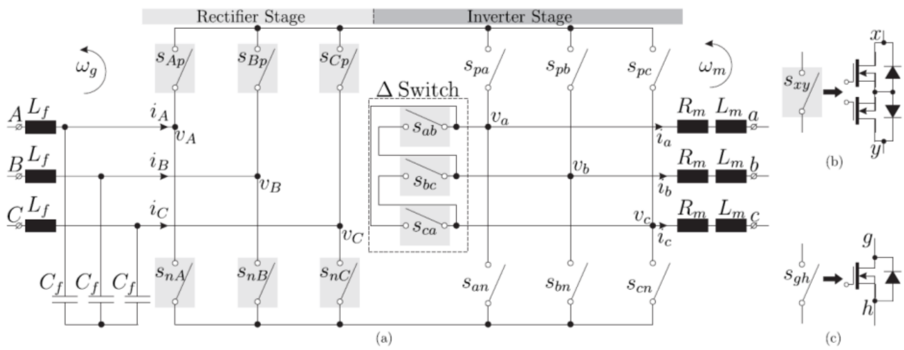

Figure 2.42: SiC based indirect MC (S Raju et al.,2013)

A hybrid MC topology is presented by the authors . This topology provides the following parameters at the converter output: phase input, line voltage and half of the phase voltages, a feature which is not present in the conventional MC. This features are possible due to the inclusion of more switches and clamping capacitors. The THD in this converter is minimized, the voltage stress is also minimum when compared to the traditional matrix converter. The presented topology is shown by Figure 2.43 and it's suitable for three phase power applications.

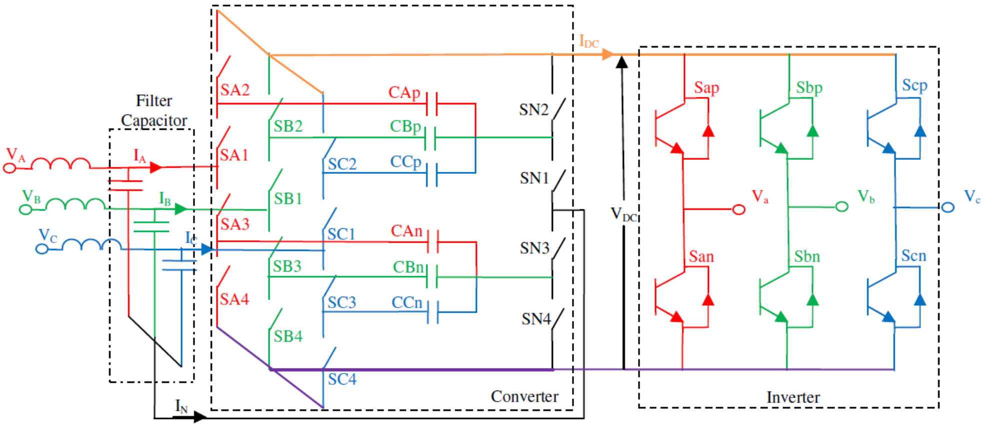

Figure 2.43: Hybrid indirect MC

A novel quasi based indirect MC topology is presented in (A Shahani et al., 2012). This topology combines the advantages of the impedance network and matrix converters thereby overcoming the major limitation of the matrix converter by providing high voltage boosting and buck-boost functionality. Figure 2.44 shows the circuit of the presented topology and also the boosting factor equation and the relationship between the boosting factor and gain is given by:

$$\begin{cases} B = \frac{1}{1-2D} \\ B = Gm \end{cases} \tag{2.22}$$

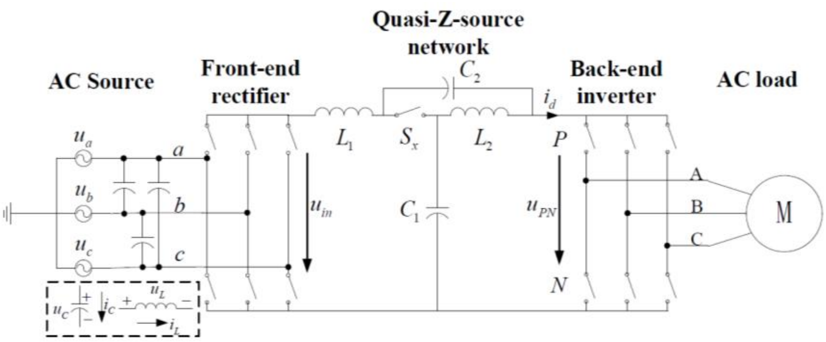

Figure 2.44: Quasi ZS indirect MC

A high frequency based single stage indirect MC topology is presented in (G. T. Chiang et al., 2011). This topology offers several advantages and is mostly suitable for renewable energy applications. Some merits of the proposed topology are high power density due to HFT, high reliability, PFC, high efficiency. Figure 2.45 shows the proposed topology.

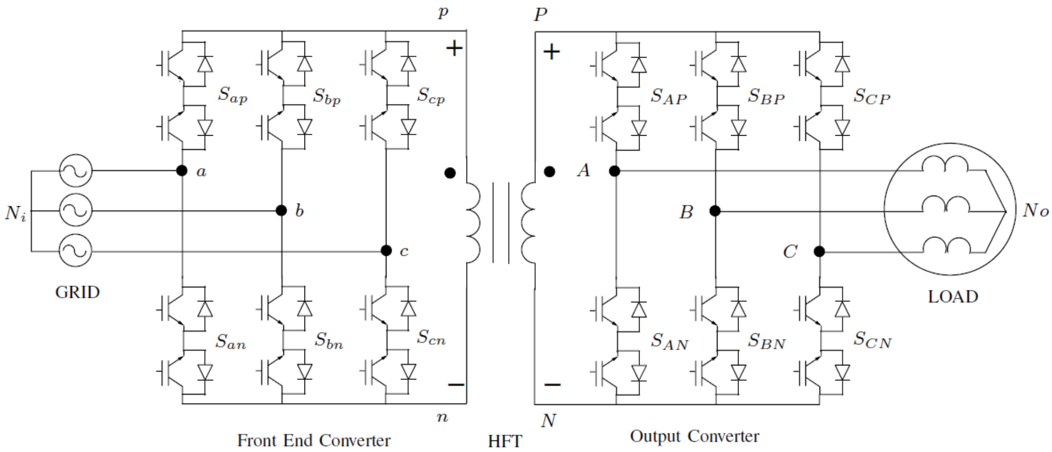

Figure 2.45: HFT based indirect MC

An indirect MC with dc boosting converter imbedded in between the first and second converter is presented by (Anand et al., 2018). The presented topology is applied in induction motor control. Also the voltage transfer ratio of the proposed topology is increased from 86.6% the conventional standard to a new value of 97%. Battery ripples caused by neutral point voltage fluctuations is minimized by use of feed forward control technique. Figure 2.46 is the circuit of the proposed topology.

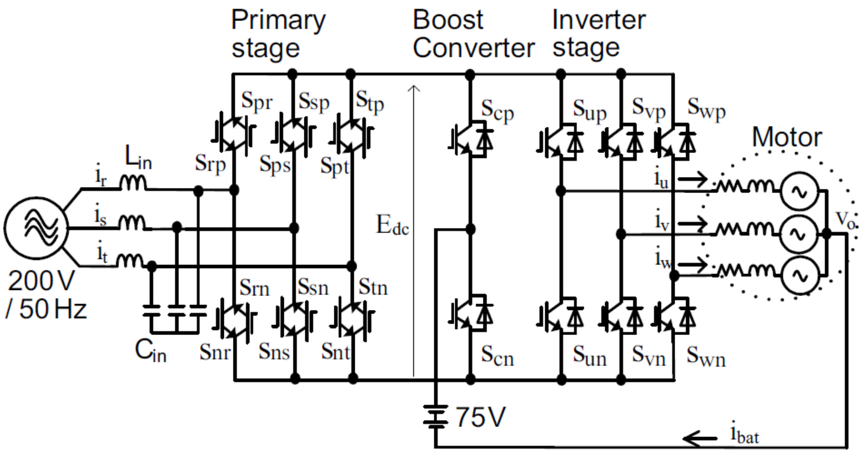

Figure 2.46: High boost indirect MC (Anand et al., 2018)

2.5 Direct AC-AC Topologies

An efficient ac-ac converter for induction cooking is presented by (S. A. Deraz et al., 2019). Induction cooking has replaced the conventional cooking technologies because of its efficiency hence any proposed converter should have very high efficiency and also high boosting capabilities. The presented topology provides high frequency and high boosting abilities with reduced component number and also minimum voltage stress on components. The proposed topology is shown by Figure 2.47 and the two modes of operation are also shown by Figure 2.48 and Figure 2.49 respectively. The circuit is composed of two diodes, one boosting capacitor, two switches, one inductor and two capacitors and the induction heating element. The boosting factor is

$$B = \frac{1}{1-D} \quad (2.23)$$

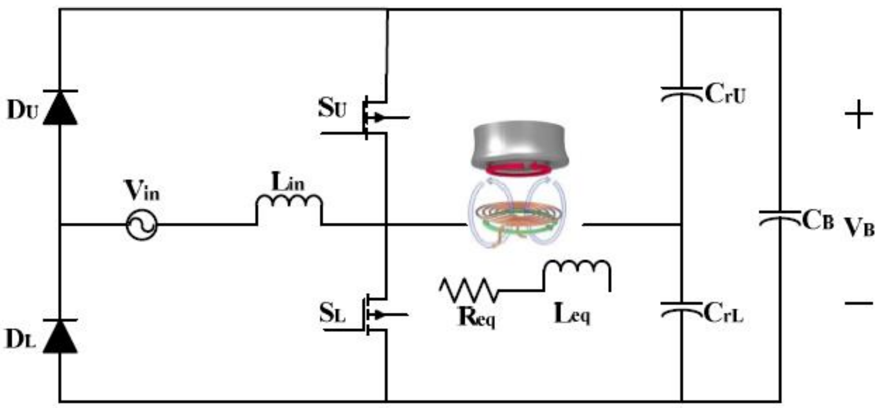

Figure 2.47: High frequency converter

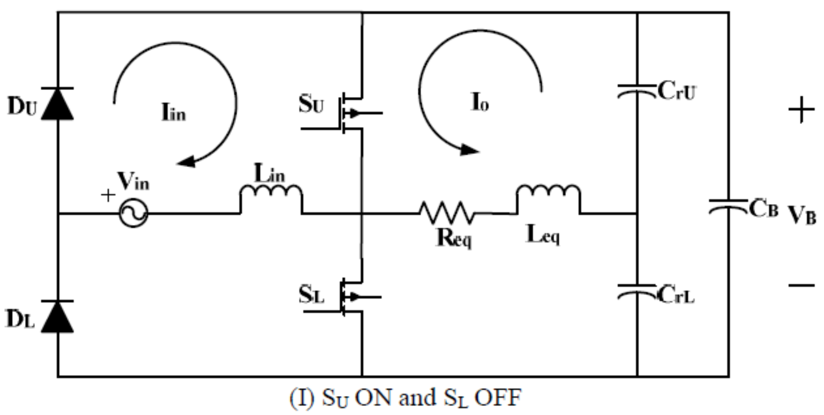

Figure 2.48: First mode of operation

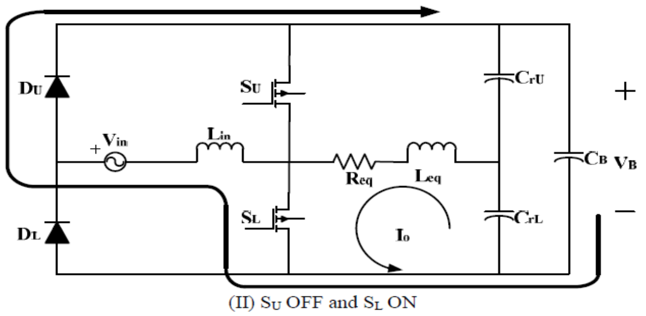

Figure 2.49: Second mode of operation

Investigation of a three phase ac-ac converter with minimum component count is analyzed in (C. Liu et al., 2019). The goal of this research is to provide a converter having reduced component count such that the following advantages will be attained: simple structure, reliability, reduced converter cost, high efficiency and reduced converter losses. Two topologies of converter are presented; boost and buck topologies.

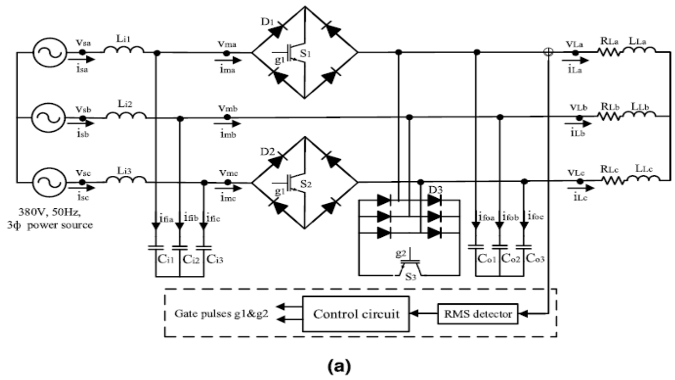

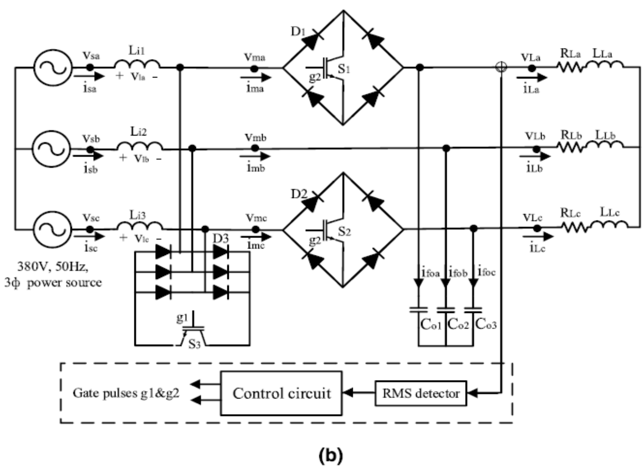

Figure 2.50: a) Buck topology b) Boost topology

A novel bipolar based on T-type converter is proposed in (A. Pareek et al., 2018). This topology combines two converters to achieve the desired converter and also apply PWM control technique. The input and output voltage are related by equation (2.24) where d1 and d2 are duty cycles.

$$V_o = (d_1 - d_2)V_{in} \tag{2.24}$$

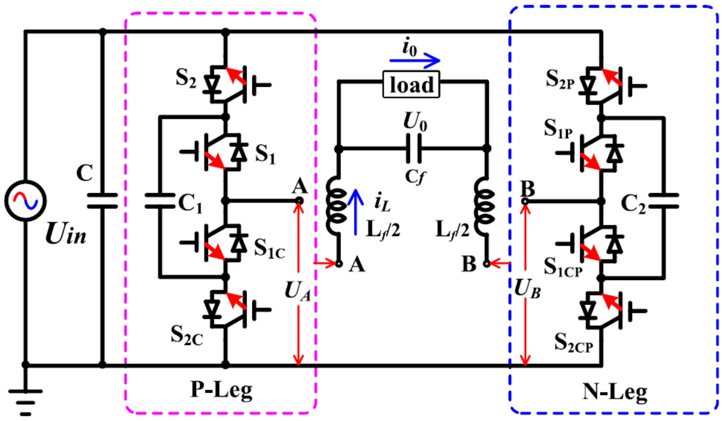

Figure 2.51: Bipolar based T-type converter (A. Pareek et al., 2018)

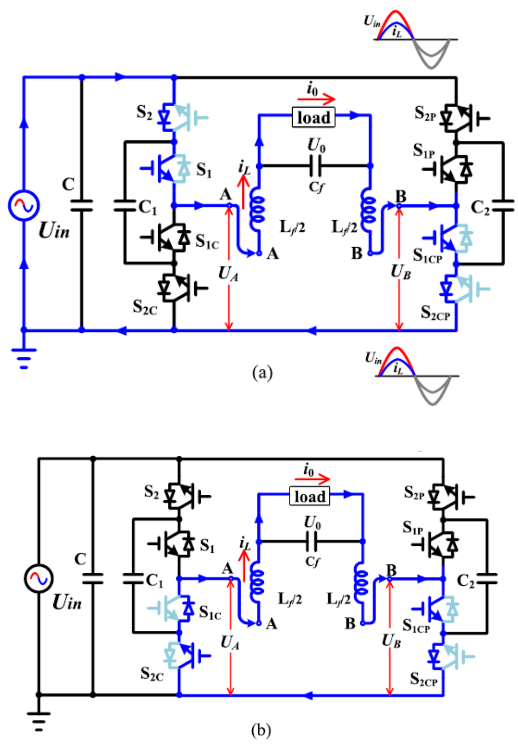

Figure 2.52: BTC modes of operation (A. Pareek et al., 2018)

An inverting and non-inverting based ac-ac converter is presented in (Sanghun et al.,2018). This topology is composed of four bidirectional switches for current flow in both directions. Using PWM method provides all the advantages of this unique control method. Buck-boost functionality is provided by this converter. Figure 2.53 shows the proposed topology. The modes of operation is that, switches S1 and S3 are switched on in the first mode whiles the remaining switches are turned off, in the second mode switches S2 and S4 are turned on and the remaining turned off.

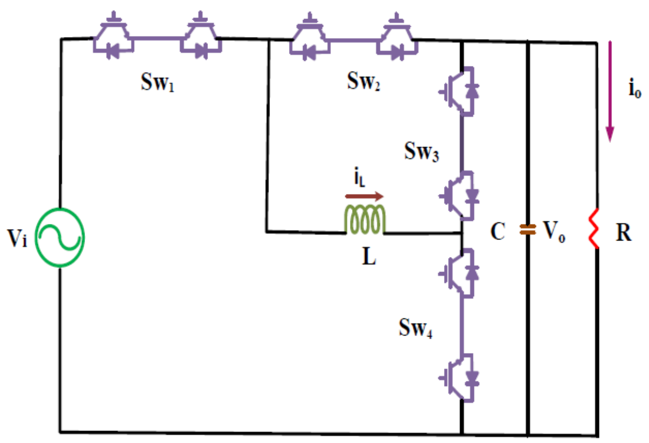

Figure 2.53: Proposed converter (Sanghun et al.,2018)

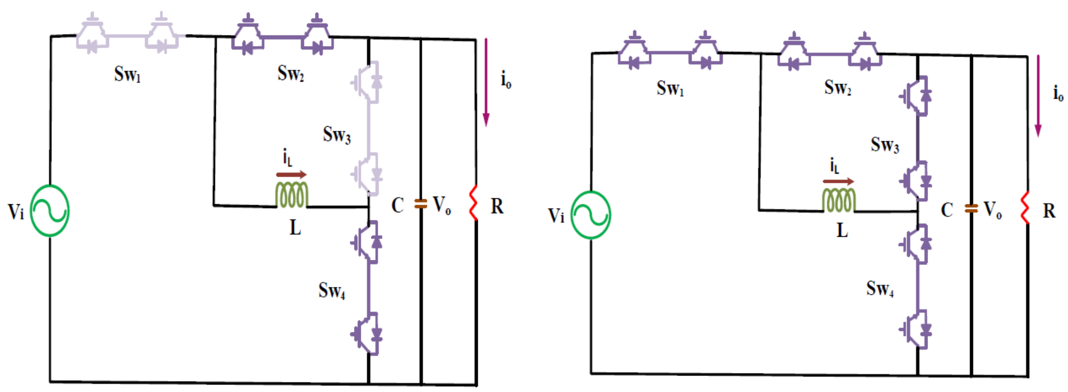

Figure 2.54: Modes of operation (Sanghun et al.,2018)

A new cascaded ac-ac converter is proposed in (Suvendu et al., 2017). The proposed topology does not have problems about the following factors: commutation difficulties, shoot through problems, but offers higher efficiency when compared to other conventional cascaded topologies. One other major limitation of this topology is the increased number of inductors which are utilized. Figure 2.55 shows the circuit of the proposed topology.

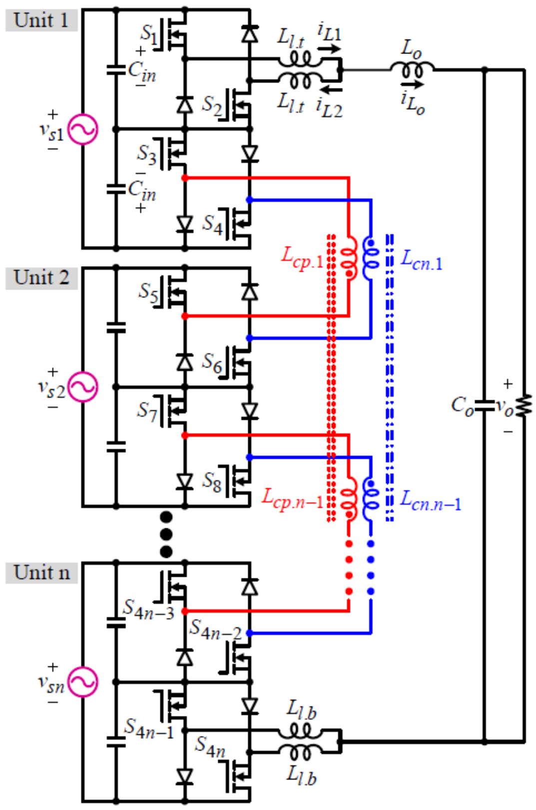

Figure 2.55: Cascaded topology (Suvendu et al., 2017)

The voltage gain relationship is given by:

$$\frac{V_o}{V_s} = nD \tag{2.25}$$

An inductive power transfer based converter is proposed . The conventional H Bridge structure using bidirectional switches coupled with a transformer connected to a voltage booster circuit constitutes the proposed topology. One major disadvantage of inductive power transfer is the high cost of the system and reduced efficiency, hence this research proposed the use of ac-ac converters to minimize the above mentioned limitations. Fig 2.56 shows the circuit of the proposed topology.

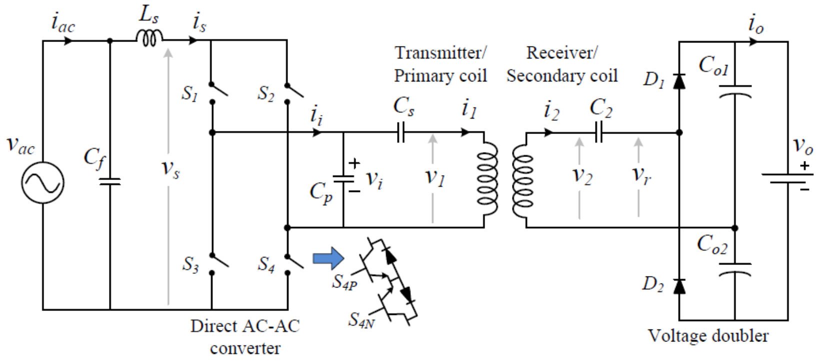

Figure 2.56: IPT based converter

The power transfer equation is given by:

$$P_{TC_{RC}} = \frac{\pi}{\sqrt{2}} \omega M I_o I_1 \tag{2.26}$$

A review of the various center point clamped ac-ac converter is investigated . Three types of topologies are review having the following features: buck, boost and buck-boost. All these topologies are ac-ac converters therefore they use bidirectional switches have minimum voltage stress on the components. The first topology which buck CPNC is shown by Figure 2.57, the second topology which is a boost converter is shown by Figure 2.58 and finally the buck-boost topology is given by Figure 2.59.

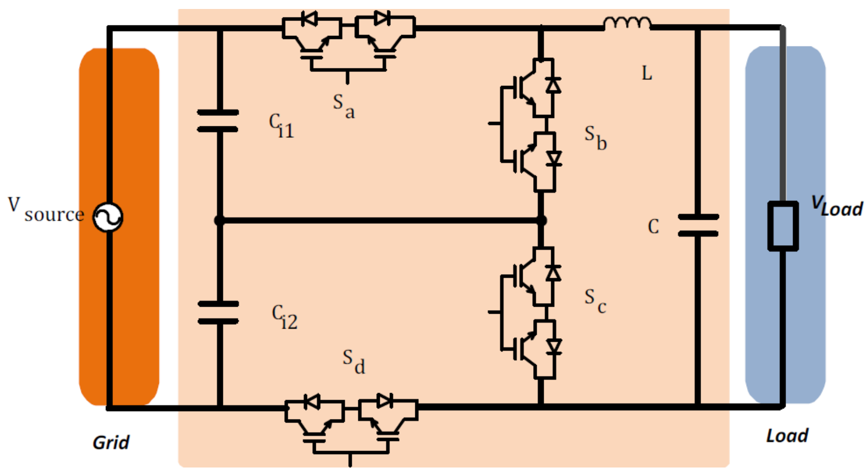

Figure 2.57: Buck CPC

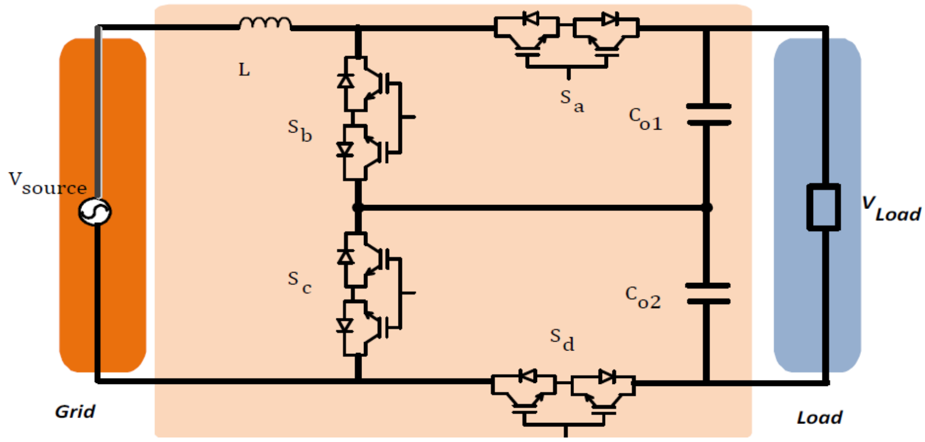

Figure 2.58: Boost CPC

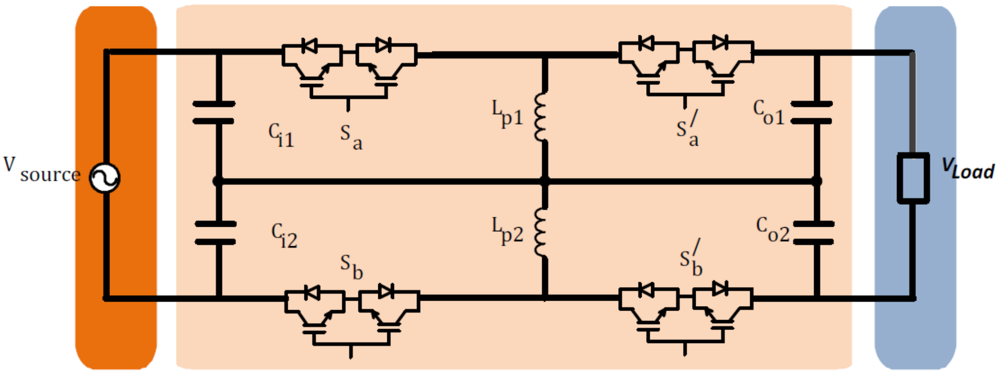

Figure 2.59: Buck-Boost CPC

2.6 Conclusion

Literature review of selected ac-ac converters were investigated in this chapter of this thesis. The review was conducted with respect to the various topologies, the differences in their structures, the type of control technique applied and their applications in industry or references for academic applications. Also investigations of their suitability for the various phases of power systems were analyzed. The first selected topology is the matrix converter followed by the impedance based topologies which are popularly called ZS converters, finally selected indirect MC topologies were also reviewed. This investigationshas exposed me to several drawbacks of the selected topologies hence further research of some of topologies will considered during my further studies.

CHAPTER THREE
RESONANT CONVERTERS AND COMMUTATION CIRCUIT

3.1 Introduction

All converters have semiconductor switches which are operated to derive the desired power conditioning. These power switches are turned on and off for these processes to be achieved. In the switching period of the converter, these power switches are subjected to maximum power losses due switching and also high voltage stress; these factors experiences a linear increase depending on the value of the switching frequency, finally the switches are also subjected EMI interferences . To best explain the switching experiences of power switches, consider the diagrams below.

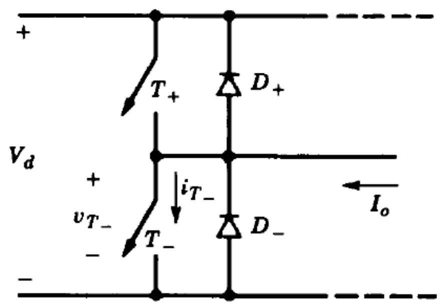

Figure 3.1: One leg of an inverter

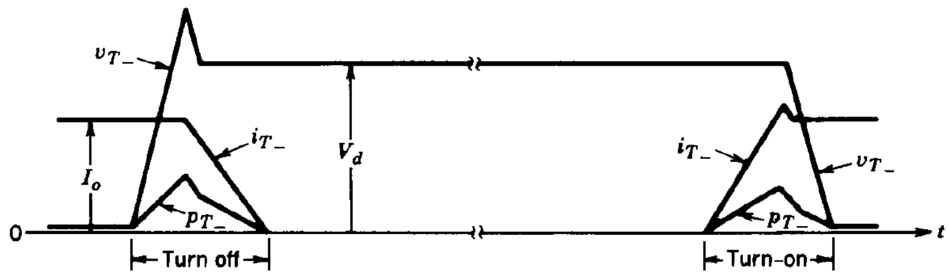

Figure 3.2: Turn on and turn off mode of the inverter leg.

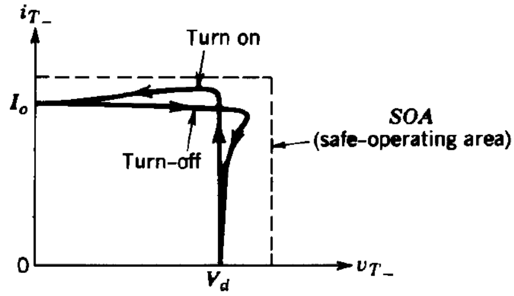

Figure 3.3: Turn on curve.

Figure 3.1 shows the graph of one leg of an inverter and the load current is shown by Io, the current direction is assumed to be in both direction because of the load type; inductance load. Figure 3.2 shows the graph on switching for one of the power switches of Figure 3.1 and the safe operating area of the above switching period is shown in Figure 3.3.

3.2 Zero Voltage and Zero Current Switching

High switching frequencies provides numerous advantages in power electronic system applications; the quality of output voltage of converters are highly improved, transformer size and weight are drastically reduced and also filter component sizes are minimized. However the use of high switching frequency introduces some limitation such as high switching losses, high component stress and finally EMI interferences .Therefore it's advisable to introduce solution to the above limitations. Some solutions to high switching losses is the introduction of snubbercircuit which are composed of passive components and diodes, connected in series or parallel to the circuit. Nevertheless the switching losses are not reduced but rather transferred to the snubber circuit. Figure 3.4a shows a snubber circuit based converter and Figure 3.4b shows the switching diagram.

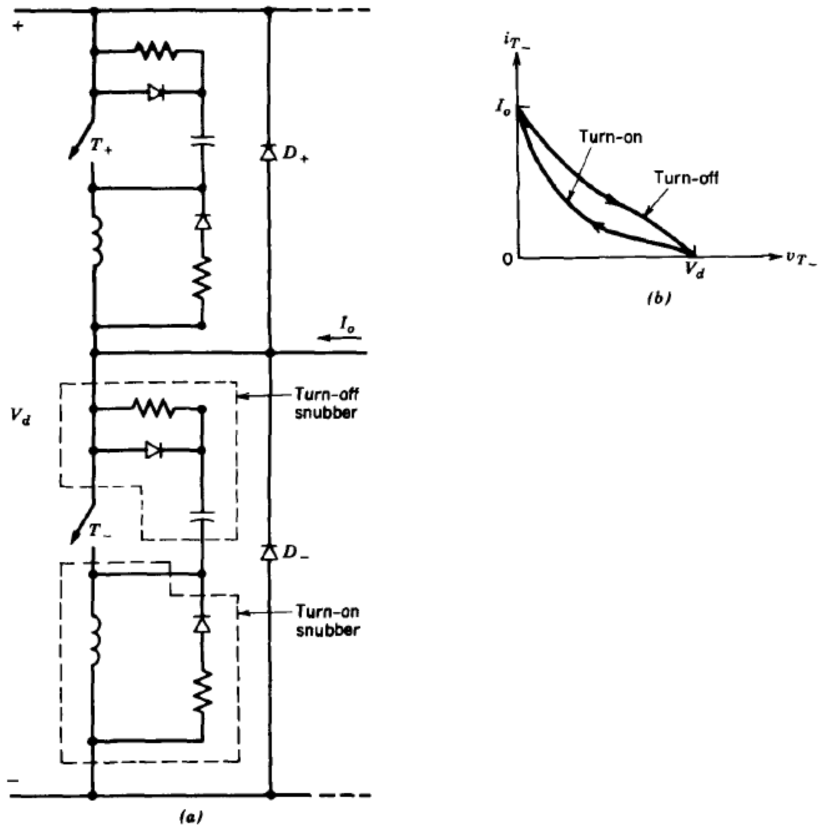

Figure 3.4: Snubber circuit.

A better solution is turn-on or turn-off the power switch when either the switch voltage or switch current has a magnitude of zero (0). This will automatically give zero switching power losses. It’s preferable to have zero switch voltage and zero switch current. Figure 3.5 shows the desired zero voltage and zero current diagram.

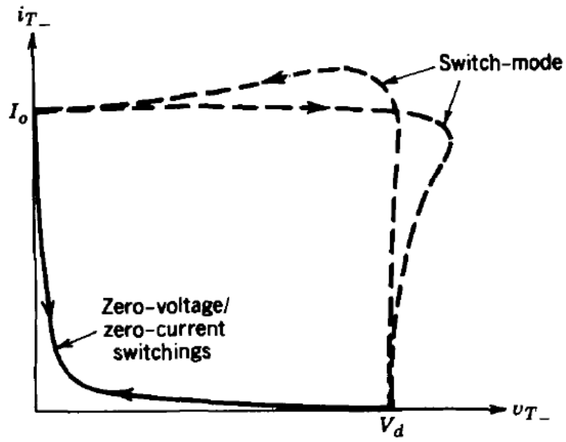

Figure 3.5: ZV-ZC switching

3.3 Resonant Converters (RC)

Resonant converter are amalgamation of converter topologies and appropriate switching or control techniques which results in ZV-ZC configurations. Resonant converter are generally put into four categories:

- Load resonant converters
- Resonant switch converters
- Resonant dc link converter
- High frequency resonant converters

The high frequency resonant converters are converters which have high frequency input and provides variable low frequency at the using ZV-ZC switching mechanism. In the resonant dc link converter the input voltage is made to wigwag via an inductor-capacitor resonance to achieve zero input voltage for a specific period hence ZV-ZC switching is obtained. In the switch topology, an LC is used to form the switch current and voltage in other to achieve the desired zero voltage and zero current switching. In the load resonant converter, an LC resonant tank is connected to the load so that zero voltage or zero current switching of the switches is permissible. The load RC are sub divided into the following categories:

- Voltage Source Series-RC
- Current Source Parallel-RC
- Class E and Subclass E RC

Voltage source series-RC is also further divided into three groups:

- Series-load RC
- Parallel-load RC
- Hybrid RC

3.4 Series-loaded RC (SL-RC) Topologies

Series-loaded RC is a type of resonant converter where the resonance is connected in series with the load or between the main converter and the rectifier circuit. The resonant tank is mostly of LC type although other structure like LLC exist. Figure 3.6a show a half bridge structure with a SL-RC whiles its equivalent circuit is given by Figure 3.6b.

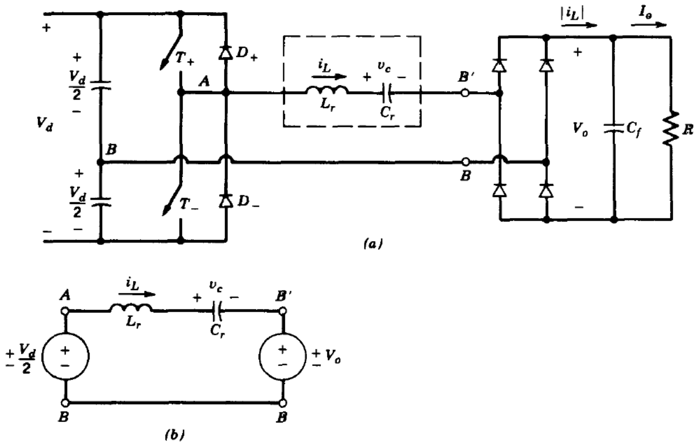

Figure 3.6: Half-bridge SL-RC

The applications of series-loaded RC can be found varied areas of power electronic system fields such as microgrid, UPS (uninterrupted power supplies), direct current distribution networks, and light emitting diode drivers . Applying SL-RC in these systems will yield higher efficiency, provide system isolation, reduced EMI interference (H. Wang et al.,2018). A soft switching SL-RC based dc-dc converter with high efficiency, high switching frequency and minimum EMI is presented in (H. Wang et al.,2018). The circuit of the presented topology is represented by Figure 3.7 and its equivalent structure is shown by Figure 3.8. The structure is composed of the conventional H-Bridge which feds the resonant tank made up of two inductors (L/2) and one capacitor (C_r) which is connected to a transformer plus a rectifier circuit. The transformer is composed of two equal turns on both the primary and secondary windings. The h-Bridge is fed from a constant current source; a typical feature of SL-RC topologies.

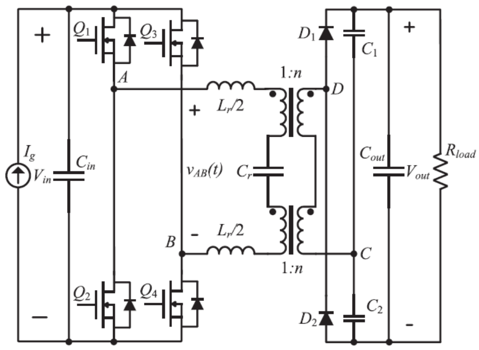

Figure 3.7: SL-RC equivalent circuit(H. Wang et al.,2018)

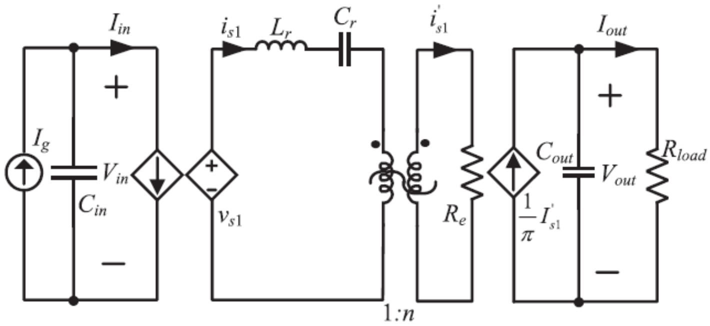

Figure 3.8: equivalent circuit of SL-RC (H. Wang et al.,2018)

Mathematical expression of the output current I_o, input voltage V_i and the output power P_o with respect the resonant tank and harmonized switching frequency is given below. Let Q be resonant tank and F_{SW} be the switching frequency.

$$\begin{cases} P_o = (1 + Q^2 \left[F - \frac{1}{F}\right]^2) \frac{I_g^2 R_{load}}{4n^2 \sin^2(\frac{\alpha}{2})} \\ V_i = (1 + Q^2 \left[F - \frac{1}{F}\right]^2) \frac{I_g R_{load}}{4n^2 \sin^2(\frac{\alpha}{2})} \\ I_o = \frac{I_g}{2n \sin^2(\frac{\alpha}{2})} \sqrt{(1 + Q^2 \left[F - \frac{1}{F}\right]^2)} \end{cases} \quad (3.1)$$

A dc link converter with series resonance tank having current limiting capabilities is presented in (E. da Silva et al., 1999), this topology utilizes PWM control technique. The structure of the presented topology is shown by Figure 3.9 and its equivalent circuit is given by Figure 3.10. The six stages of operation is represented by the equivalent circuits of Figure 3.11. The circuit of Figure 3.9 is composed of both input and output filters which are made of *LC* structure. A stiff inductor L_d interconnects the rectifier circuit at the input section to the inverter at the output section.

The current limiting capabilities of the proposed converter is achieved by utilizing a saturable reactor having turns ratio represented by (3.2). The resonant tank is represented by capacitor Co and inductor Lo which is obtained after saturation of the reactor.

$$k = \frac{n_1}{n_2} \tag{3.2}$$

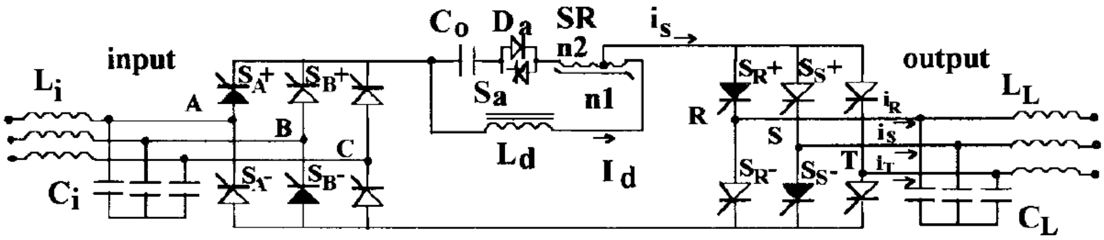

Figure 3.9: PWM SL-RC (E. da Silva et al., 1999)

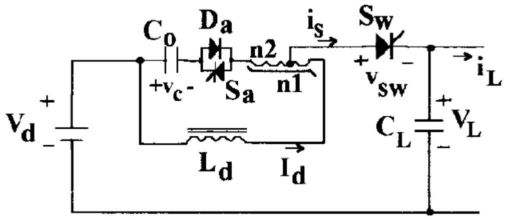

Figure 3.10: Equivalent circuit of PWM SL-RC (E. da Silva et al., 1999)

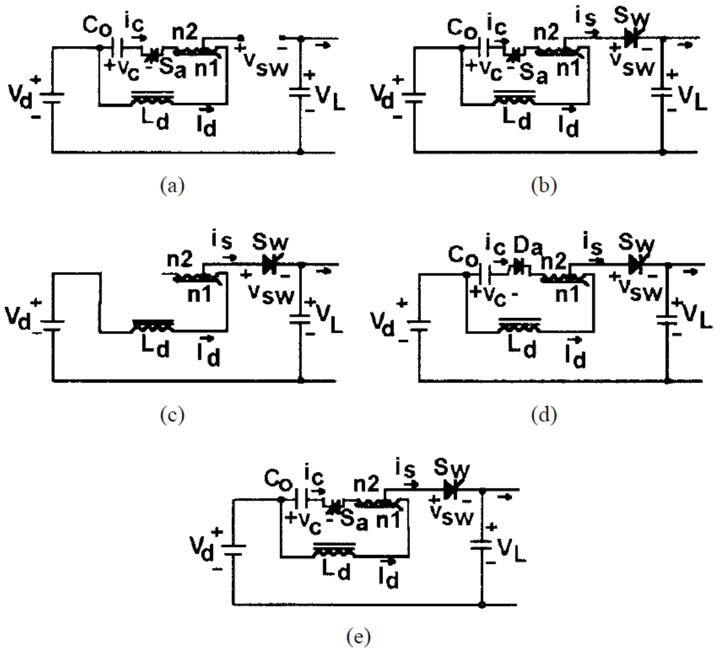

Figure 3.11: Various equivalent circuit of PWM SL-RC (E. da Silva et al., 1999)

A dual SL resonant converter based dc-dc topology is presented by (Amir et al., 2019). This dual topology offers higher efficiency and better power transfer capabilities when compared to the traditional single SL-RC structures .It's mainly applied in telecommunication industry where dc-dc converters having high frequency but low voltage is required. Another important feature of this topology is the buck-boost functionality. Figure 3.12 shows the structure of the presented topology.

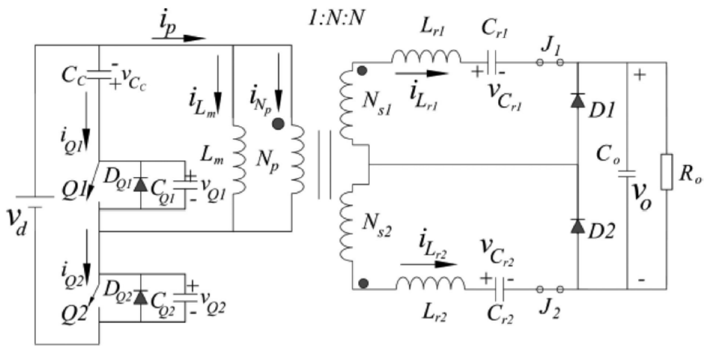

Figure 3.12: Dual SL-RC (Amir et al., 2019)

A bidirectional series RC is presented in (S. Hu et al.,2018). This topology is presented to address the issue of reduced efficiency in high frequency isolated RC. The reduced efficiency is caused by low losses due to switching. To resolve the above problem, it's necessary to minimize the current of the resonant tank; this is achieved by utilizing the bidirectional switch based series RC with the appropriate control techniques such as phase shift and modified phase shift PWM. Modified PS-PWM enables ZVS of the switches when light loads are used. The circuit of the presented topology is shown by Figure 3.13; the structure is composed of two H-Bridges separated by a high frequency transformer and the resonant tank. Snubber capacitors are connected across the switches. The symmetric nature of the topology allows for voltage transfer from first H-bridge to the second H-Bridge.

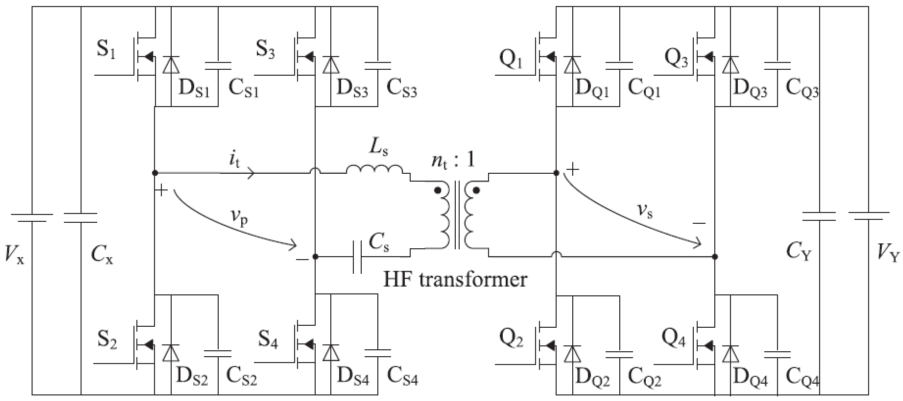

Figure 3.13: Bidirectional series RC (S. Hu et al.,2018)

The base value parameters and the voltage gain M are given by:

$$\begin{cases} V_B = V_X \\ M = \frac{n_t V_Y}{V_X} \\ Z_B = \frac{n_t^2 V_Y^2}{P_{rate}} \\ \omega_B = \sqrt{(L_s C_s)^{-1}} \end{cases} \tag{3.3}$$

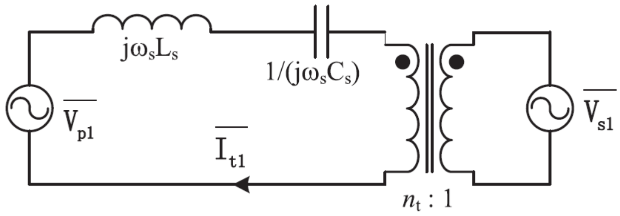

Figure 3.14: Equivalent circuit (S. Hu et al.,2018)

A novel isolated LLC series RC is presented in (S. M. Showybul et al.,2017). The proposed converter is a dc-dc converter and it's suitable for wide input voltage applications. The appropriate control method applied is the frequency adaptive PS-PWM. The control technique enables high boosting capabilities and zero voltage switching; irrespective of the load state. The input side of the topology is made up of cascaded Half-Bridge structure; this provides minimum switching stress on the components of the input side. Figure 3.15 shows the circuit of the proposed converter. The resonant tank is connected to an HFT, transformer saturation is prevented by utilizing capacitor C_r(resonant capacitor) to absorb the dc component of the ac voltage. The switch stress is minimized to half the source voltage. High capacitor value is chosen for the output section in other to eliminate ripples. The voltage gain is given by:

$$G = \frac{1}{\sqrt{\left\{\left(1+K-\frac{K}{F^2}\right)-\left[\frac{Q(F^2-1)}{F}\,x\left(\frac{FK+F-\frac{K}{F}}{Q(F^2-1)}-cot\varphi\right)\right]\right\}^2+\left\{\frac{Q(F^2-1)}{F}\right\}}} \tag{3.4}$$

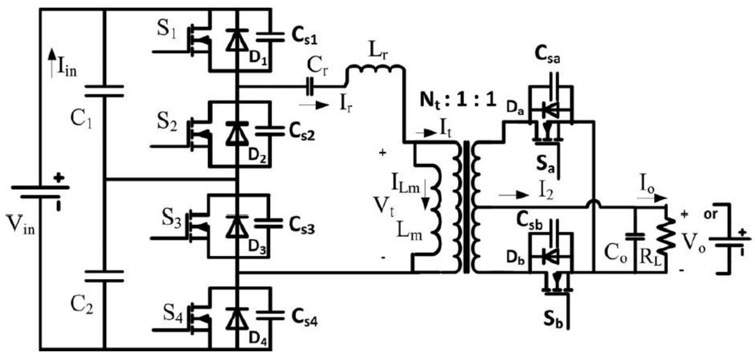

Figure 3.15: Novel LLC converter (S. M. Showybul et al.,2017)

3.5 Parallel-loaded RC (PL-RC) Topologies

In the parallel-loaded RC , the components of the resonant tank are connected in parallel with respect to the load. A typical example if the LC tank of Figure 3.16. The resonant tank is connected between the H-Bridge structure and the rectifier circuit. The model circuit of Figure 3.16 is represented by Figure 3.17. The Fourier expression for the following parameters is given the mathematical expression below:

$$V_T = \frac{4V_{in}}{\pi} \sum_{n=1}^{\infty} \frac{1}{2n-1} \sin[(2n-1)\omega_o]\, t \tag{3.5}$$

$$V_{RO}(t) = \sum_{n=-\infty}^{\infty} C_m e^{jm\omega_o t} \tag{3.6}$$

$$V_{RI}(t) = \sum_{m=-\infty}^{\infty} X_n e^{jm\omega_o t} \tag{3.7}$$

The output current is given by:

$$i_o(t) = I_o + \sum_{m=2}^{\infty} I_m \cos(m\omega_o t + \varphi_m) \tag{3.8}$$

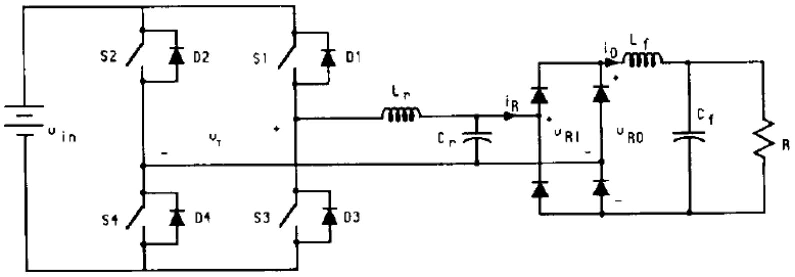

Figure 3.16: PL-RC

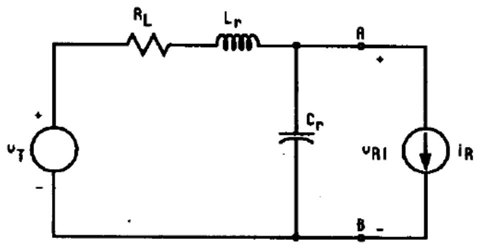

Figure 3.17: Equivalent model of PL-RC

A three phase cascaded LLC PL-RC is presented in (Feng et al., 2018). This topology improves the efficiency and the power density of the converter because of the application of LLC with the transformer. Also the desire of achieving zero voltage and zero current switching is obtained. The circuit of the presented topology is composed of main blocks; filter section, square wave generator section, resonant section and a rectifier section. Figure 3.18 shows the structure of the presented topology.

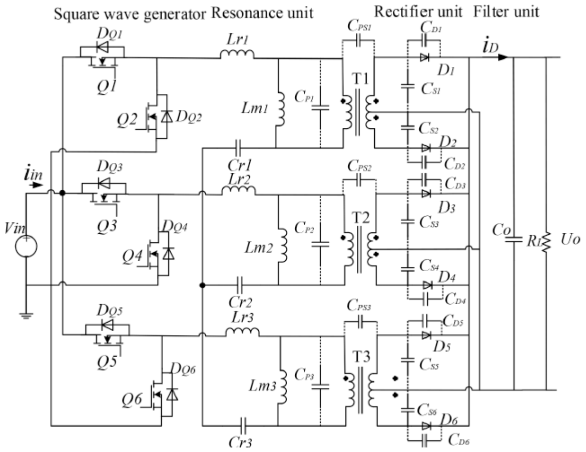

Figure 3.18: Three-phase PL-RC (Feng et al., 2018)

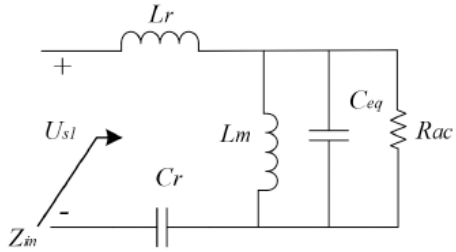

Figure 3.19: Single phase model of 3ph PL-RC (Feng et al., 2018)

The voltage gain equation is given by:

$$M = \frac{\left(\frac{L_m}{L_r}\right)\left(\frac{f_s}{f_r}\right)^2}{\sqrt{\left[\left(\frac{L_m}{L_r}\right)\left(\frac{f_s}{f_r}\right)^2+\left\{1-\left(\frac{f_s}{f_r}\right)^2\right\}\left\{\left(\frac{L_m}{L_r}\right)\left(\frac{f_s}{f_r}\right)^2-1\right\}\right]^2+\left[\left(\frac{f_s}{f_r}\right)\left(\frac{L_m}{L_r}\right)\left(\sqrt{\frac{L_r C_r}{R_{ac}}}\right)\left\{\left(\frac{f_s}{f_r}\right)^2-1\right\}\right]}} \quad (3.9)$$

A half H-Bridge which has been modified and with asymmetric features is presented in (Neilor et al., 2019). The dc offset current in the transformer has been eliminated. The method of control of this inverter is similar to the traditional H-Bridge topology where a sustained frequency and asymmetric PWM technique is utilized. To prevent the flow of dc component of the inverter output to the transformer, a voltage doubler is connected to the transformers output. The resonant tank of parallel connection is fixed between the inverter output and the transformer input. Figure 3.20 shows the circuit of the presented topology. Two switches of the inverter have different conduction times, switch S1 operates during the time period of DT_s whiles the remaining switch S2 conducts during the time period of

$T_s(1\text{-}D)$ which the complementary mode of conduction. The voltage multiplier increases the magnitude of the output voltage hence minimum turns ratio is required in the transformer. The parallel resonant tank provides the ZV-ZC switching. The equivalent circuit of the six modes of operating the proposed topology is provided in Figure 3.21.

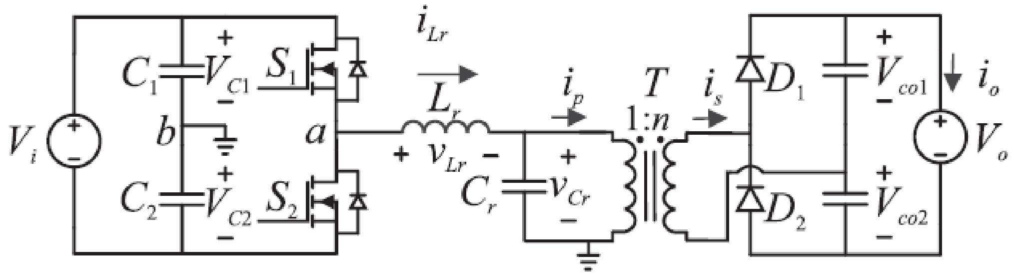

Figure 3.20: Modified HB PL-RC (Neilor et al., 2019)

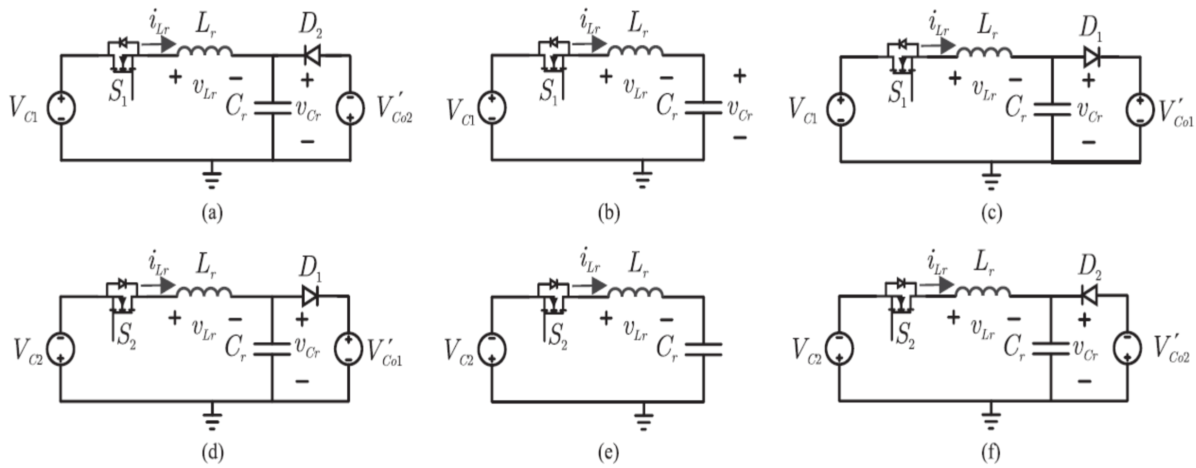

Figure 3.21: Six modes of equivalent circuit (Neilor et al., 2019)

A new parallel RC is presented in (M. Kim et al., 2015) which has wide range of values for the output voltage, also this topology has lean path of operating the switching frequency. Zero voltage switching during the period of turn-on and zero current switching during the period of turn-off is another possible feature of this topology. The turn's ratio of the transformer can be varied to determine the value of capacitance for the resonant tank. The resonant tank is stress-free at startup because of ZV gain at notch resonance frequency. The proposed topology of Figure 3.22 is mainly composed of three parts; the HB structure, the resonant tank and the rectifier component. The resonant tank has two inductors, one capacitor and a transformer. The equivalent circuit for the modes of operation is shown by Figure 3.23.

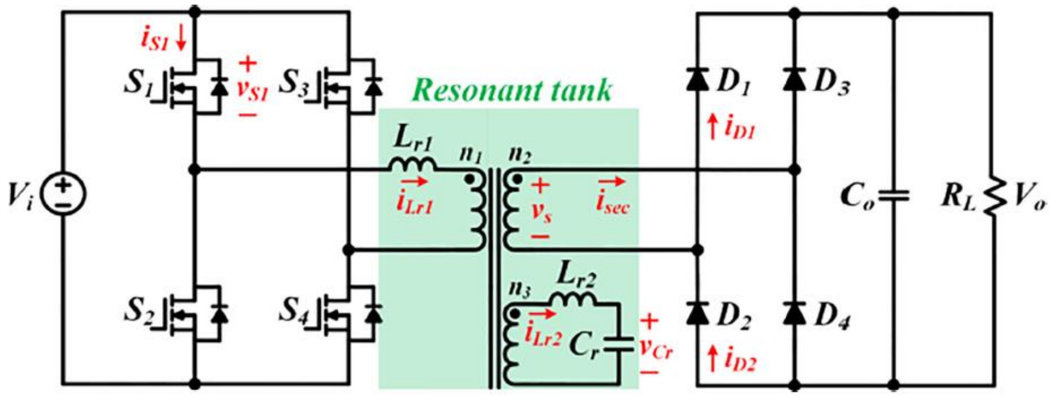

Figure 3.22: HB-PL-RC (M. Kim et al., 2015)

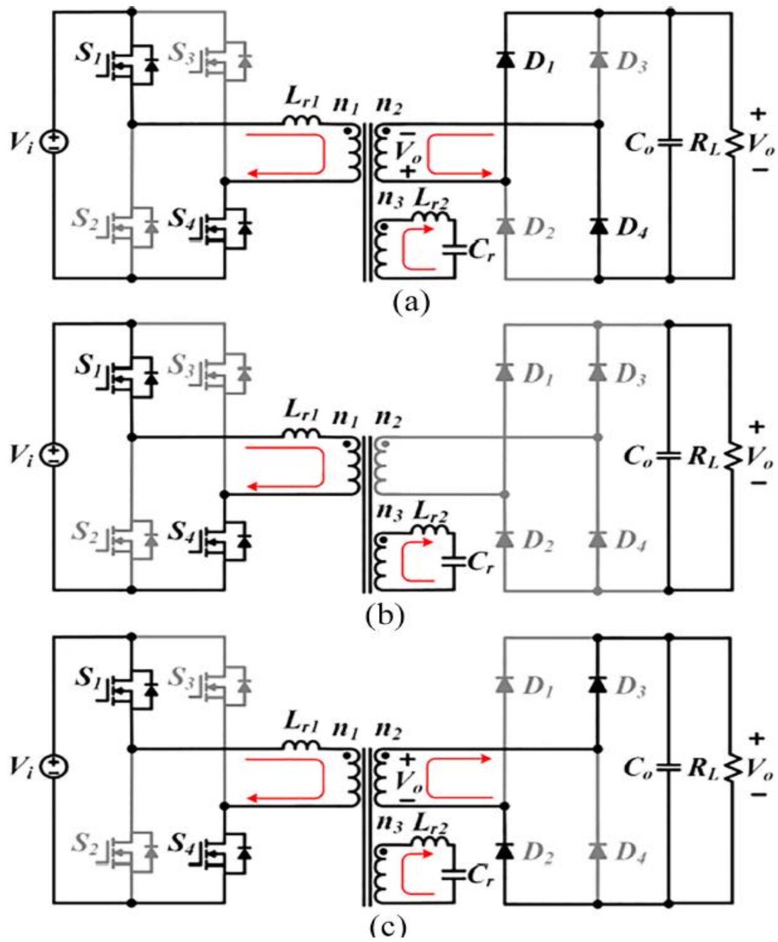

Figure 3.23: Modes of operation (M. Kim et al., 2015)

The gain of the converter is given by:

$$G = \frac{n_2}{n_1}\frac{1}{\sqrt{\left(k\frac{f_n^2}{f_n^2-1}+1\right)^2+\left(\frac{kf_n}{Q}\right)^2}} \tag{3.10}$$

A parallel loaded RC topology is presented in (Y. C. Chuang et al., 2012) for battery charging based on float charge approach; this technique ensure that the battery is constantly charged and will remain fully charged always. The proposed converter has minimum component requirements however high efficiency and minimum switching losses is delivered. The high efficiency is obtained at the point of discontinuous current mode conduction. The circuit of the presented topology is seen in Figure 3.24 and its equivalent circuit is given by Figure 3.25. The main circuit is made up three parts; the half HB, the resonant tank and finally the rectifier part to eliminate the dc component of the inverter output. This topology does not incorporate a transformer into its structure.

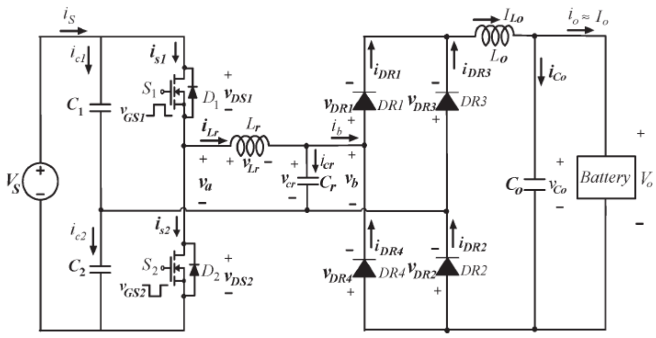

Figure 3.24: PL-RC (Y. C. Chuang et al., 2012)

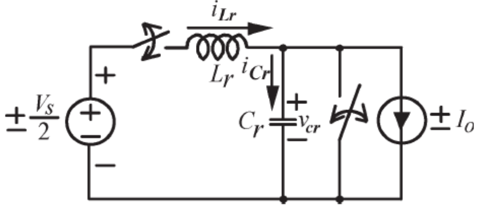

Figure 3.25: PL-RC equivalent circuit (Y. C. Chuang et al., 2012)

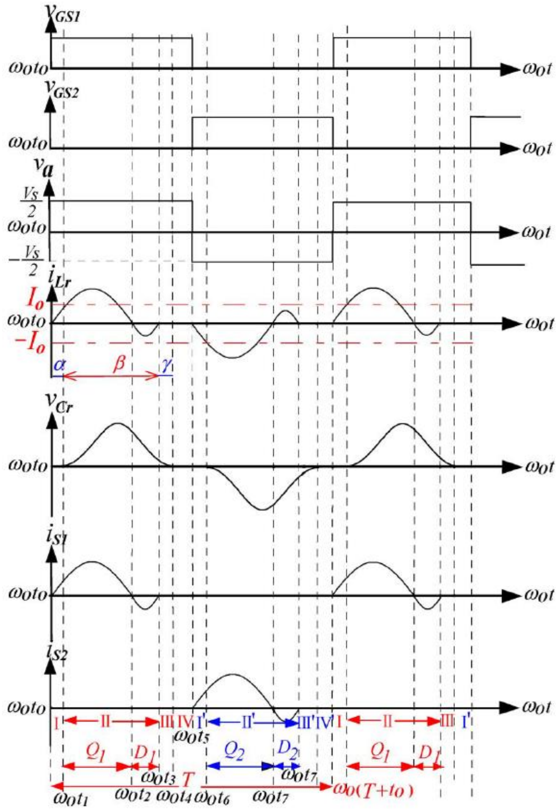

Figure 3.26: Waveforms of current and voltage (Y. C. Chuang et al., 2012)

A capacitor based push-pull PL-RC is proposed in (D. Thrimawithana et al., 2008) this topology is operated in three different states which are named as:

- Normal state
- Buck state
- Boost state

These states of operation are possible due to the variation of the switching frequency achieved by damped RF modulation via a phase shift. These modes of operation guarantees high voltage gain with wide range of values. Detailed explanation of the proposed converter is well explained in the following .

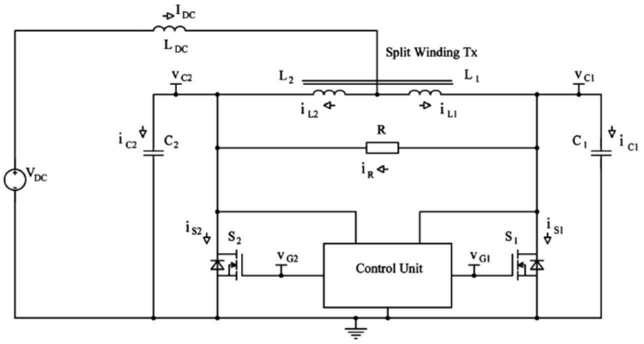

Figure 3.27: Push-pull PL-RC (D. Thrimawithana et al., 2008)

The normal state of operation, the switching frequency equals to the damped resonant frequency, in the buck state of operation, the damped resonant frequency is greater than the switching frequency and finally in the boost state of operation the switching frequency is greater than the damped resonant frequency.

The output power is given by:

$$P_{out} = \left(\frac{T_S}{T_z}\right)^2 \frac{\pi^2 V_{DC}}{2R} \tag{3.11}$$

The dc current $I_{DC}$is given by:

$$I_{DC} = \frac{P_{out}}{\eta V_{DC}} \tag{3.12}$$

$$I_{DC} = \frac{\pi^2 V_{DC}}{2R\eta} \left(\frac{T_S}{T_z}\right)^2 \tag{3.13}$$

Analysis of the characteristics of PL-RC is investigated in (M. J. Schutten et al., 1992). The circuit of the parallel network is shown by Figure 3.28. The resonant tank equation is governed by:

$$Q = \frac{R_L}{\sqrt{\frac{L_r}{C_p}}} \tag{3.14}$$

Where RL is the inverter load and the resonant tank components are represented by the inductor and capacitor. The ratio of the output voltage to the input voltage which represents the voltage gain is expressed by:

$$G = \frac{1}{\frac{\pi^2}{8}\left(1+\frac{C_p}{C_s}-\omega^2 L_r C_p\right)+jQ_s\left(\frac{\omega}{\omega_s}-\frac{\omega_s}{\omega}\right)} \qquad (3.15)$$

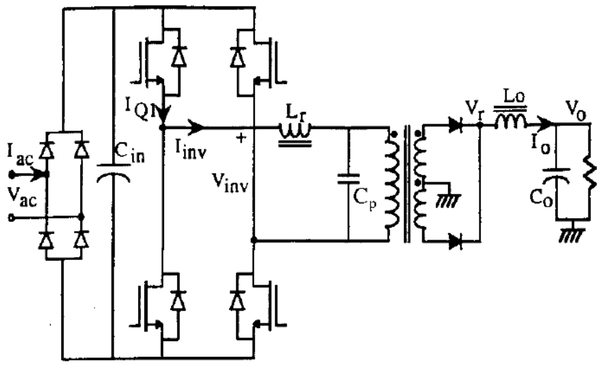

Figure 3.28: PL-RC (M. J. Schutten et al., 1992)

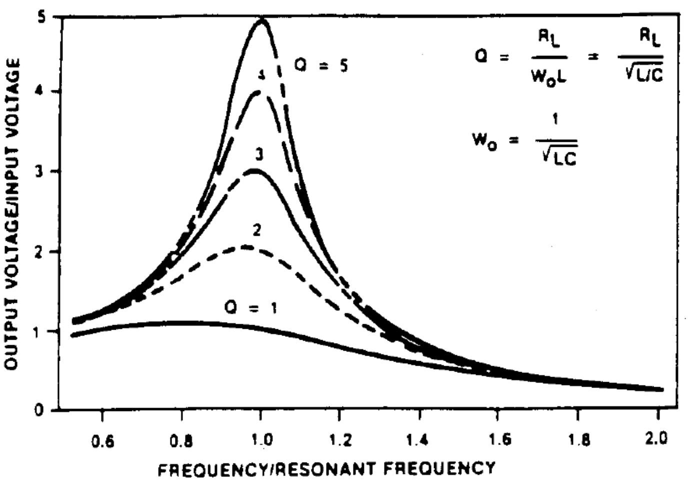

Figure 3.29: PL-RC characteristics (M. J. Schutten et al., 1992)

3.6 Series-Parallel-loaded RC (SPL-RC) Topologies

The series-parallel loaded resonant converter is a combination of the series and the parallel RC structures. Depending on the converter topology, SPL resonant converter is connected at the output of the converter to provide high efficiency by reducing the switching losses of the converter when zero-voltage and zero-current switching is attained. Some selected papers on the above mentioned subject are presented below.

A boost dual SPL resonant converter is presented .Figure 3.30 show the circuit of the proposed converter. The high boosting feature is achieved by incorporating switched capacitor network into the converter structure. This converter boast of voltage gain of wide range, better voltage regulation of light loads and continuous variation. Charge losses and current spikes are removed by resonance operation of the capacitors. Also zero-current switching for transistors and diodes at turn-on and turn-off respectively is attained. The basic unit is composed of three components; transistor, capacitor and a diode. Another diode is sandwiched between the basic units. The individual resonance frequency f_{rn} and the voltage gain M are given by:

$$f_{rn} = \frac{1}{2\pi\sqrt{2L_rC_r}} \tag{3.16}$$

$$\begin{cases} M = \frac{V_o}{V_{in}} \\ M = \frac{[(h-1)(V_{cr,max}-V_{cr,min})]m}{hV_{cr,max}-V_{cr,min}} \\ M = \frac{1+\sqrt{1+8m(N-1)}}{2} \end{cases} \tag{3.17}$$

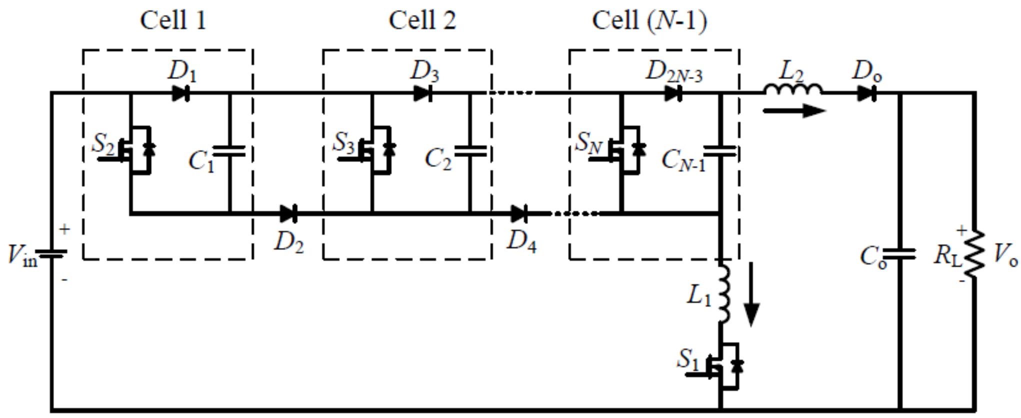

Figure 3.30: nX SPL-RC

The modes of operation are represented by Figure 3.31.

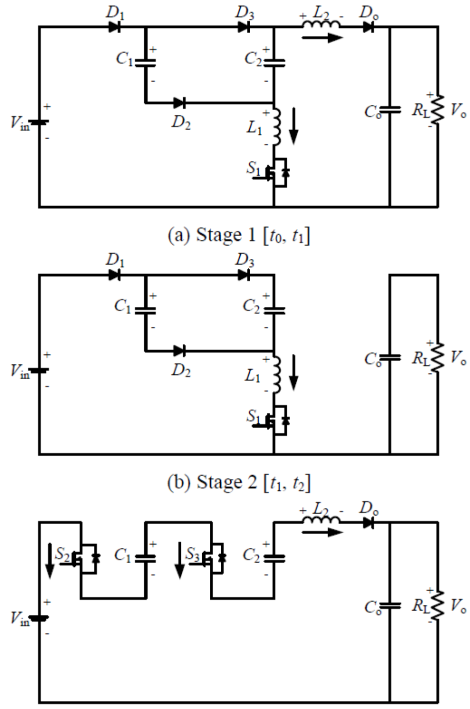

(a) Stage 1 [t_0, t_1]

(b) Stage 2 [t_1, t_2]

(c) Stage 3 [t_2, t_3]

Figure 3.31: Modes of operation of nX SPL-RC

A dual output converter is proposed . The novel features of the proposed converter is the combination of two finite topologies; the parallel input and series output resonant tank of the LLC topology and the full bridge structure. The modulation method used is the PS hybrid technique. Switching frequency and phase angle modulation are used in modulating the resonant tank and full HB respectively. The parallel LLC network is composed of two resonant inductors and capacitors plus magnetizing inductances. The series connection is obtained from the output of the resonant converter. The HB is composed of four semiconductors devices (MOSFET); which generates the pulsating voltage of high frequency. The principal output waveforms of the proposed converter is shown in Figure 3.32 whiles the main circuit of the proposed converter is shown in Figure 3.33.The converter modes of operation are shown by Figure 3.34.

$$M_B = \frac{f_n}{2n\sqrt{-K+f_n^2(1+k)}} \tag{3.18}$$

$$I_{o2,\max} = \frac{P_{out,max}}{V_{out2}} \tag{3.19}$$

$$i_{Lr}(t) = I_{Lrt}\sin(\omega_s + \theta)\sqrt{2} \tag{3.20}$$

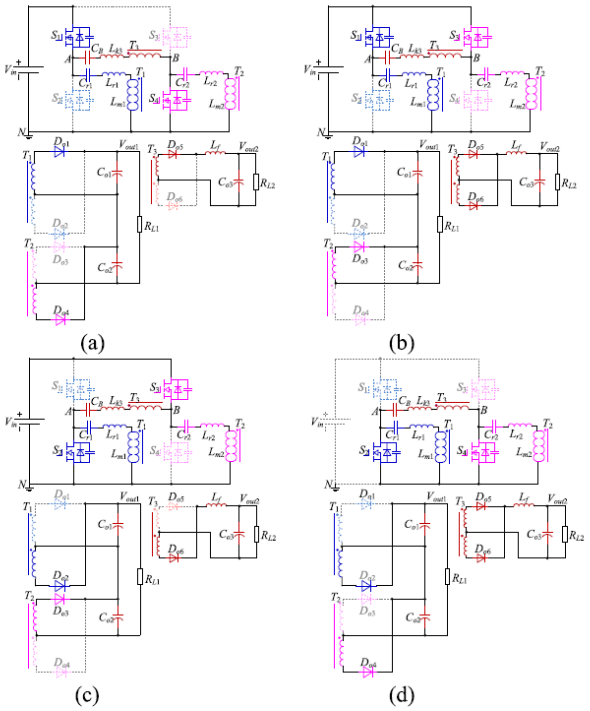

Figure 3.32: Modes of operation

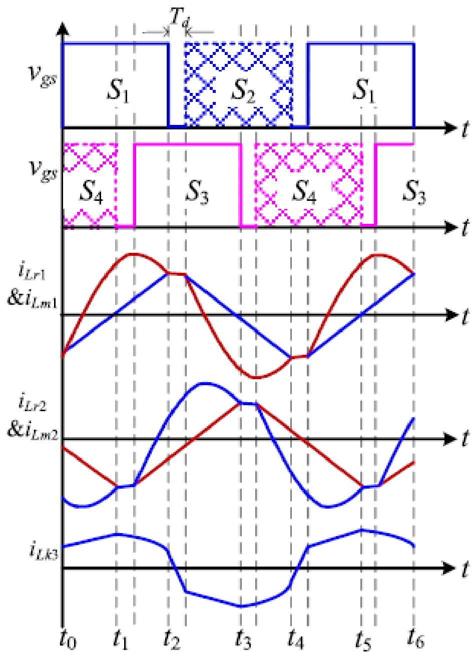

Figure 3.33: Waveforms Figure

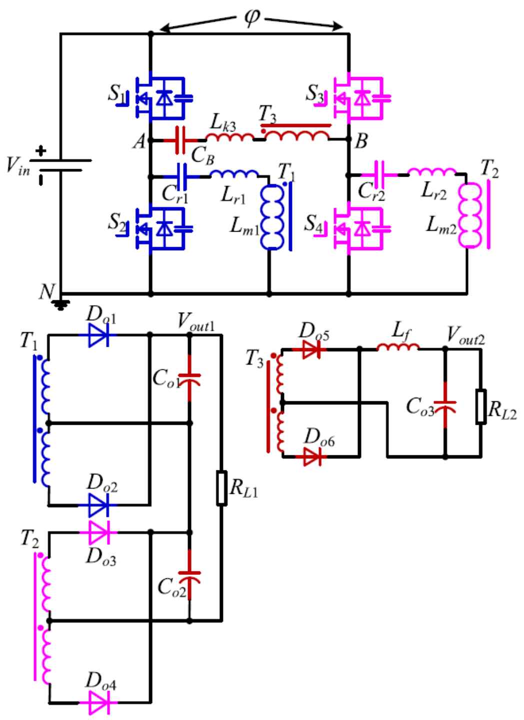

3.34: Proposed converter

A full bridge based LLC resonant converter is presented in (Y. Shen et al., 2018). The presented converter is connected a transformer and a rectifier circuit and it's used in for charging of electric vehicles. Instead of one large transformer, two medium size transformers are employed. Equal current values are attained at the primary by series connection and equal voltage values are attained at the secondary by parallel connections hence the power magnitude is balanced for both connections. To increase efficiency and reduce losses, ZVS for turn-on of switches and ZCS during turn-off of diodes is attained. When compared to conventional topologies with one large transformer, the presented topology offers better heat dissipation and minimum transformer losses. Figure 3.35 shows the presented topology. The circuit is composed of H-Bridge structure, the resonant tank and the rectifier output section. The mode of operation is divide into eight parts which are represented by Figure 3.36 and Figure 3.37.

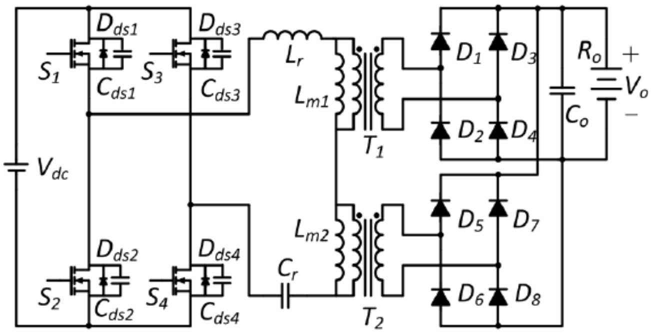

Figure 3.35: HB LLC converter (Y. Shen et al., 2018)

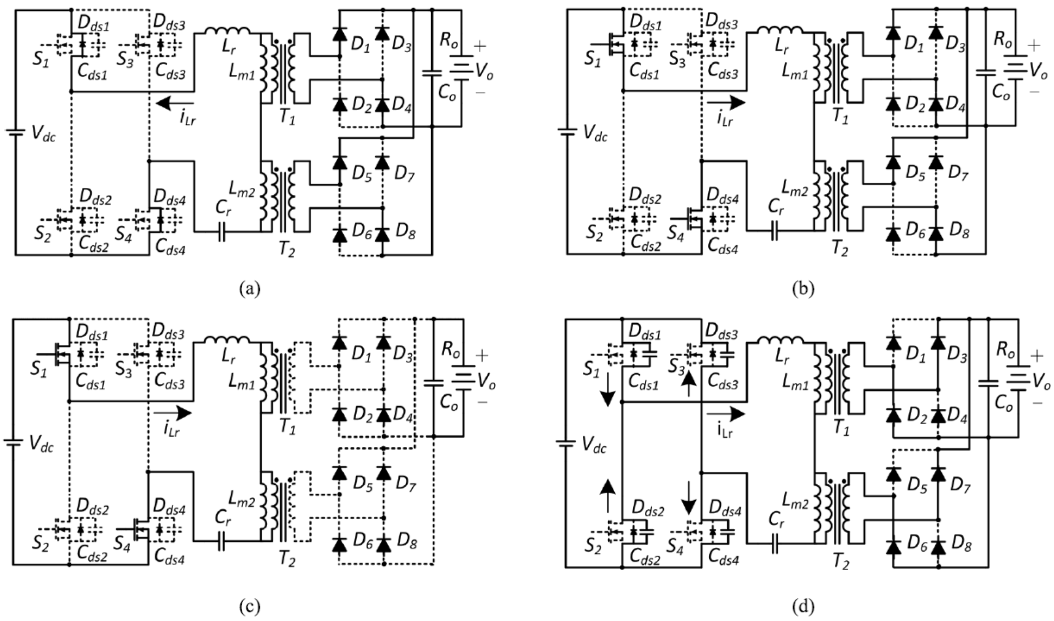

Figure 3.36: Modes of operation (Y. Shen et al., 2018)

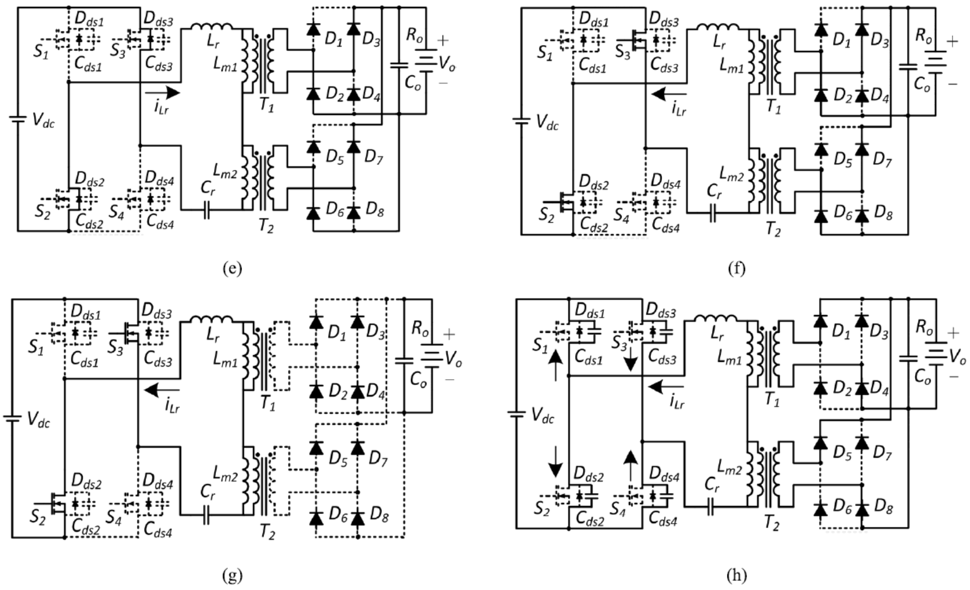

Figure 3.37: Modes of operation (Y. Shen et al., 2018)

The voltage gain is given by:

$$M = \left| \frac{R_{eq} f_s L_m C_r}{[j f_s \left(1 - \frac{f_s^2}{f_r^2}\right)(L_{lks} n^2 + L_m) + R_{ac} \left(1 - \frac{f_s^2}{f_p^2}\right)} \right| \tag{3.21}$$

The resonant tank Q is given by:

$$Q = \frac{0.95}{|M|_{max} K} \sqrt{K + \frac{|M|_{max}^2}{|M|_{max}^2 - 1}} \tag{3.22}$$

A novel dc-dc converter based on single switch coupled with a rectifier circuit and a resonant tank is presented in (Ying et al.,2017). This topology is suitable for low voltage power systems. The single switch concept reduces the component count hence the size and cost the proposed converter. The circuit of the proposed inverter is shown by Figure 3.38.

The inverter section of the topology is made up of an input filter, the semiconductor switch and the shunt capacitor. The resonant tank is sandwiched between the inverter and the rectifier. The series-parallel tank is composed of three components; one inductor and two capacitors as shown in Figure 3.38.

The rectifier circuit is of the bridge topology and has an output filter composed of LC components. There are six modes of operations, the equivalent circuit for each mode of operation is shown by Figure 3.39.

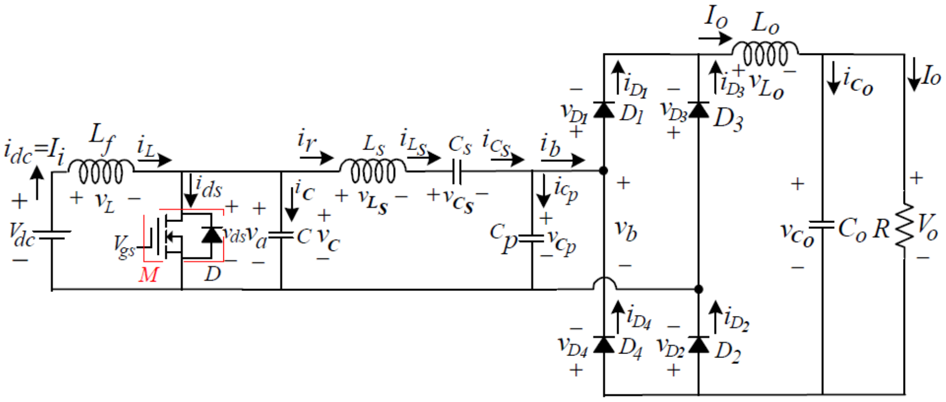

Figure 3.38: One switch SPL-RC (Ying et al.,2017)

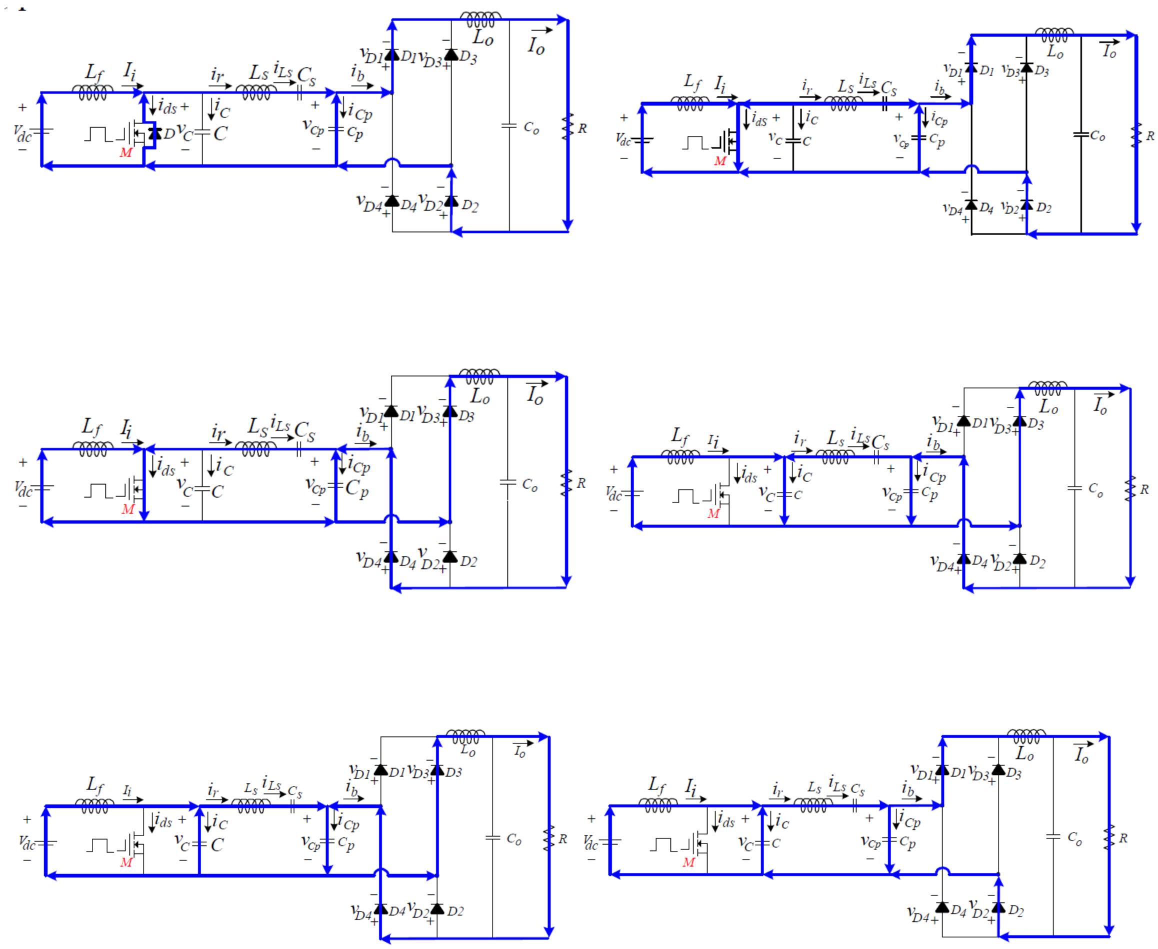

Figure 3.39: Modes of operation (Ying et al.,2017)

The design of bidirectional SPL-RC based on LCC tank topology is presented in (M. Khalil et al., 2016). The used switches will have bidirectional current flow capabilities and also a ratio transformer is used to separate the high and low current components. The transformer can also be utilized for both buck and boost functions. Figure 3.40 shows the circuit of the presented converter and its generated waveforms are shown by Figure 3.41. The circuit of Figure 3.40 is composed of two converters sandwiched by the SPL topology and a transformer. The two converters have independent dc sources. The series section of the resonant tank is composed two components; inductor and capacitor whiles the remaining capacitor constitutes the parallel section. Operation of the H-Bridge structure is similar to the conventional operation states; diagonal switches are turned-on to produce the desired polarity of power.

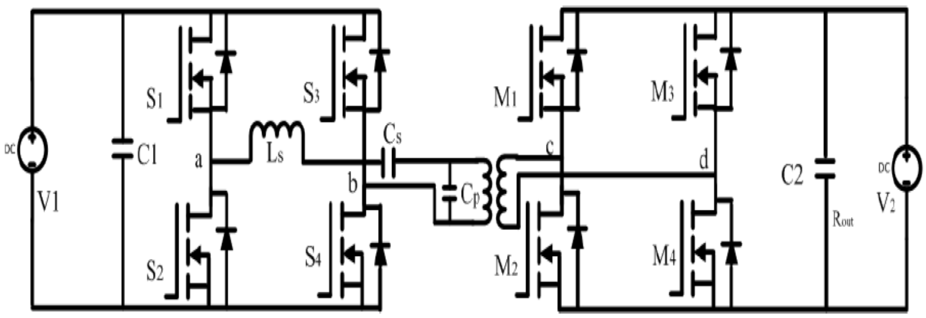

Figure 3.40: Bidirectional SPL-RC (M. Khalil et al., 2016)

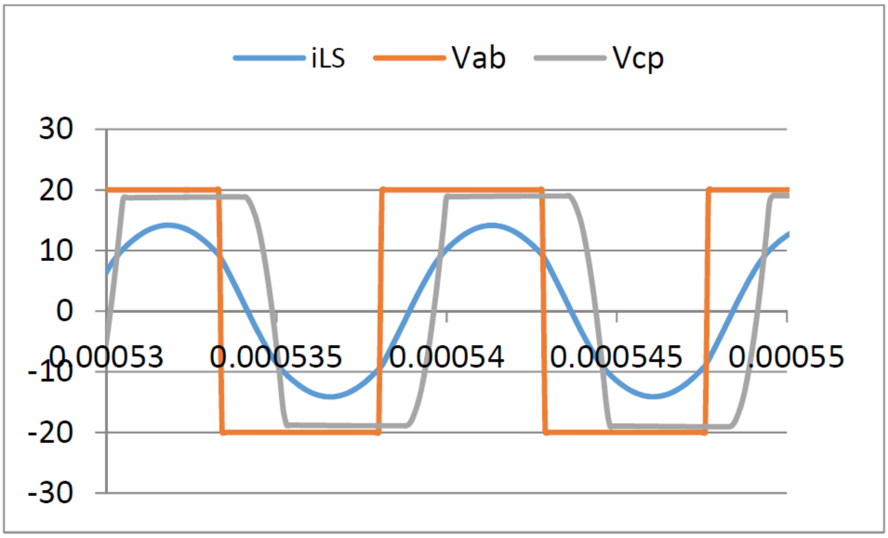

Figure 3.41: Generated waveforms (M. Khalil et al., 2016)

Output voltage equation is given by:

$$V_2 = 2nR_L \left(\frac{I_{in} - nk\omega_s C_p V_d}{\pi + 2n^2 R_L \omega_s C_p} \right) \tag{3.23}$$

A novel dc-dc converter based on SPL-RC topology is presented in (Yueshi et al., 2016). The proposed converter is suitable light emitting diode (LED) driver applications. The presented topology has an important feature in which there's equal phase of the input voltage and input current due to the resistive nature of the input impedance. The structure of the proposed converter is shown by Figure 3.42. The inverter section is composed of half HB made up of two switches. The resonant tank is sandwiched between the inverter and the rectifier circuit. The resonant tank is connected to a transformer. The equivalent circuit is shown in Figure 3.43 and the simplified circuit is given by Figure 3.43.

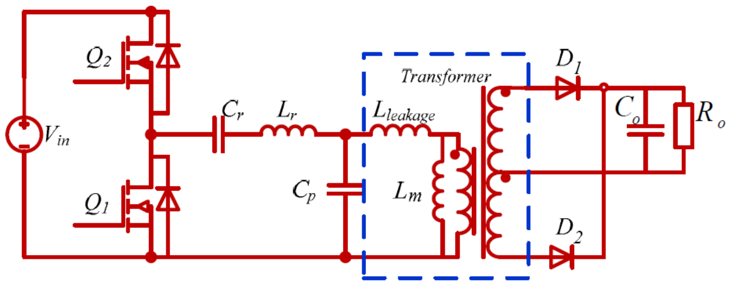

Figure 3.42: DC-DC SPL-RC (Yueshi et al., 2016)

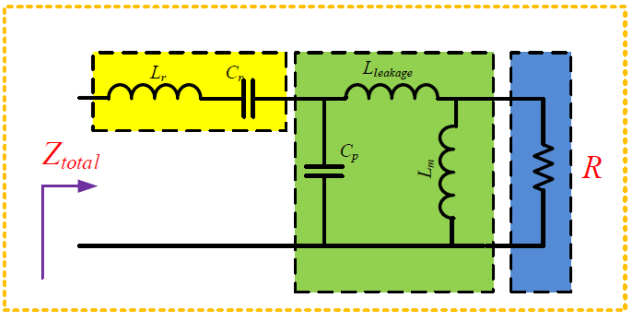

Figure 3.43: Equivalent circuit of DC-DC SPL-RC(Yueshi et al., 2016)

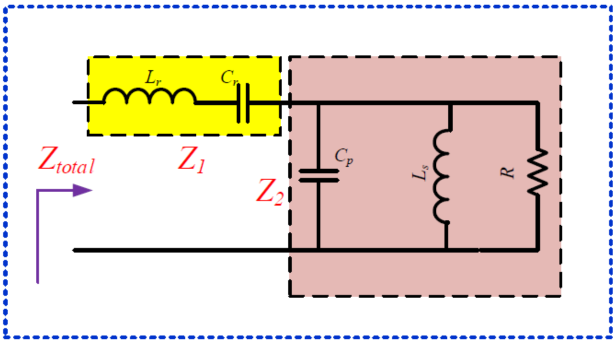

Figure 3.44: Simplified DC-DC SPL-RC (Yueshi et al., 2016)

The voltage gain is given by:

$$M = \frac{s^2 C_r L_s R}{(1+s^2 C_r L_r)(s^2 C_p L_s R + s L_s + R) + s^2 (C_r L_s R)} \tag{3.24}$$

A novel battery charging system based on half H-Bridge SPL-RC is presented. Source or input of the proposed topology is derived from photovoltaic systems. The design of the proposed topology makes possible to eliminate low frequency current ripples and high frequency current ripples of the battery; this feature increases the lifespan of the battery. Figure 3.45 shows the proposed circuit topology. The circuit is composed of the following parts:

- PV input
- Half H-Bridge
- Resonant Tank
- Rectifier Circuit
- Filter

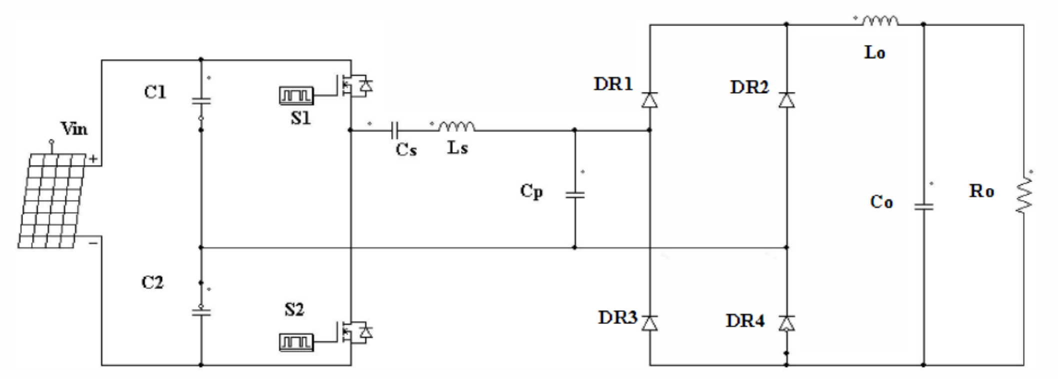

Figure 3.45: PV based SPL-RC

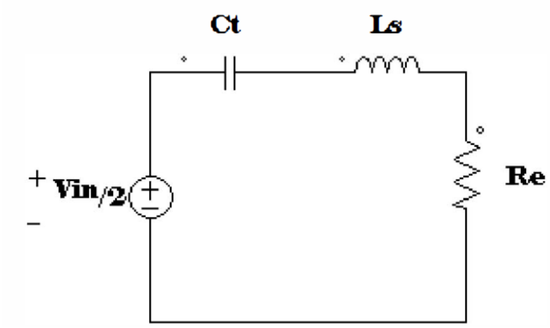

Figure 3.46: Equivalent circuit of PV based SPL-RC

Bidirectional power flow of isolated LLC SPL-RC offers numerous advantages such as both directional power flow, higher efficiency and higher power density. This topology of SPL-RC is presentedin (A, Hillers et al., 2012). The presented converter is composed of two H-Bridges in both ends of the structure and have independent power sources. Analysis of the primary side HB is similar to the methods presented in the following papers . A square wave is generated by the H-Bridge at the primary and it's applied to the SPL tank; this produces an almost sinusoidal current. Rectification of the produced power is done by the secondary H-Bridge; this process increases the efficiency of the converter . First harmonic approximation is achieved because the resonant tank functions as a filter (Bandpass) hence power transfer is done by the fundamental components of current and voltage . The circuit of the presented topology is givenFigure 3.47.

The voltage gain of the converter is given by:

$$M = \frac{1}{\sqrt{\left[Q\left(K-\frac{1}{K}\right)\right]^2+\left[1+\frac{1}{h}-\frac{1}{hK^2}\right]^2}} \tag{3.25}$$

The voltage gain for the reverse power flow is given by:

$$M_{rev} = \frac{1}{\sqrt{\left(QK-\frac{Q}{K}\right)^2+1}} \tag{3.26}$$

Where Q is defined by:

$$Q = \frac{R_{ac}}{Z_o} \tag{3.27}$$

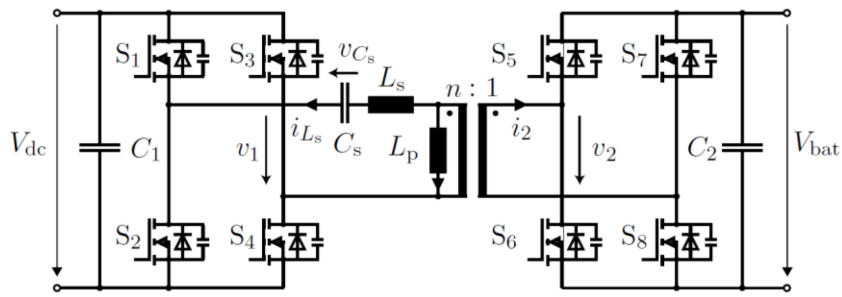

Figure 3.47: Bidirectional SPL-RC (A, Hillers et al., 2012)

3.7 Hybrid Resonant Converter Topologies

Soft switching of semiconductor switches is a technique where the power losses due to switching is minimized or eliminated. Currently two types of soft switching are widely being applied in industry and these are:

- Zero voltage switching (ZVS)
- Zero-voltage/zero-current switching (ZVSZCS)

Because of the lower voltage ratings of MOSFET when compared to IGBT, ZVS is mostly suitable for the MOSFETS whiles ZCS is suitable for IGBT. The hybrid resonant converter is derived by combining structures of the already existing topologies to derive a new converter, also hybrid control techniques are proposed. The main idea of the hybrid topology is resolve any of the limitations of the existing topologies. Below are some published papers on the hybrid RC converter topologies.

A hybrid controller to provide control and stabilization of dc-dc RC is presented . This method does not use the conventional small signal approximation or the average signal approximation method. Two features are used in the design of the proposed control method; converter switch behavior and piecewise affine technique. A hybrid modulation technique for the control of dc-dc RC is presented . The hybrid control technique is composed of phase shift and pulse frequency PWM. The output voltage of the proposed converter and the resonant tank are independently controlled because phase angle and switching frequency are used to control the two parameters respectively.

A novel converter with both three-level and two-level output voltage generation capabilities is presented . This converter is derived from the full bridge structure and its combines the advantages of HB and the resonant tank. It’s capable of accepting input voltage with wide variations hence suitable for fuel cell applications. The size of the output filter and the input ripples are minimized when compared to the traditional HB. Zero voltage switching is possible with the presented converter. Figure 3. 48 shows the circuit of the presented converter.

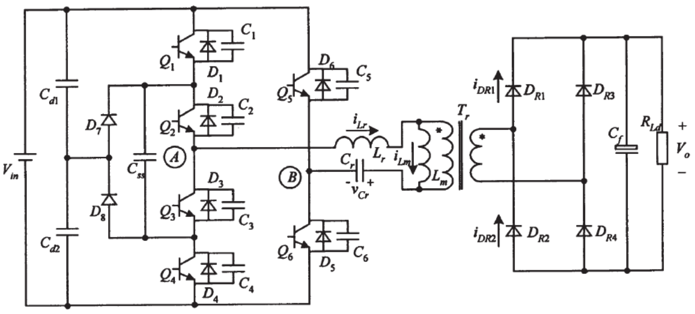

Figure 3.48: Hybrid HB LLC converter

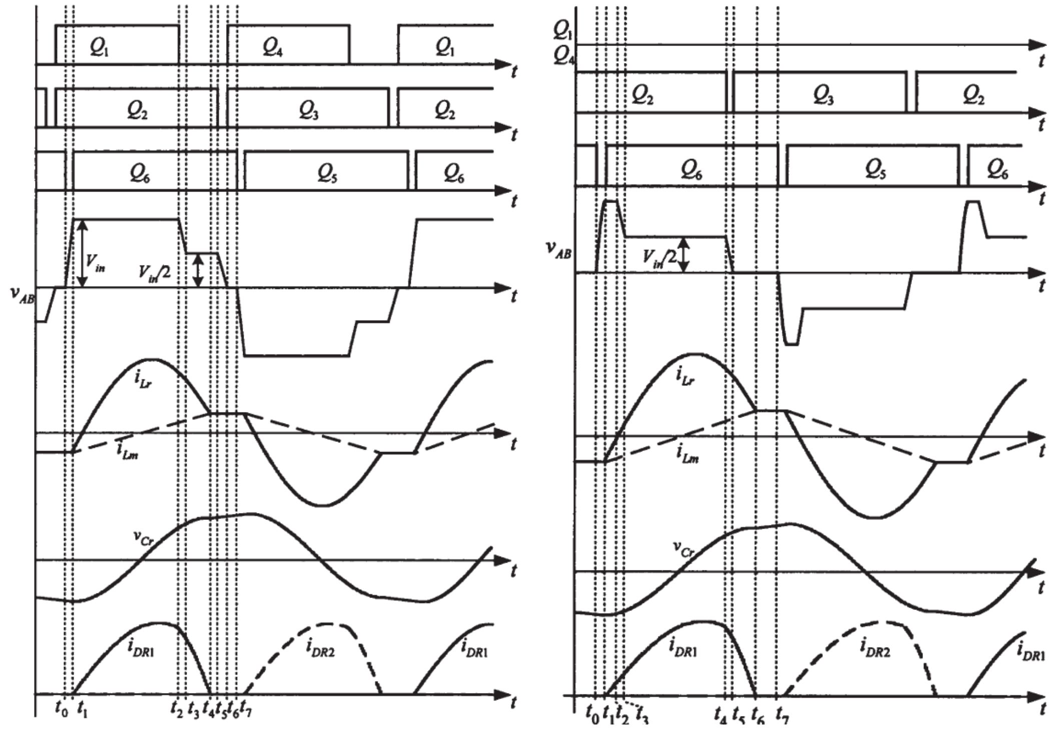

Figure 3.49: Major waveforms

The structure of the proposed inverter is composed three major parts; the inversion section, the resonant tank and the rectifier section. The structure of the inversion section is similar to the NPC converter. Each power switch is connected with antiparallel diode and capacitor, there are six of these switches, one dc source, two capacitors, LLC tank and HB rectifier.

3.8 Commutation Circuit

Commutation basically is the process of turning off the power electronic switch so as to bring the current value to zero. Basically commutation can be explained as the switching behavior of power electronic switches. Commutation of power switching experiences two types of commutation known as hard commutation and soft commutation. In the case of hard switching, the power switch holds a considerable amount of voltage or current when it immediately changes state. Hard commutation if a forced process by either gate signal or other power electronic switches. Soft switching on the other end occurs at a state when the current and voltage values are at zero (0). Soft commutation is achieved by employing circuit of RLC to achieve the zero current or zero voltage switching . There are two other types of commutation known as synchronous and asynchronous commutation which are well explained . Below are some published commutation circuits.

Load-Adoptive commutation control of a three-phase inverter termed RDCL (resonant DC link) is presented . The RDCL is a novel topology composed of the usual suspects in any resonant tank based topology; converter, resonant tank and rectifier circuit. This presented control techniques achieves soft switching thus reduced losses, high efficiency and finally minimum voltage stress of components. Also a new soft switching known as pseudo ZVS/ZCS is achieved by this method. Comparing this method to the fixed time control method, this control offers higher efficiency because the commutation switching points can be positively controlled. The commutation current (inductor) waveform for the proposed control method is shown by Figure 2.51.

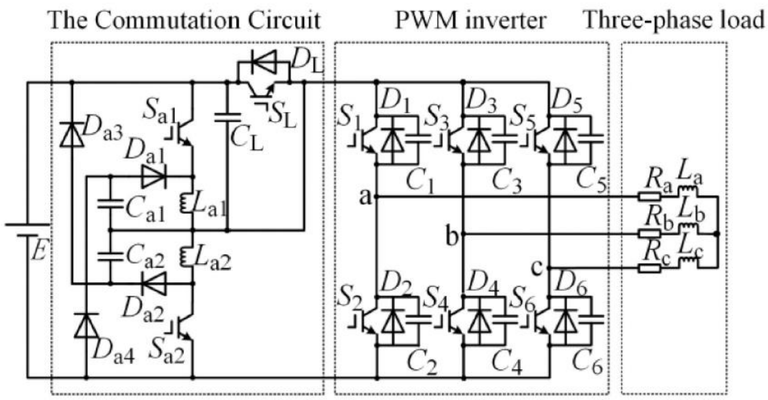

Figure 2.50: RDCL inverter

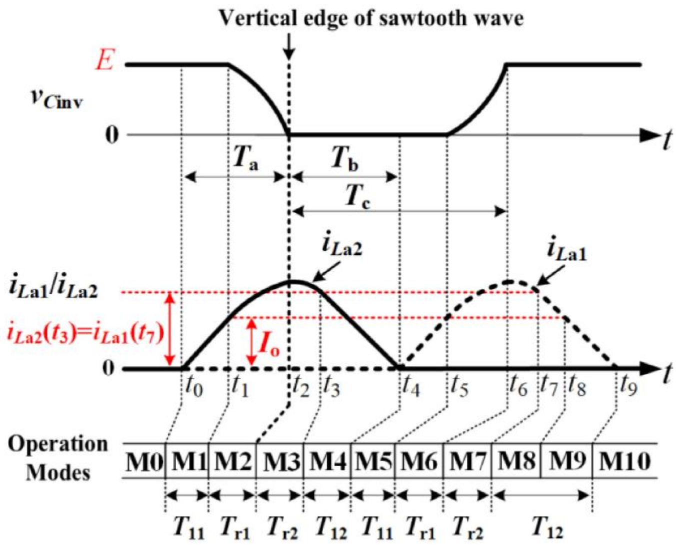

Figure 3.51: Inductor current commutation waveform

A unique commutation and PWM technique are presented which yields the following positives results:

Soft switching

Snubber circuit elimination

Leakage current recovery

The topology of the presented system is a single stage solid state transformer which comes with numerous advantages such as frequency regulation, VAR application and high power density. This converter is suitable for distribution of modern power and high power density drives, it also has bidirectional power-flow and PF correction in open loop systems. The component count is at its barest minimum; semiconductor switches and copper. Figure 3.52 shows the structure of presented topology (type 1)

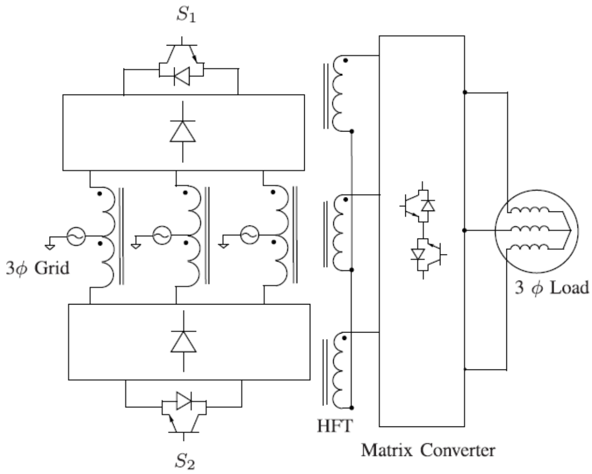

Figure 3.52: Single stage transformer

3.9 Conclusion

Resonant converters as a topic as well as selected publications on different topologies of resonant converters were investigated in this section of this thesis. The investigations revealed that resonant converters minimize switching losses by providing zero voltage and zero current switching of the semiconductor switches. Four main types of selected resonant converters were reviewed, these topologies are derived from the load side connection of the resonant tank. The basic type of resonant tank is LC structure which can be connected in series, parallel, series-parallel and hybrid with respect to the load of the converter.

CHAPTER FOUR
PROPOSED TOPOLOGY AND SIMULATION RESULTS

4.1 Proposed Topology

The proposed topology in this research is a novel single switch which is coupled with a resonant tank of parallel nature and it's applied the application of induction heating. This topology boast of several advantages such as minimum component count hence reduced converter losses and also minimum switching loss due to the application of the resonant tank; therefore the total converter efficiency is improved. Operation of the proposed topology is done in soft commutation state therefore the converter is able to generate the high frequency required for induction heating applications. The switching frequency is used to regulate the output power. Figure 4.1 shows the structure of the proposed converter which is made up of an input LC filter, a H-Bridge diode rectifier, a unidirectional switch connected with an antiparallel diode, the parallel resonance and the load.

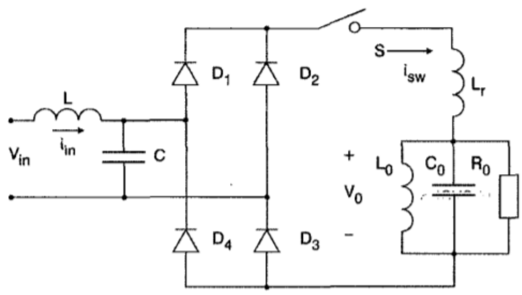

Figure 4.1: Proposed converter

The modes of operation of the proposed converter is in three states; these states are shown by Figure 4.2a to Figure 4.2c. In the first state, which can be described as the charging state or filtering state, the diodes and the switches are off; Figure 4.2a illustrate this mode. In the second state, the switch is gated on and the diodes D1 and D3 conducts; this state is illustrated by Figure 4.2b and finally the last or third state occurs when all diodes and the switch are conducting; Figure 4.2c illustrates this state.

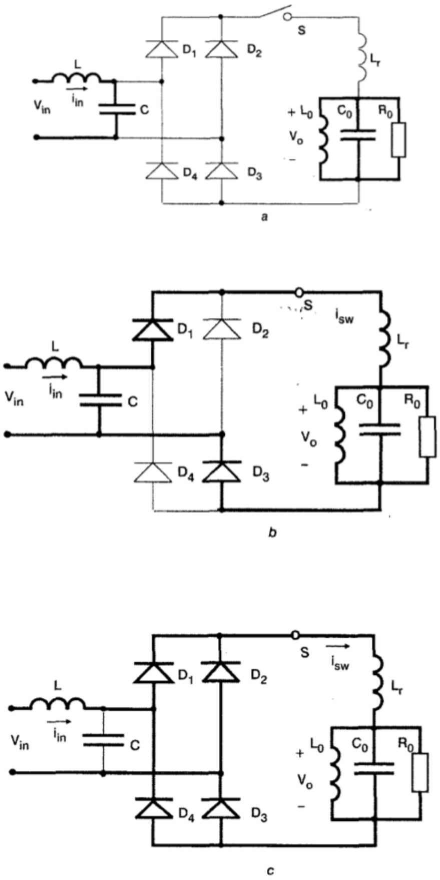

Figure 4.2: States of operation

The desired theoretical output waveforms for the operation of the proposed converter is illustrated by Figure 4.3. There are three period of switching for the above converter; these periods are t_0 to t_1, t_1 to t_2 and t_2 to t_3. These time periods correspond to the three modes of operation of the converter. Let these three periods of interval be represented by Period A, Period B and Period C.

Period A: From t_o - t_1,

As shown in Figure 4.3, in this interval, all the diodes and the switch of Figure 4.1 are off hence they do not conduct. This period is used in charging linearly the capacitor of the input LC structure. At this period, the input voltage and capacitor voltage have the same polarity.

Period B: From t_1 - t_2

In this interval, only three active components conducts, the main power switch S and two diodes (D1 and D3) conducts. During this period, the power to the semiconductor switch is provided by the capacitor and it last until the capacitor finally discharges its voltage.

Period C: From t_2 - t_3

In this state or interval, all the diodes and the power switch are conducting hence the current to the switch has two paths, either paths of the diode bridge. When the current through the switch finally reduces to zero, the period ends and the whole switching period starts all over again from Period A.

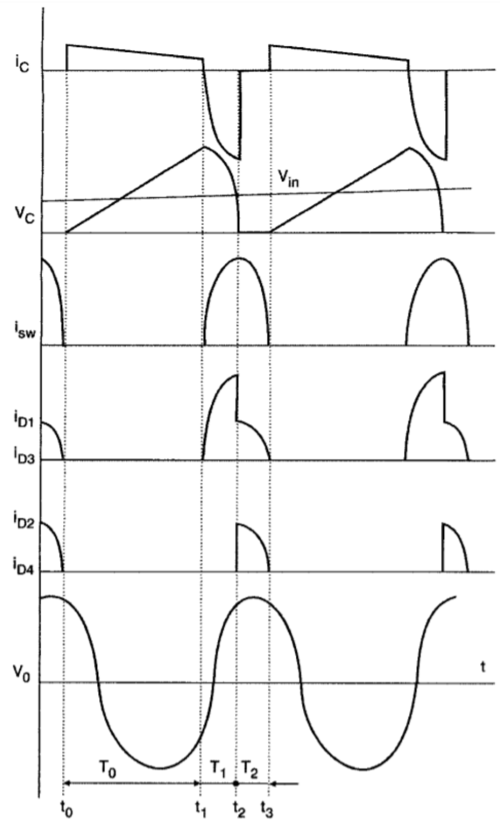

Figure 4.3: Output waveforms

4.2 Operational Investigations

As in the case of all circuit analysis, the components and devices are assumed to be ideal hence this assumption is used in the circuit analysis. Two more assumptions are made which will aid in the analysis of the circuit; these assumptions are:

- Approximation of the switch current to be semi-sinusoidal
- First harmonic component of the output voltage determines the load power

The following expressions are derived from the above assumption. The base voltage is given by:

$$V_B = V_{in} \tag{4.1}$$

Base impedance RB is given by:

$$R_B = \sqrt{\frac{L_o}{C_o}} \tag{4.2}$$

Base current is expressed as:

$$I_B = \frac{V_B}{R_B} \tag{4.3}$$

The base power is given by:

$$P_B = I_B V_B \tag{4.4}$$

The base frequency is expressed as:

$$\omega_B = \frac{1}{\sqrt{L_o C_o}} \tag{4.5}$$

The base period is expressed by:

$$T_B = \frac{2\pi}{\omega_B} \tag{4.6}$$

The maximum switch current is expressed below and should fall within the range 6– 10(A)

$$i_{max}^{sw} = \frac{I_{max}}{I_B} \tag{4.7}$$

The maximum switch voltage is expressed below and should fall within the range 4 –5(V)

$$v_{max}^{sw} = \frac{V_m}{V_B} \tag{4.8}$$

The switch current is the sum of the input current and the capacitor current:

$$i_{in}(i_{Lin}) + i_{Cin} = i_{sw} \tag{4.9}$$

$$I_{max}^{1sw} = \sqrt{a_1^2 + b_1^2} \tag{4.10}$$

$$a_1 = \frac{1}{\pi}\int_0^{2\pi D} I_{max}^{1sw} \sin\left(\frac{\omega_{st}}{2D}\right) cos\, \omega_{st} d(\omega_{st}) \tag{4.11}$$

$$b_1 = \frac{1}{\pi}\int_0^{2\pi D} I_{max}^{1sw} \sin\left(\frac{\omega_{st}}{2D}\right) sin\, \omega_{st} d(\omega_{st}) \tag{4.12}$$

The efficiency of the proposed converter can be calculated from the expression given by:

$$Efficiency = \frac{P_{in} - P_{Total\, loss}}{P_{in}} \tag{4.13}$$

However the power losses of the converter is derived from three major parameters; these are the switching power losses, conduction power losses and blocking power losses. These losses can only be calculated when experimental investigations are carried out because real components will provide certain information needed in the calculating these losses.

Table 4.1: Parameters for Simulation

Component	Value
Input Voltage V_{in}	230V
Filter capacitor C_{in}	0.94 x 10^{-6}F
Filter inductor L_{in}	8 x 10^{-3}H
Switching frequency f_{sw}	20kHz
Resonance inductor L_r	22 x 10^{-6}H
Output inductor L_o	150x 10^{-6}H
Output capacitor C_o	2.35 x 10^{-6}F
Output resistor R_o	60Ω

4.3 Simulation Results

Simulation results for the proposed single switch resonant converter is represented below. The necessary component parameters are show in Table 4.1. This simulation is carried out in MATLAB R2015a edition. Figure 4.4 shows the MATLAB layout for simulation, the input section has an LC filter connected an H-Bridge diode rectifier, the output which is connected to the single switch then the resonance inductor and the parallel RCL load.

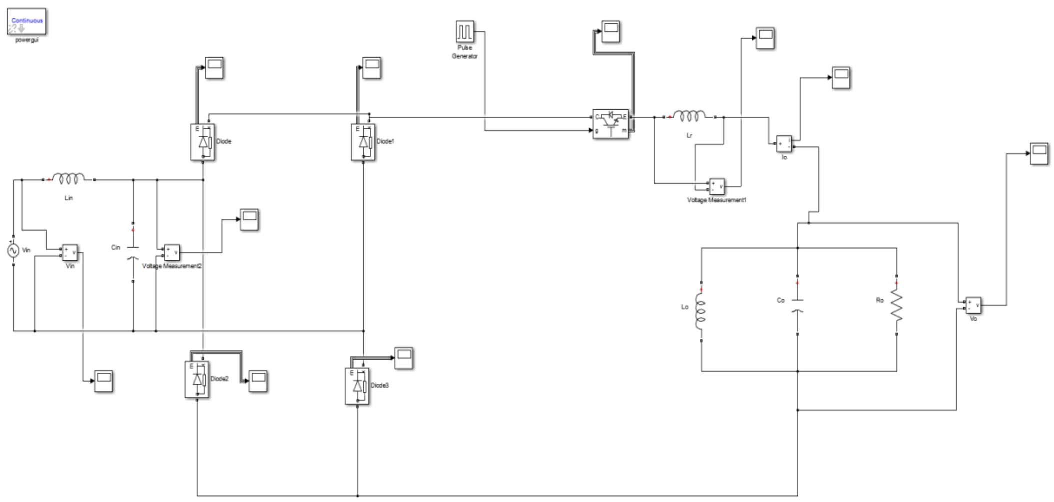

Figure 4.4: The MATLAB layout for simulation

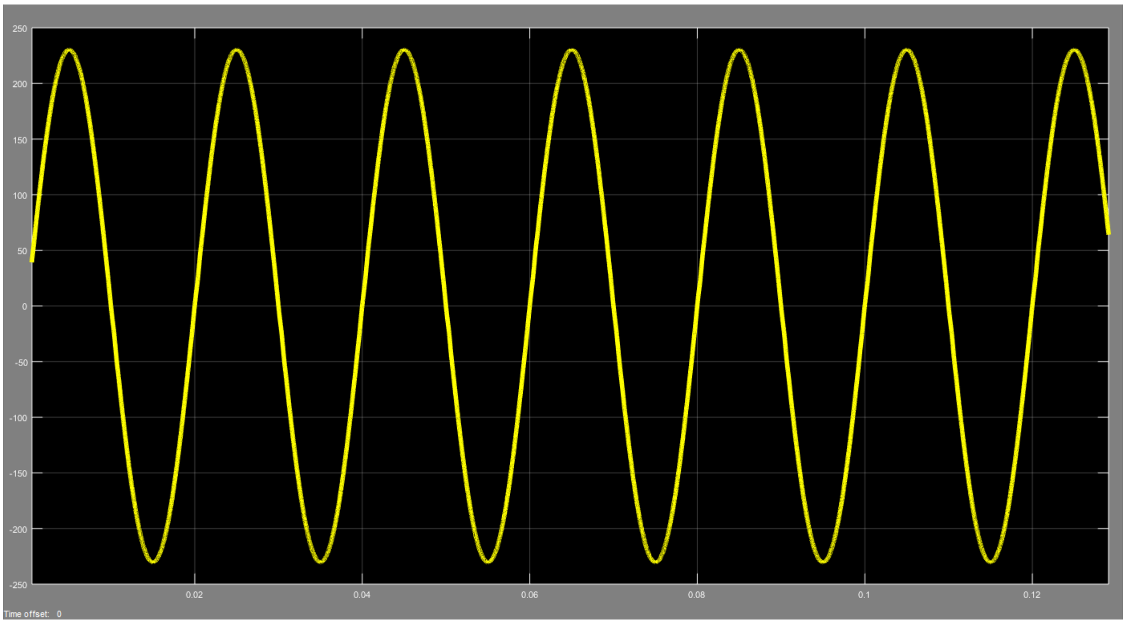

Figure 4.5: Input voltage waveform

The sinusoidal voltage input is shown by Figure 4.5. The peak to peak value of this voltage is 230V. Also the sinusoidal current input is shown by Figure 4.6. It should be noted that these values of measurements were carried out after the input filter. Hence the filter capacitor value is equivalent to the measurement of Figure 4.5 and the inductor measurement is equivalent to that of Figure 4.6.

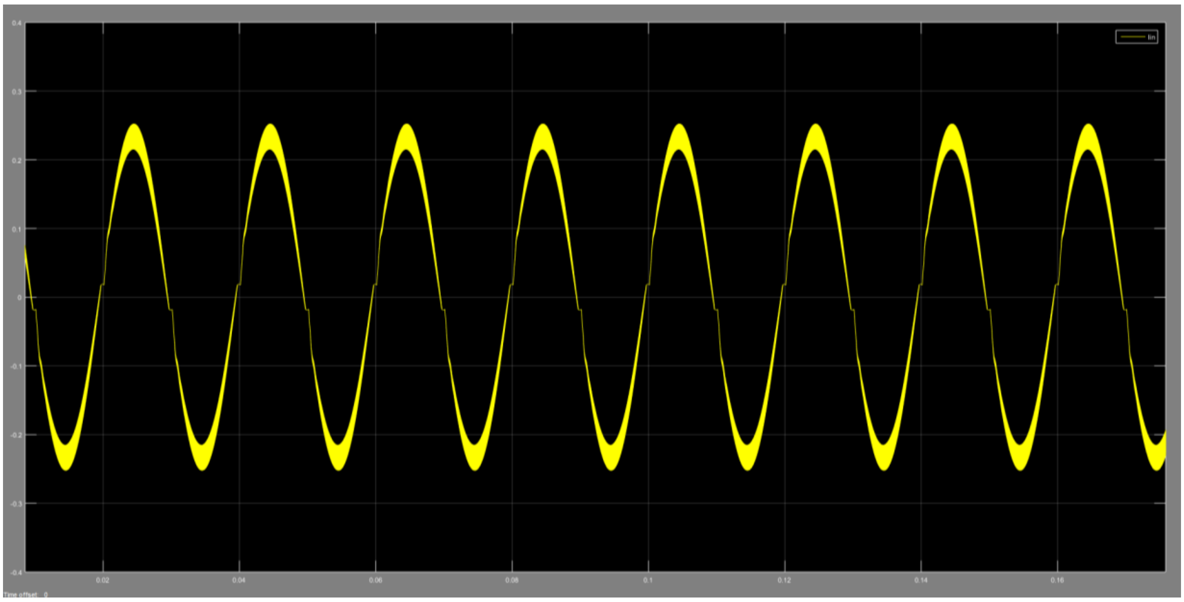

Figure 4.6: Input current

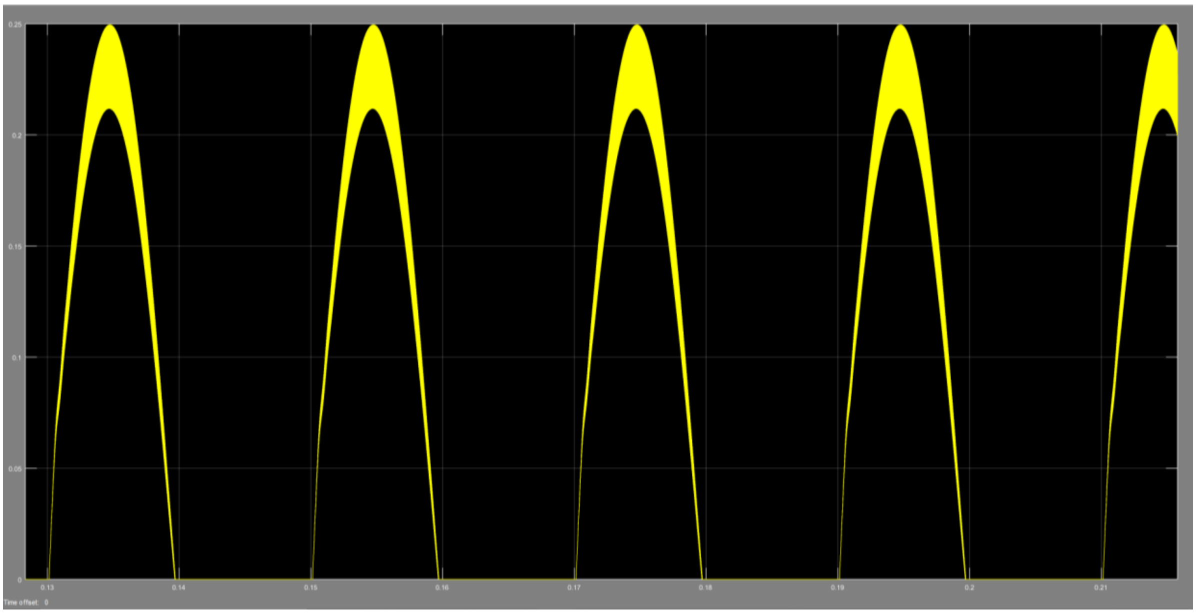

Figure 4.7: Diode current waveform

Figure 4.7 and Figure 4.8 shows the diode current and voltage waveforms during the process of changing the ac voltage into dc voltage. These waveforms are obtained from one diode and it can be used to represent the four diodes in the rectifier circuit because the input voltage values to change.

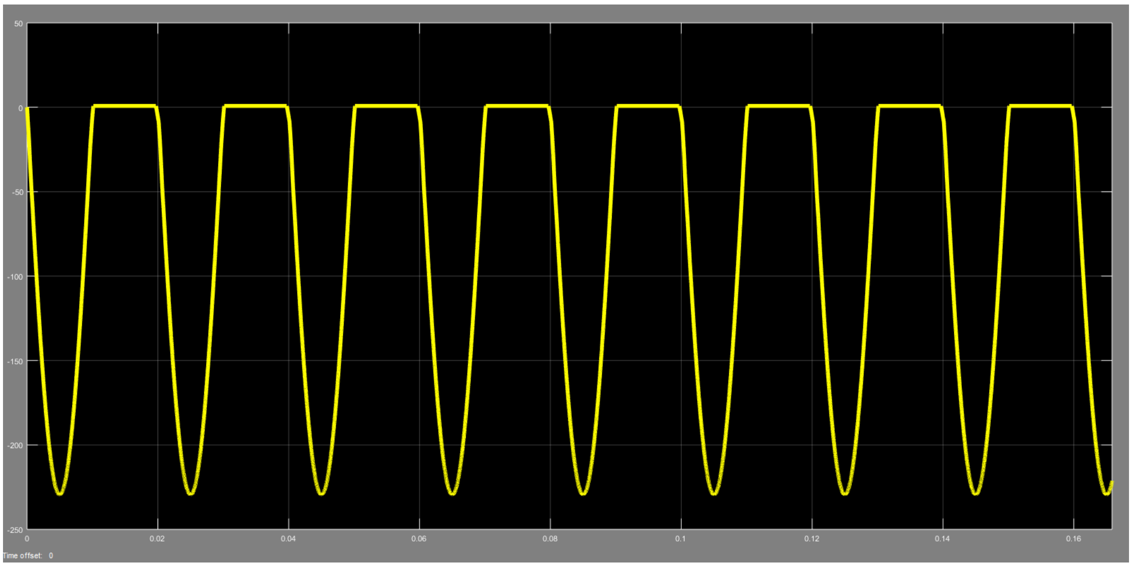

Figure 4.8: Diode voltage waveform

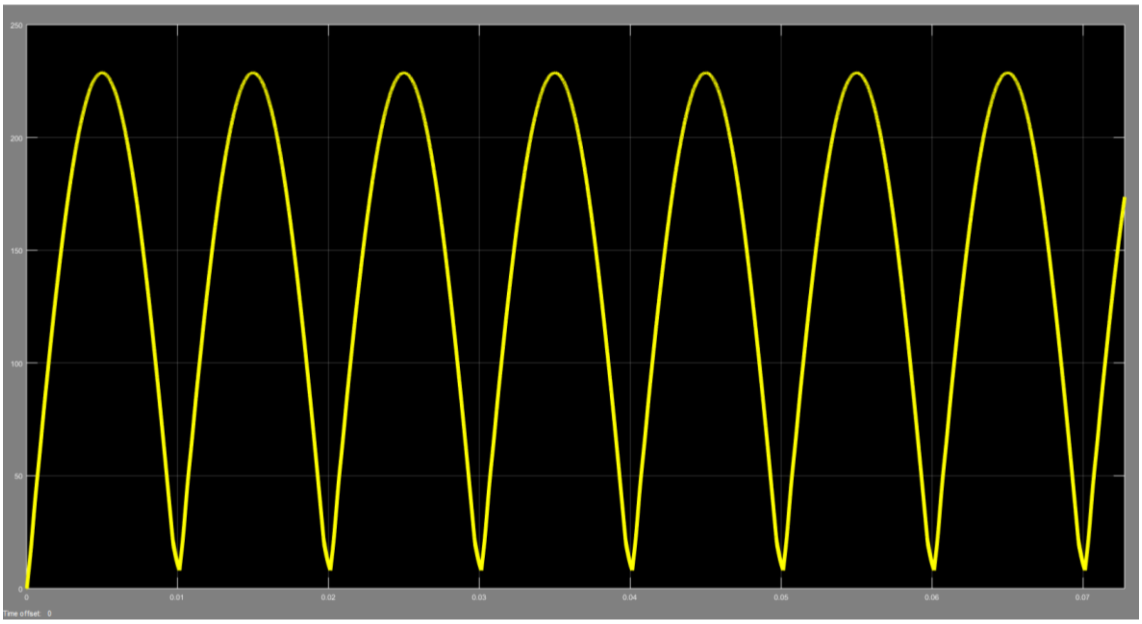

Figure 4.9: Rectifier output voltage

The rectified voltage of Figure 4.9 derived by changing the 230 ac voltage at the filter output to the desired dc voltage is shown by Figure 4.9. This rectified voltage is used to feed the single switch with unidirectional voltage flow; so as to converter the rectified voltage in sinusoidal ac voltage.

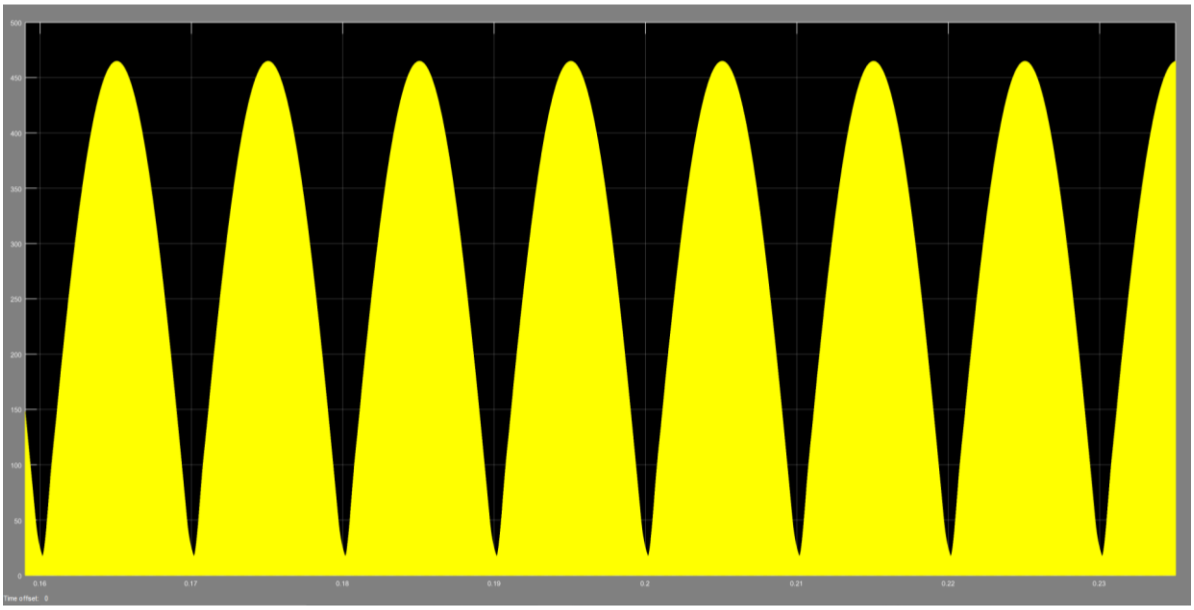

Figure 4.10: Switch voltage

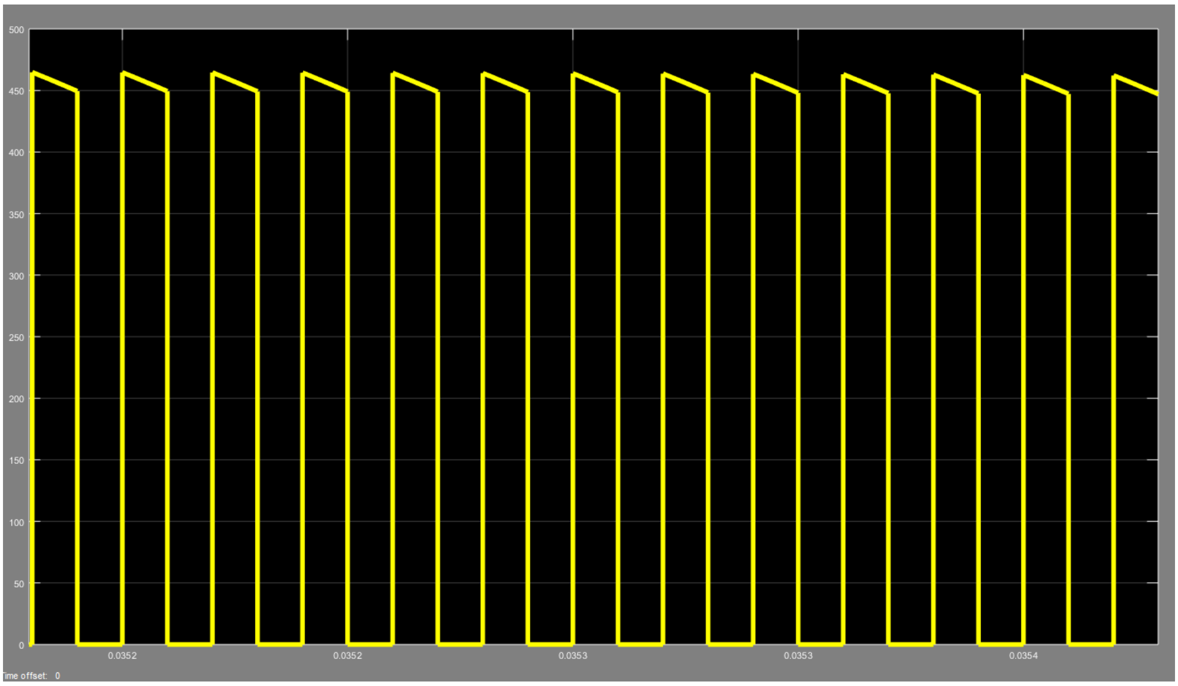

Figure 4.11: Switch voltage zoomed output

Figure 4.10 and Figure 4.11 shows the voltage across the unidirectional switch during the period of conduction. Figure 4.11 shows the zoomed out waveforms of the voltage across the switch. With a switching frequency of 20 kHz, the generated output voltage is shown by Figure 4.12 to Figure 4.14.

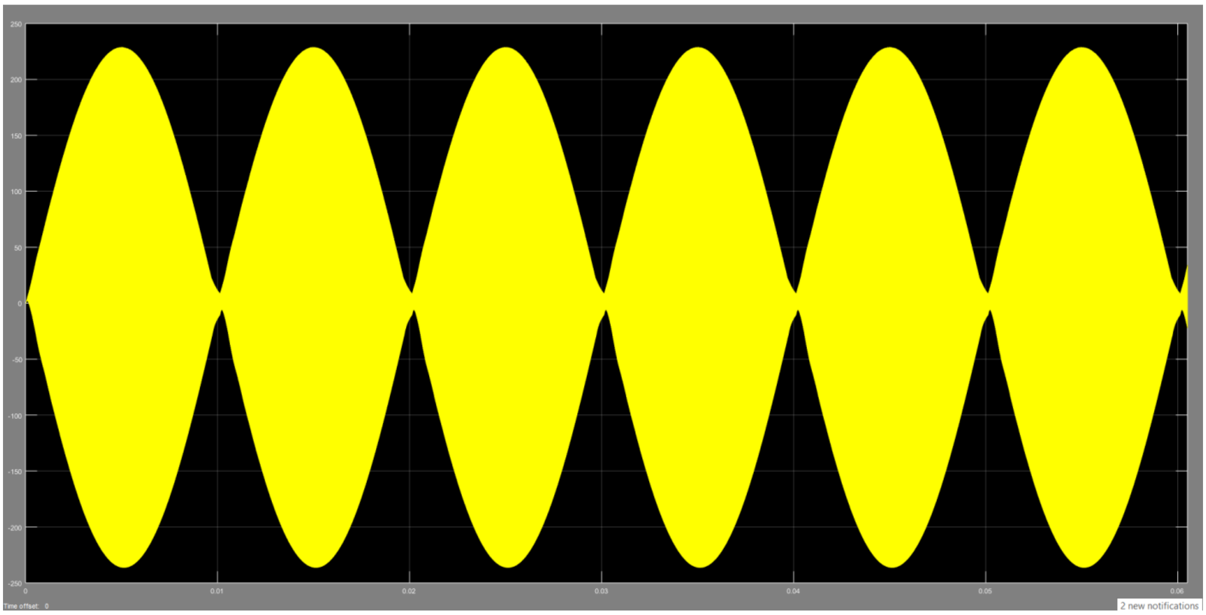

Figure 4.12: Output voltage

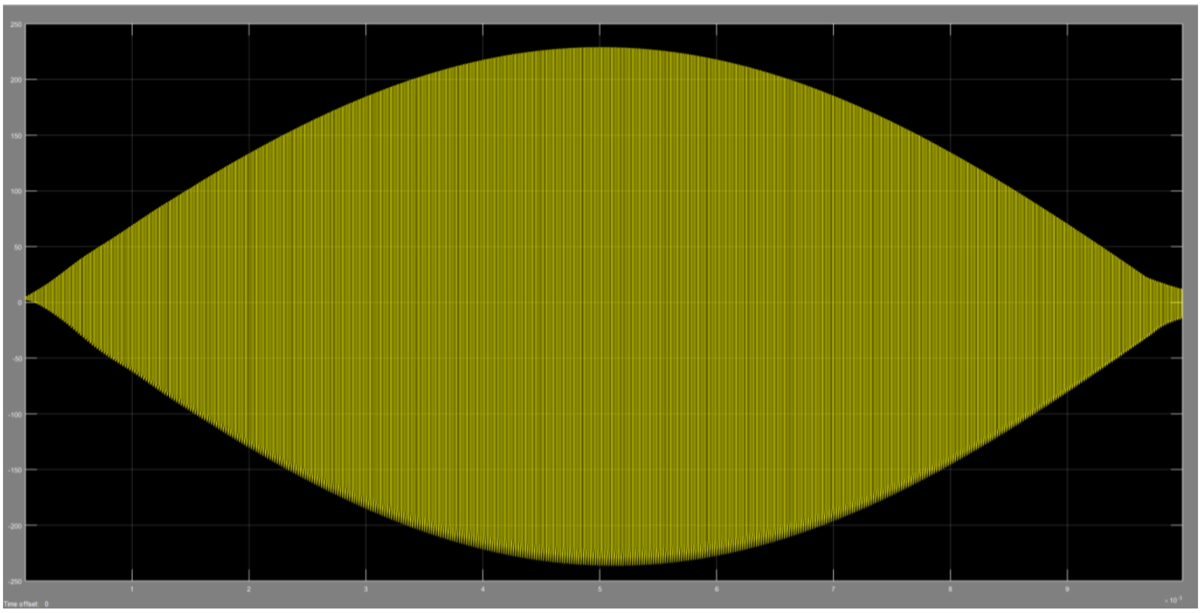

Figure 4.13: Output voltage zoomed out

Figure 4.12 shows the generated output voltage across the resonant tank and the load and Figure 4.13 shows the semi zoomed out of one of the output voltage. A further zoomed out of the output voltage is represented by Figure 4.14.

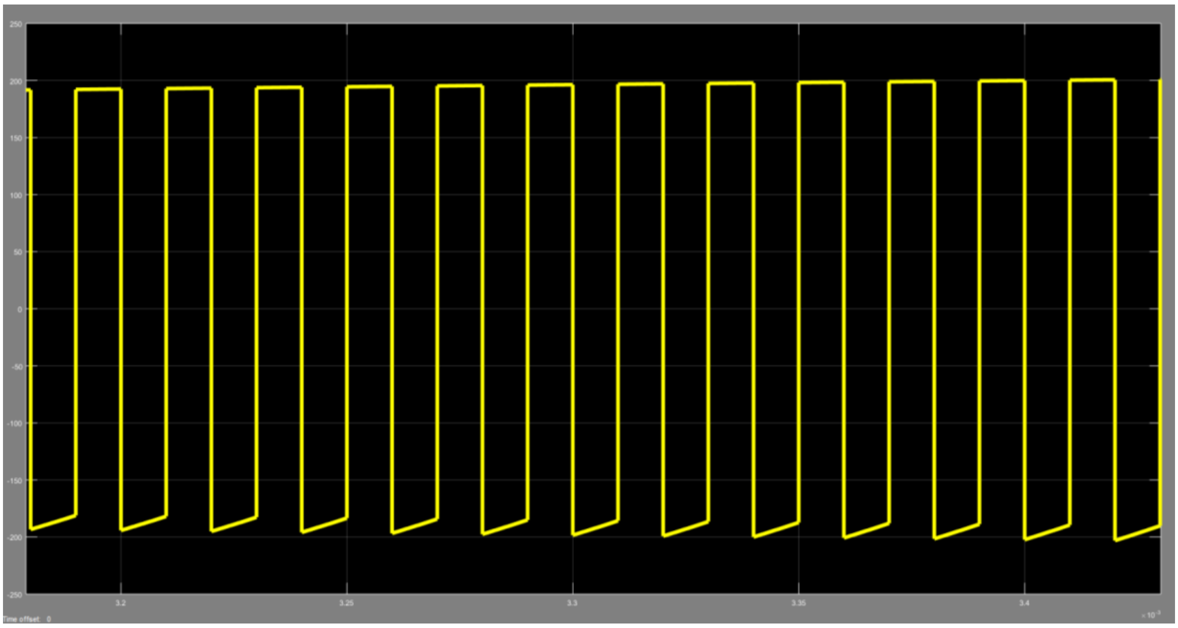

Figure 4.14: Output voltage further zoomed out

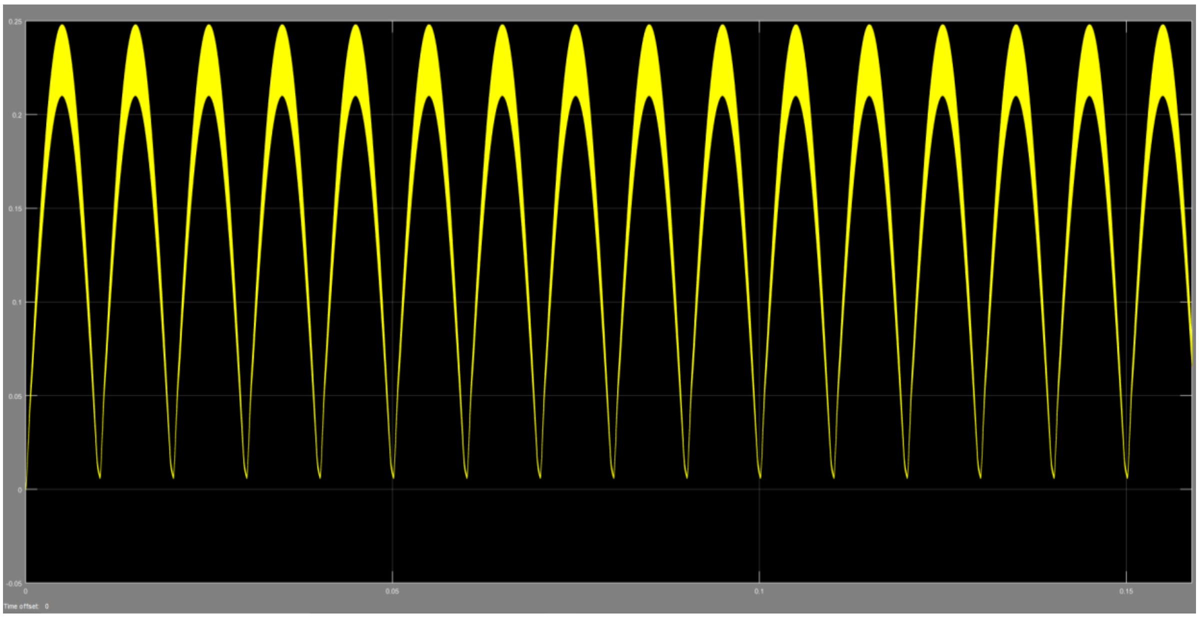

Figure 4.15: Output current

The generated output current which is the same as the resonant inductor current is shown by Figure 4.15. This currents feeds the parallel RLC load. Putting a scope across the resistor in the parallel RLC load will results in the measurement of the resistor current as shown by Figure 4.16.

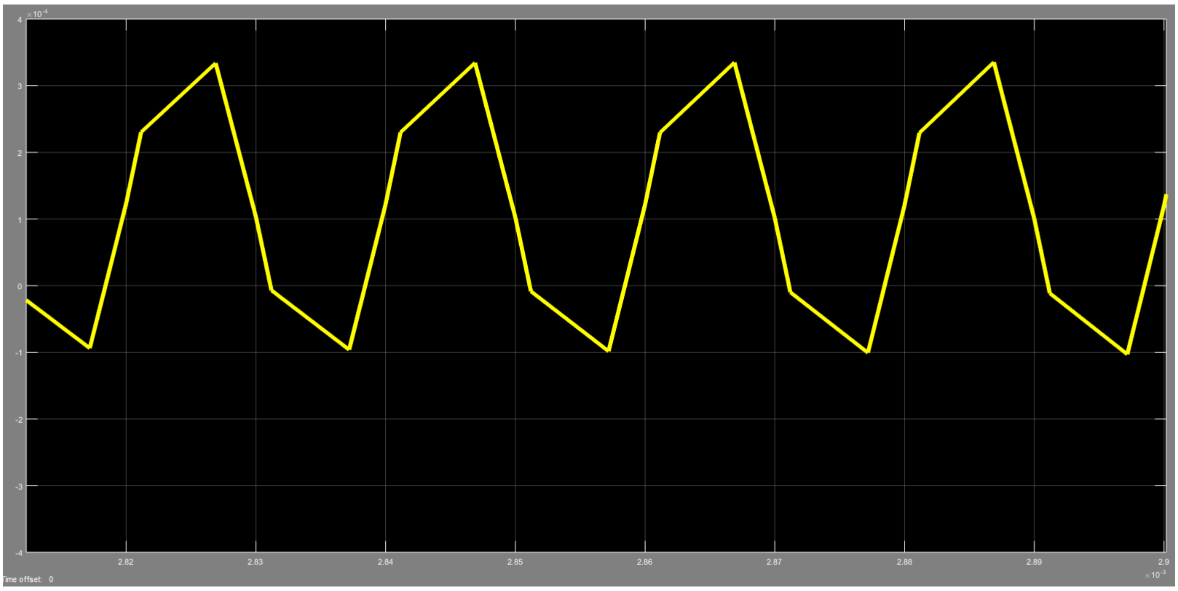

Figure 4.16: Resistor output current

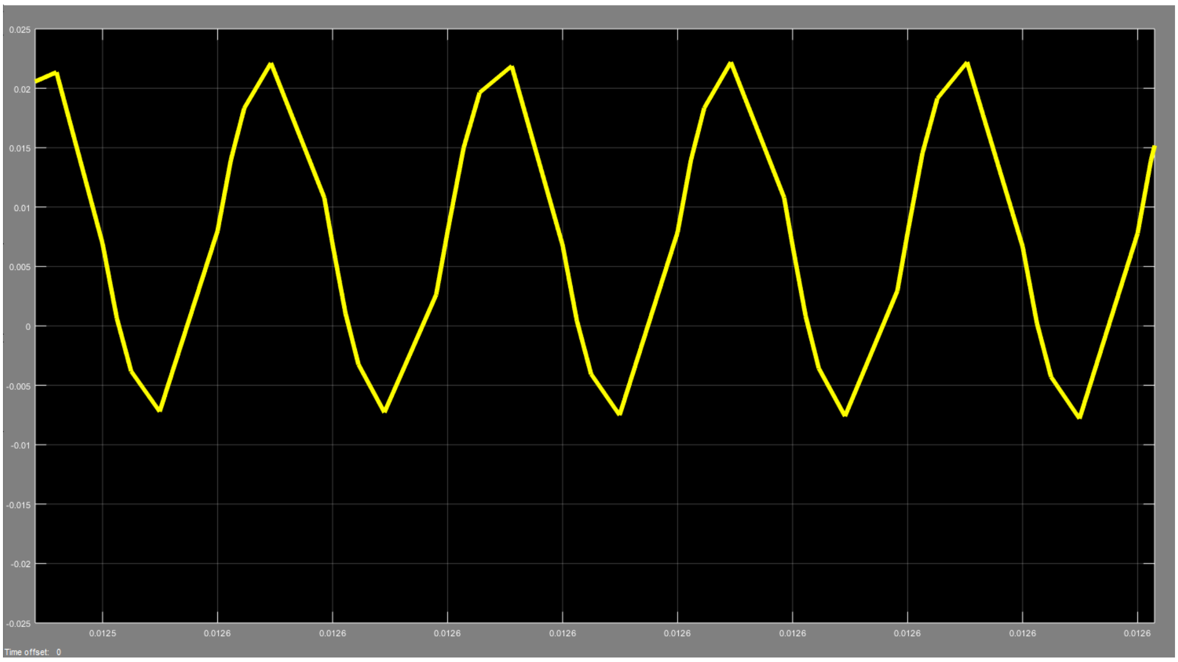

Figure 4.17: Capacitor voltage zoomed out.

The voltage across the parallel RLC load when measured is represented by Figure 4.17. This voltage shown in the figure is zoomed out to indicate the exact nature of its waveform. The above waveforms were generated for the simulation of the proposed single switch converter. The application of a single switch reduces the converter losses, reduces the volume and the size of the converter also. In the proposed topology, an input filter is used which minimises the input ripples and also resonant tank is applied which increases the efficiency of the topology.

4.4 Conclusion

The goal of this section of this thesis is to provide simulation results which will validate the theoretical analysis for the proposed topology. The generated output waveforms from simulating the proposed topology in MATLAB Software using the parameters of Table 4.1 proves a successful implementation of the proposed topology.

CHAPTER FIVE

CONCLUSION AND FUTURE WORKS

5.1 Conclusion

In this research, a single unidirectional converter is proposed which is fitted with an input LC filter and parallel resonant tank at the output which provides soft commutation of the power switch. As in the case of all ac-ac converters, this topology can be utilized as a high frequency generator and thereby using the frequency as the medium to control the converter output power. Due to laboratory constraints, analysis of the proposed converter is only investigated via simulation results. The generated waveforms obtained from simulations are shown and explained in chapter four of this thesis. Advantages of the presented topology when compared to similar converters can boast of minimum switching devices which results in minimization of the converter losses due to switching and conduction. An input filter is utilized to minimize the input ripples and alsominimize the harmonic content. The resonant tank structure provides the needed soft switching of the power switches so as to reduce the converter losses generated during the periods of blocking, conduction and switching. In all, the proposed converter, archives the needed goal of providing high frequency at the output and also provide the ac-dc-ac power conversion with minimum components and minimum losses.

5.2 Future Works

All the goals set out before conducting this research were achieved perfectly, however the current happenings in the world of power conversion needs a review of this research hence the following future works are recommended. A trade-off between this proposed topology which is a double stage conversion system but has only one power switch and four diodes and a single stage matrix converter with four bidirectional switches can be analysed. Incorporating any of the impedance based networks will provide buck-boost functionality and also provide very high voltage gains. Therefor future works will investigate the inclusion of the latest impedance network structure to boast the voltage gain.

REFERENCES

A. Hakemi, M. Monfared, (2017). Very high gain three-phase indirect matrix converter with two Z-source networks in its structure.*IET Renew Power Gener, 11*(5), 633-640.

A. Hillers, D Christen, J. Biela, (2012). Design of a highly efficient bidirectional isolated LLC resonant converter. *In International Power Electronics and Motion Control Conference*(vol. 15,6, pp. 1-8).

A. Pareek, A. K. Sharma, S. C. Mittal, A. Gautam, R. Singh (2018). Investigation of Operational Principle for Integrated Inverting and Non- Inverting PWM AC-AC Converter. *In International Conference on Inventive Research in Computing Applications*(vol. 12,8, pp. 5-14).

A. Shahani, K. Basu, N. Mohan, (2012). A power electronic transformer based on indirect matrix converter for PWM ac drive with lossless commutation of leakage energy. I*n Proceeding 6th IET International Conference*(vol. 14,5, pp. 1-6)

Amir Tahavorgar and John E. Quaicoe, (2019).Stability and Small-Signal Analyses of the Dual Series-Resonant DC–DC Converter. *IEEE Trans Power Electron,30*(2),82-89 .

C. Liu, D. Guo, R. Shan, G. Cai ; W. Ge, Z. Huang Yibo Wang, H. Zhang, P. Wang, (2019). Novel Bipolar-Type Direct AC–AC Converter Topology Based on Non-Differential AC Choppers .*IEEE Transactions on Power Electronics,34*(10), 9585-9599.

D. Thrimawithana, U. Madawala, (2008). Analysis of split-capacitor push-pull parallel-resonant converter in boost mode .*IEEE Trans. Power Electron, 23*(1), 359-368.

E. da Silva, S. Abeyratne, Y. Murai, (1999).PWM series resonant DC-link converter with current clamping by the use of saturable core. *IEEE. Trans. Power Electron, 14*(1), 82-89.

Emerson J. A. da Silva ; Bruno R. de Ameida ; Paulo P. Praça ; Demercil S. de Oliveira ; Luiz H. S. C. Barreto ; Fernando Luiz Marcelo Antunes, An Indirect AC-AC Converter With Power Factor Correction and High Frequency Insulation. *In IEEE International Conference on Industry Applications*(vol. 17,5, pp. 45-54).

Feng Xingtian ; Wan Manman ; Tao Yuanyuan ; Shao Kang, (2018).Self-adaptation load change control strategy for three-phase staggered parallel LLC resonant converter.*IET Power Electron, 11*(14), 2338-2345.

G. T. Chiang, J. I. Itoh, (2011). Performance optimization of a square wave operation in an indirect matrix converter with a reactor free DC boost converter. *In Proceedings of the 2011 14th European Conference on Power Electronics and Applications*(vol. 11,6, pp. 1-10).

.H. F. Ahmed, H., Cha, A. A. Khan, (2016). A single-phase quasi-Z-source AC-AC converter with high-frequency transformer isolation. *In Power Electron Motion Control Conference* (vol. 13,4, pp. 1111-1115).

H. Wang, T. Saha, B.S. Riar, R. Zane, (2018).Design Considerations for Current Regulated Series Resonant Converters with Constant Input Current. *IEEE Transaction on Power Electronics, 15*(6), 56-61.

L. Wang et al., (2017). A three-level T-type indirect matrix converter based on the third-harmonic injection technique. *IEEE J. Emerg. Sel. Topics Power Electron, 5*(2), 841-852.

M. J. Schutten, R. L. Steigerwald, M. H. Kheraluwala, (1992). Characteristics of load resonant converters operated in a high-power factor mode. *IEEE Trans. Power Electron, 7*(2), 304-314.

M. K. Nguyen, Y. G. Jung, Y. C. Lim, (2010). Single-phase ac-ac converter based on quasi-Z-source topology. *IEEE Trans Power Electron, 25*(8), 2200-2210.

M. Khalil-Abaker, J. Shi, A. Kalam, (2016). Design of a 100W bi-directional LCC series-parallel resonant DC-DC converter. *In Australasian Universities Power Engineering Conference*(vol. 14,8, pp. 1-5).

M. Kim, S. Noh, S. Choi, (2015). New Parallel Loaded Resonant Converter with Wide Input and Output Voltage Range. *In International Conference on Power Electronics*(vol. 9,2, pp. 12-20) .

M. R. Banaei, R. Alizadeh, N. Jahanyari, E. S. Najmi, (2016). An ac Z-source converter based on gamma structure with safe-commutation strategy. *IEEE Trans Power Electron, 31*(2), 1255-1262.

Minh-KhaiNguyen ; Young-Gook Jung ; Young-Cheol Lim, (2009). Single-Phase AC/AC Buck-Boost Converter with Single-Phase Matrix Topology. *In European Conference on Power Electronics and Applications* (vol. 6,2, pp. 14-21).

Neilor C. Dal Pont ;Delvanei G. Bandeira ; Telles B. Lazzarin ; Ivo Barbi, (2019).A ZVS APWM Half-Bridge Parallel Resonant DC–DC Converter With Capacitive Output.*EEE Transactions on Industrial Electronics, 66*(7), 5231-5241.

S. A. Deraz, H. Z. Azazi, M. S. Zaky, M. K. Metwaly, M. E. Dessouki, (2019). Performance investigation of three-phase three-switch direct PWM AC/AC voltage converters. *IEEE Access, 7*(2), 11485-11501.

S. Hu, X. Li, A. K. S. Bhat, (2018).Operation of a bidirectional series resonant converter with minimized tank current and wide ZVS range. *IEEE Trans Power Electron, 34*(1), 904-915.

S. Liu, B. Ge, H. Abu-Rub, X. Jiang, F.Z. Peng, (2013). A novel indirect quasi-Z-source matrix converter applied to induction motor drives. *IEEE Energy Conversion Congress and Exposition, 14*(3), 2440-2444.

S. M. Showybul Islam Shakib and Saad Mekhilef, (2017). A Frequency Adaptive Phase Shift Modulation Control Based LLC Series Resonant Converter for Wide Input Voltage Applications. *IEEE Trans Power Electron, 32*(11), 8360-8370.

S. Raju, N. Mohan, (2013).Space vector modulated hybrid indirect multilevel matrix converter. *In Annual Conference of the IEEE Industrial Electronics Society*(vol. 11,4, pp. 4931-4936) .

S. Z. Mohammad Noor, N. F. Abdul Rahman, and A. Mohamad Aris, (2011). Modeling and simulation of a single-phase boost AC-AC converter using Single-Phase Matrix Converter topology. *In Computer Applications and Industrial Electronics, 2011IEEE International Conference*(vol. 15,3, pp. 208-213).

Sanghun Kim, Duekjin Jang, Heung-Geun Kim, Honnyong Cha, (2018). Cascaded Dual-Buck AC-AC Converter Using Coupled Inductors. *In International Power Electronics Conference (IPEC-Niigata 2018-ECCE Asia)*(vol. 7,5, pp. 15-22).

Suvendu Samanta, Akshay Kumar Rathore, (2017). A New Inductive Power Transfer Topology Using Direct AC-AC Converter with Active Source Current Control. *IEEE Industry Applications Society Annual Meeting, 16*(4), 41-49.

Tang, Y., Xie, S., Wei, J. (2013).Grid-tied photovoltaic system with series Z-source inverter. *IET Renew Power Gener 7*(3), 275-283.

Tiago Kommers Jappe ; Marcelo Lobo Heldwein ; Samir Ahmad Mussa, (2015). Design of a high performance ac-ac drive system based on indirect matrix converters employing MOSFET. *In Brazilian Power Electronics Conference and 1st Southern Power Electronics Conference* (vol. 16,2, pp. 28-36).

X. Fang, M. Cao, Z. Chen, (2010). Z-source AC-DC-AC converter for mining applications. I*n Proceeding International Conference Electronics*(vol. 14,5, pp. 44-47)

X. Peng Fang, Z. Ming Qian, F. Zheng Peng, (2005). Single-phase Z-source PWM AC-AC converters. *IEEE Power Electron, 3*(4), 121-124 .

Y. C. Chuang, Y. L. Ke, H. S. Chuang, S. Y. Chang,(2012). Battery Float Charge Technique Using Parallel-Loaded Resonant Converter for Discontinuous Conduction Operation. *IEEE Transactions on Industry Applications,* 4*8*(3), 1070-1078.

Y. Shen, W. Zhao, Z. Chen, C. Cai, (2018). Full-bridge LLC resonant converter with series-parallel connected transformers for electric vehicle on-board charger. *IEEE Access, 6*(2), 13490-13500.

Ying-Chun Chuang, Hung-Shiang Chuang, Chun-Hsiang Yang, Tien-Chi Chen, (2017).Low-power DC energy conversion system based on a novel single-switch current-fed series-parallel resonant converter. *In IEEE International Conference on Industrial Technology* (vol. 12,5, pp. 76-81).

Yueshi Guan, Na Qi, Yijie Wang, Xiangjun Zhang, Dianguo Xu, Wei Wang, (2016).A novel DC/DC converter based on series-parallel resonant network for LED driver, *In International Power Electronics and Motion Control Conference,,* (vol. 6,2, pp. 126-130).

Z. Aleem, M. Hanif, (2016).Single-phase transformer based Z-source AC–AC converters. *In Proceedings IEEE 2nd Annu. Southern Power Electron International Conference14*(2), 1-6.

Z. Shao, K. J. Tseng, T. D. Nguyen, (2009). Novel three-phase AC-AC Z-Source converters using matrix converter theory. *Energy Conversion Congress and Exposition, 15*(7), 3063-3070.

Zhang, S. Tseng, K.J. Nguyen, T.D, (2009). Novel three-phase AC-AC Z-Source converters using matrix converter theory. *IEEE Energy Conversion and Exposition, 13*(2), 3065-3074.